

University of Windsor

## Scholarship at UWindor

---

Electronic Theses and Dissertations

Theses, Dissertations, and Major Papers

---

4-24-2018

# Digital Filter Design Using Multiobjective Cuckoo Search Algorithm

Jiajun Liang  
*University of Windsor*

Follow this and additional works at: <https://scholar.uwindsor.ca/etd>

---

### Recommended Citation

Liang, Jiajun, "Digital Filter Design Using Multiobjective Cuckoo Search Algorithm" (2018). *Electronic Theses and Dissertations*. 7431.

<https://scholar.uwindsor.ca/etd/7431>

This online database contains the full-text of PhD dissertations and Masters' theses of University of Windsor students from 1954 forward. These documents are made available for personal study and research purposes only, in accordance with the Canadian Copyright Act and the Creative Commons license—CC BY-NC-ND (Attribution, Non-Commercial, No Derivative Works). Under this license, works must always be attributed to the copyright holder (original author), cannot be used for any commercial purposes, and may not be altered. Any other use would require the permission of the copyright holder. Students may inquire about withdrawing their dissertation and/or thesis from this database. For additional inquiries, please contact the repository administrator via email ([scholarship@uwindsor.ca](mailto:scholarship@uwindsor.ca)) or by telephone at 519-253-3000ext. 3208.

**Digital Filter Design Using Multiobjective Cuckoo Search Algorithm**

By

**Jiajun Liang**

A Thesis  
Submitted to the Faculty of Graduate Studies  
through the Department of Electrical and Computer Engineering  
in Partial Fulfillment of the Requirements for  
the Degree of Master of Applied Science  
at the University of Windsor

Windsor, Ontario, Canada

2018

© 2018 Jiajun Liang

# **Digital Filter Design Using Multiobjective Cuckoo Search Algorithm**

by

**Jiajun Liang**

APPROVED BY:

---

X. Guo  
Odette School of Business

---

C. Chen  
Department of Electrical and Computer Engineering

---

H.K. Kwan, Advisor  
Department of Electrical and Computer Engineering

April 12, 2018

## DECLARATION OF ORIGINALITY

I hereby certify that I am the sole author of this thesis and that no part of this thesis has been published or submitted for publication.

I certify that, to the best of my knowledge, my thesis does not infringe upon anyone's copyright nor violate any proprietary rights and that any ideas, techniques, quotations, or any other material from the work of other people included in my thesis, published or otherwise, are fully acknowledged in accordance with the standard referencing practices. Furthermore, to the extent that I have included copyrighted material that surpasses the bounds of fair dealing within the meaning of the Canada Copyright Act, I certify that I have obtained a written permission from the copyright owner(s) to include such material(s) in my thesis and have included copies of such copyright clearances to my appendix.

I declare that this is a true copy of my thesis, including any final revisions, as approved by my thesis committee and the Graduate Studies office, and that this thesis has not been submitted for a higher degree to any other University or Institution.

## ABSTRACT

Digital filters can be divided into finite impulse response (FIR) digital filters and infinite impulse response (IIR) digital filters. Evolutionary algorithms are effective techniques in digital filter designs. One such evolutionary algorithm is Cuckoo Search Algorithm (CSA). The CSA is a heuristic algorithm which emulates a special parasitic hatching habit of some species of cuckoos and have been proved to be an effective method with various applications.

This thesis compares CSA with Park-McClellan algorithm on linear-phase FIR Type-1 lowpass, highpass, bandpass and bandstop digital filter design. Furthermore, a multiobjective Cuckoo Search Algorithm (MOCSA) is applied on general FIR digital design with a comparison to Non-dominated Sorting Genetic Algorithm III (NSGA-III). Finally, a constrained multiobjective Cuckoo Search Algorithm is presented and used for IIR digital filter design. The design results of the constrained MOCSA approach compares favorably with other state-of-the-art optimization methods.

CSA utilizes Levy flight with wide-range step length for the global walk to assure reaching the global optimum and the approach of local walk to orientate the direction toward the local minima. Furthermore, MOCSA incorporates a method of Euclidean distance combing objective-based equilibrating operations and the searching for the optimal solution into one step and simplifies the procedure of comparison.

## ACKNOWLEDGEMENTS

I am very grateful to Dr. H. K. Kwan for his patient instruction and invaluable suggestions on this thesis. Dr. Kwan has enlightened me on the research of evolutionary algorithms and in particular the use of Cuckoo Search Algorithm for designing linear phase FIR digital filters, asymmetric FIR digital filters and IIR digital filters by multiobjective approach. He shares his precious experiences and inspires me to make greater progress on my research area. Furthermore, I would like to express my appreciation to Dr. Chunhong Chen and Dr. Xiaolei Guo for their great insight and professional advice on my thesis. Besides, I expect to thank Jason Liu and Miao Zhang for their sincere solicitude.

## TABLE OF CONTENTS

DECLARATION OF ORIGINALITY .....	iii
ABSTRACT.....	iv
ACKNOWLEDGEMENTS .....	v
LIST OF TABLES .....	ix
LIST OF FIGURES .....	xiii
LIST OF ABBREVIATIONS/SYMBOLS.....	xvii
CHAPTER 1 Introduction to Digital Filters .....	1
1.1 Introduction .....	1
1.2 Analog-to-digital Conversion .....	1
1.2.1 Limitation of Sampling Frequency.....	2
1.2.2 Normalized Frequency.....	2
1.3 Z-transform to A Digital Filter .....	2
1.4 Four Main Types of Ideal Filter Shapes .....	4
1.4.1 Ideal Lowpass Digital Filters .....	4
1.4.2 Ideal Highpass Digital Filters .....	4
1.4.3 Ideal Bandpass Digital Filters .....	5
1.4.4 Ideal Bandstop Digital Filters .....	6
CHAPTER 2 Introduction to Evolutionary Algorithms .....	8
2.1 Introduction .....	8
2.2 Optimization Problems .....	8
2.3 Evolutionary Algorithms .....	9
2.4 Basic Methodologies of An Evolutionary Algorithm .....	10
2.4.1 Configuration of Solutions .....	10
2.4.2 Objective Functions .....	11
2.4.3 Initialization .....	12
2.4.4 Elite Selection .....	12
2.4.5 Variation for New Solutions.....	13

2.4.5.1 <i>Inheritance</i> .....	13
2.4.5.2 <i>Mutation</i> .....	14
2.4.6 <i>Survivor Determination</i> .....	15
2.4.7 <i>Termination Criterion</i> .....	16
CHAPTER 3 <i>Linear Phase FIR Digital Filter Design Using Cuckoo Search</i>	
Algorithm .....	17
3.1 <i>Introduction of CSA</i> .....	17
3.1.1 <i>Biological Background of CSA</i> .....	17
3.1.2 <i>Biological Rules of CSA for Algorithm Realization</i> .....	18
3.1.3 <i>Levy Flight</i> .....	18
3.1.4 <i>Random Walk</i> .....	19
3.2 <i>Design of Linear-Phase Type-1 FIR Digital Filters</i> .....	20
3.3 <i>Design Examples and Results</i> .....	22
3.3.1 <i>Lowpass Digital Filters</i> .....	23
3.3.1.1 <i>24th-order Lowpass Digital Filter</i> .....	23
3.3.1.2 <i>48th-order Lowpass Digital Filter</i> .....	25
3.3.2 <i>Highpass Digital Filters</i> .....	27
3.3.2.1 <i>24th-order Highpass Digital Filter</i> .....	27
3.3.2.2 <i>48th-order Highpass Digital Filter</i> .....	29
3.3.3 <i>Bandpass Digital Filters</i> .....	31
3.3.3.1 <i>24th-order Bandpass Digital Filter</i> .....	31
3.3.3.2 <i>48th-order Bandpass Digital Filter</i> .....	33
3.3.4 <i>Bandstop Digital Filters</i> .....	35
3.3.4.1 <i>24th-order Bandstop Digital Filter</i> .....	35
3.3.4.2 <i>48th-order Bandstop Digital Filter</i> .....	37
3.4 <i>Conclusion</i> .....	39
CHAPTER 4 <i>General FIR Digital Filter Design Using Multiobjective Cuckoo</i>	
Search Algorithm .....	40
4.1 <i>Introduction</i> .....	40
4.2 <i>Multiobjective Cuckoo Search Algorithm</i> .....	41
4.3 <i>Design of General FIR Digital Filters</i> .....	42
4.4 <i>Design Examples and Results</i> .....	42
4.4.1 <i>24th-order Lowpass Digital Filters</i> .....	44



4.4.1.1 Lowpass Digital Filter with Group Delay in Passband at 10.....	44
4.4.1.2 Lowpass Digital Filter with Group Delay in Passband at 12.....	47
4.4.1.3 Lowpass Digital Filter with Group Delay in Passband at 14.....	51
4.4.2 24th-order Highpass Digital Filters .....	54
4.4.2.1 Highpass Digital Filter with Group Delay in Passband at 10 .....	54
4.4.2.2 Highpass Digital Filter with Group Delay in Passband at 12.....	57
4.4.2.3 Highpass Digital Filter with Group Delay in Passband at 14.....	61
4.4.3 24th-order Bandpass Digital Filters.....	64
4.4.3.1 Bandpass Digital Filter with Group Delay in Passband at 10 .....	64
4.4.3.2 Bandpass Digital Filter with Group Delay in Passband at 12 .....	67
4.4.3.3 Bandpass Digital Filter with Group Delay in Passband at 14 .....	71
4.4.4 24th-order Bandstop Digital Filters .....	74
4.4.4.1 Bandstop Digital Filter with Group Delay in Passband at 10.....	74
4.4.4.2 Bandstop Digital Filter with Group Delay in Passband at 12.....	77
4.4.4.3 Bandstop Digital Filter with Group Delay in Passband at 14.....	81
4.5 Conclusion .....	84
<b>CHAPTER 5 IIR Digital Filter Design Using Constrained Multiobjective Cuckoo Search Algorithm .....</b>	<b>85</b>
5.1 Introduction .....	85
5.2 Constrained Multiobjective Cuckoo Search Algorithm.....	85
5.3 Design of IIR Digital Filters .....	86
5.4 Design Examples and Results .....	89
5.4.1 Example 1.....	91
5.4.2 Example 2.....	94
5.4.3 Example 3.....	98
5.5 Conclusion .....	101
<b>CHAPTER 6 Conclusion Remarks.....</b>	<b>102</b>
<b>REFERENCES .....</b>	<b>103</b>
<b>VITA AUCTORIS .....</b>	<b>105</b>

## LIST OF TABLES

Table 3.1 Pseudocode of Cuckoo Search Algorithm .....	20
Table 3.2 Filter specifications and CSA parameters .....	22
Table 3.3 LP-FIR1 digital filter cutoff frequencies .....	23
Table 3.4 Frequency grid for LP-FIR1 digital filter design .....	23
Table 3.5 Coefficients of 24th-order LP-FIR1 lowpass digital filter.....	23
Table 3.6 Design results of 24th-order LP-FIR1 lowpass digital filter.....	24
Table 3.7 Computational record of 24th-order LP-FIR1 lowpass digital filter .....	24
Table 3.8 Coefficients of 48th-order LP-FIR1 lowpass digital filter.....	25
Table 3.9 Design results of 48th-order LP-FIR1 lowpass digital filter.....	26
Table 3.10 Computational record of 48th-order LP-FIR1 lowpass digital filter .....	26
Table 3.11 Coefficients of 24th-order LP-FIR1 highpass digital filter.....	27
Table 3.12 Design results of 24th-order LP-FIR1 highpass digital filter .....	28
Table 3.13 Computational record of 24th-order LP-FIR1 highpass digital filter .....	28
Table 3.14 Coefficients of 48th-order LP-FIR1 highpass digital filter.....	29
Table 3.15 Design results of 48th-order LP-FIR1 highpass digital filter .....	30
Table 3.16 Computational record of 48th-order LP-FIR1 highpass digital filter .....	30
Table 3.17 Coefficients of 24th-order LP-FIR1 bandpass digital filter .....	31
Table 3.18 Design results of 24th-order LP-FIR1 bandpass digital filter.....	32
Table 3.19 Computational record of 24th-order LP-FIR1 bandpass digital filter.....	32
Table 3.20 Coefficients of 48th-order LP-FIR1 bandpass digital filter .....	33
Table 3.21 Design results of 48th-order LP-FIR1 bandpass digital filter.....	34
Table 3.22 Computational record of 48th-order LP-FIR1 bandpass digital filter.....	34
Table 3.23 Coefficients of 24th-order LP-FIR1 bandstop digital filter .....	35
Table 3.24 Design results of 24th-order LP-FIR1 bandstop digital filter .....	36
Table 3.25 Computational record of 24th-order LP-FIR1 bandstop digital filter.....	36
Table 3.26 Coefficients of 48th-order LP-FIR1 bandstop digital filter .....	37
Table 3.27 Design results of 48th-order LP-FIR1 bandstop digital filter .....	38
Table 3.28 Computational record of 48th-order LP-FIR1 bandstop digital filter.....	38
Table 4.1 Parameters of MOCSA and NSGA-III .....	43
Table 4.2 G-FIR digital filter cutoff frequencies .....	43
Table 4.3 Frequency grid for G-FIR digital filter design.....	43
Table 4.4 Coefficients of lowpass digital filter with group delay in passband at 10 .....	44

Table 4.5 Magnitude error of lowpass digital filter with group delay in passband at 10..	45
Table 4.6 Group delay error of lowpass digital filter with group delay in passband at 10 .....	45
Table 4.7 Computational record of lowpass digital filter with group delay in passband at 10 .....	45
Table 4.8 Coefficients of lowpass digital filter with group delay in passband at 12 .....	47
Table 4.9 Magnitude error of lowpass digital filter with group delay in passband at 12..	48
Table 4.10 Group delay error of lowpass digital filter with group delay in passband at 12 .....	48
Table 4.11 Computational record of lowpass digital filter with group delay in passband at 12 .....	49
Table 4.12 Coefficients of lowpass digital filter with group delay in passband at 14 .....	51
Table 4.13 Magnitude error of lowpass digital filter with group delay in passband at 14 .....	52
Table 4.14 Group delay error of lowpass digital filter with group delay in passband at 14 .....	52
Table 4.15 Computational record of lowpass digital filter with group delay in passband at 14 .....	52
Table 4.16 Coefficients of highpass digital filter with group delay in passband at 10 .....	54
Table 4.17 Magnitude error of highpass digital filter with group delay in passband at 10 .....	55
Table 4.18 Group delay error of highpass digital filter with group delay in passband at 10 .....	55
Table 4.19 Computational record of highpass digital filter with group delay in passband at 10 .....	55
Table 4.20 Coefficients of highpass digital filter with group delay in passband at 12 .....	57
Table 4.21 Magnitude error of highpass digital filter with group delay in passband at 12 .....	58
Table 4.22 Group delay error of highpass digital filter with group delay in passband at 12 .....	58
Table 4.23 Computational record of highpass digital filter with group delay in passband at 12 .....	59
Table 4.24 Coefficients of highpass digital filter with group delay in passband at 14 .....	61
Table 4.25 Magnitude error of highpass digital filter with group delay in passband at 14 .....	62
Table 4.26 Group delay error of highpass digital filter with group delay in passband at 14 .....	62

Table 4.27 Computational record of highpass digital filter with group delay in passband at 14 .....	62
Table 4.28 Coefficients of bandpass digital filter with group delay in passband at 10 ....	64
Table 4.29 Magnitude error of bandpass digital filter with group delay in passband at 10 .....	65
Table 4.30 Group delay error of bandpass digital filter with group delay in passband at 10 .....	65
Table 4.31 Computational record of bandpass digital filter with group delay in passband at 10 .....	65
Table 4.32 Coefficients of bandpass digital filter with group delay in passband at 12 ....	67
Table 4.33 Magnitude error of bandpass digital filter with group delay in passband at 12 .....	68
Table 4.34 Group delay error of bandpass digital filter with group delay in passband at 12 .....	68
Table 4.35 Computational record of bandpass digital filter with group delay in passband at 12 .....	69
Table 4.36 Coefficients of bandpass digital filter with group delay in passband at 14 ....	71
Table 4.37 Magnitude error of bandpass digital filter with group delay in passband at 14 .....	72
Table 4.38 Group delay error of bandpass digital filter with group delay in passband at 14 .....	72
Table 4.39 Computational record of bandpass digital filter with group delay in passband at 14 .....	72
Table 4.40 Coefficients of bandstop digital filter with group delay in passband at 10.....	74
Table 4.41 Magnitude error of bandstop digital filter with group delay in passband at 10 .....	75
Table 4.42 Group delay error of bandstop digital filter with group delay in passband at 10 .....	75
Table 4.43 Computational record of bandstop digital filter with group delay in passband at 10 .....	75
Table 4.44 Coefficients of bandstop digital filter with group delay in passband at 12.....	77
Table 4.45 Magnitude error of bandstop digital filter with group delay in passband at 12 .....	78
Table 4.46 Group delay error of bandstop digital filter with group delay in passband at 12 .....	78
Table 4.47 Computational record of bandstop digital filter with group delay in passband at 12 .....	79

Table 4.48 Coefficients of bandstop digital filter with group delay in passband at 14.....	81
Table 4.49 Magnitude error of bandstop digital filter with group delay in passband at 14 .....	82
Table 4.50 Group delay error of bandstop digital filter with group delay in passband at 14 .....	82
Table 4.51 Computational record of bandstop digital filter with group delay in passband at 14 .....	82
Table 5.1 Parameters of constrained MOCSA.....	90
Table 5.2 Frequency grid for IIR digital filter design.....	91
Table 5.3 Filter specification of designed IIR lowpass digital filter in Example 1.....	91
Table 5.4 Performance requirements of designed IIR lowpass filter in Example 1.....	91
Table 5.5 Design results of the IIR lowpass digital filter in Example 1 .....	92
Table 5.6 Computational record of designed IIR lowpass digital filter in Example 1.....	92
Table 5.7 Coefficients of designed IIR lowpass digital filter in Example 1 .....	92
Table 5.8 Filter specification of designed IIR highpass digital filter in Example 2 .....	94
Table 5.9 Performance requirements of designed IIR highpass filter in Example 2 .....	95
Table 5.10 Design results of the IIR highpass digital filter in Example 2 .....	95
Table 5.11 Computational record of designed IIR highpass digital filter in Example 2... ..	95
Table 5.12 Coefficients of designed IIR highpass digital filter in Example 2.....	95
Table 5.13 Filter specification of designed IIR bandpass digital filter in Example 3.....	98
Table 5.14 Performance requirements of designed IIR bandpass filter in Example 3.....	98
Table 5.15 Design results of the IIR bandpass digital filter in Example 3 .....	98
Table 5.16 Computational record of designed IIR bandpass digital filter in Example 3.. ..	99
Table 5.17 Coefficients of designed IIR bandpass digital filter in Example 3 .....	99

## LIST OF FIGURES

Fig. 1.1 Input-filtering-output correspondence of a digital filter for its impulse response .	3
Fig. 1.2 Magnitude response of an ideal lowpass digital filter .....	4
Fig. 1.3 Magnitude response of an ideal highpass digital filter .....	5
Fig. 1.4 Magnitude response of an ideal bandpass digital filter.....	6
Fig. 1.5 Magnitude response of an ideal bandstop digital filter.....	7
Fig. 2.1 Configuration of a chromosome in GA .....	11
Fig. 2.2 Initialization of a chromosome in GA .....	12
Fig. 2.3 Roulette wheel for a population in GA.....	13
Fig. 2.4 An example of elite selection in GA.....	13
Fig. 2.5 Crossover operation in GA.....	14
Fig. 2.6 Mutation operation in GA.....	15
Fig. 3.1 Magnitude response, impulse response, the passband and stopband errors of designed 24th-order LP-FIR1 lowpass digital filter .....	24
Fig. 3.2 Convergence curve of designed 24th-order LP-FIR1 lowpass digital filter .....	25
Fig. 3.3 Magnitude response, impulse response, the passband and stopband errors of designed 48th-order LP-FIR1 lowpass digital filter .....	26
Fig. 3.4 Convergence curve of designed 48th-order LP-FIR1 lowpass digital filter .....	27
Fig. 3.5 Magnitude response, impulse response, the passband and stopband errors of designed 24th-order LP-FIR1 highpass digital filter .....	28
Fig. 3.6 Convergence curve of designed 24th-order LP-FIR1 highpass digital filter.....	29
Fig. 3.7 Magnitude response, impulse response, the passband and stopband errors of designed 24th-order LP-FIR1 highpass digital filter .....	30
Fig. 3.8 Convergence curve of designed 48th-order LP-FIR1 highpass digital filter.....	31
Fig. 3.9 Magnitude response, impulse response, the passband and stopband errors of designed 24th-order LP-FIR1 bandpass digital filter.....	32
Fig. 3.10 Convergence curve of designed 24th-order LP-FIR1 bandpass digital filter ....	33
Fig. 3.11 Magnitude response, impulse response, the passband and stopband errors of designed 48th-order LP-FIR1 bandpass digital filter.....	34
Fig. 3.12 Convergence curve of designed 48th-order LP-FIR1 bandpass digital filter ....	35
Fig. 3.13 Magnitude response, impulse response, the passband and stopband errors of designed 24th-order LP-FIR1 bandstop digital filter.....	36
Fig. 3.14 Convergence curve of designed 24th-order LP-FIR1 bandstop digital filter ....	37
Fig. 3.15 Magnitude response, impulse response, the passband and stopband errors of designed 48th-order LP-FIR1 bandstop digital filter.....	38

Fig. 3.16 Convergence curve of designed 48th-order LP-FIR1 bandstop digital filter ....	39
Fig. 4.1 Magnitude response, impulse response, the passband and stopband errors of designed G-FIR lowpass digital filter with group delay in passband at 10 obtained by MOCSA .....	46
Fig. 4.2 Magnitude response, impulse response, the passband and stopband errors of designed G-FIR lowpass digital filter with group delay in passband at 10 obtained by NSGA-III .....	46
Fig. 4.3 Convergence curve of designed G-FIR lowpass digital filter with group delay in passband at 10 obtained by MOCSA .....	47
Fig. 4.4 Magnitude response, impulse response, the passband and stopband errors of designed G-FIR lowpass digital filter with group delay in passband at 12 obtained by MOCSA .....	49
Fig. 4.5 Magnitude response, impulse response, the passband and stopband errors of designed G-FIR lowpass digital filter with group delay in passband at 12 obtained by NSGA-III .....	50
Fig. 4.6 Convergence curve of designed G-FIR lowpass digital filter with group delay in passband at 12 obtained by MOCSA .....	50
Fig. 4.7 Magnitude response, impulse response, the passband and stopband errors of designed G-FIR lowpass digital filter with group delay in passband at 14 obtained by MOCSA .....	52
Fig. 4.8 Magnitude response, impulse response, the passband and stopband errors of designed G-FIR lowpass digital filter with group delay in passband at 14 obtained by NSGA-III .....	53
Fig. 4.9 Convergence curve of designed G-FIR lowpass digital filter with group delay in passband at 14 obtained by MOCSA .....	53
Fig. 4.10 Magnitude response, impulse response, the passband and stopband errors of designed G-FIR highpass digital filter with group delay in passband at 10 obtained by MOCSA .....	56
Fig. 4.11 Magnitude response, impulse response, the passband and stopband errors of designed G-FIR highpass digital filter with group delay in passband at 10 obtained by NSGA-III .....	56
Fig. 4.12 Convergence curve of designed G-FIR highpass digital filter with group delay in passband at 10 obtained by MOCSA .....	57
Fig. 4.13 Magnitude response, impulse response, the passband and stopband errors of designed G-FIR highpass digital filter with group delay in passband at 12 obtained by MOCSA .....	59
Fig. 4.14 Magnitude response, impulse response, the passband and stopband errors of designed G-FIR highpass digital filter with group delay in passband at 12 obtained by NSGA-III .....	60

Fig. 4.15 Convergence curve of designed G-FIR highpass digital filter with group delay in passband at 12 obtained by MOCSA .....	60
Fig. 4.16 Magnitude response, impulse response, the passband and stopband errors of designed G-FIR highpass digital filter with group delay in passband at 14 obtained by MOCSA .....	62
Fig. 4.17 Magnitude response, impulse response, the passband and stopband errors of designed G-FIR highpass digital filter with group delay in passband at 14 obtained by NSGA-III .....	63
Fig. 4.18 Convergence curve of designed G-FIR highpass digital filter with group delay in passband at 14 obtained by MOCSA .....	63
Fig. 4.19 Magnitude response, impulse response, the passband and stopband errors of designed G-FIR bandpass digital filter with group delay in passband at 10 obtained by MOCSA .....	66
Fig. 4.20 Magnitude response, impulse response, the passband and stopband errors of designed G-FIR bandpass digital filter with group delay in passband at 10 obtained by NSGA-III .....	66
Fig. 4.21 Convergence curve of designed G-FIR bandpass digital filter with group delay in passband at 10 obtained by MOCSA .....	67
Fig. 4.22 Magnitude response, impulse response, the passband and stopband errors of designed G-FIR bandpass digital filter with group delay in passband at 12 obtained by MOCSA .....	69
Fig. 4.23 Magnitude response, impulse response, the passband and stopband errors of designed G-FIR bandpass digital filter with group delay in passband at 12 obtained by NSGA-III .....	70
Fig. 4.24 Convergence curve of designed G-FIR bandpass digital filter with group delay in passband at 12 obtained by MOCSA .....	70
Fig. 4.25 Magnitude response, impulse response, the passband and stopband errors of designed G-FIR bandpass digital filter with group delay in passband at 14 obtained by MOCSA .....	72
Fig. 4.26 Magnitude response, impulse response, the passband and stopband errors of designed G-FIR bandpass digital filter with group delay in passband at 14 obtained by NSGA-III .....	73
Fig. 4.27 Convergence curve of designed G-FIR bandpass digital filter with group delay in passband at 14 obtained by MOCSA .....	73
Fig. 4.28 Magnitude response, impulse response, the passband and stopband errors of designed G-FIR bandstop digital filter with group delay in passband at 10 obtained by MOCSA .....	76



Fig. 4.29 Magnitude response, impulse response, the passband and stopband errors of designed G-FIR bandstop digital filter with group delay in passband at 10 obtained by NSGA-III .....	76
Fig. 4.30 Convergence curve of designed G-FIR bandstop digital filter with group delay in passband at 10 obtained by MOCSA .....	77
Fig. 4.31 Magnitude response, impulse response, the passband and stopband errors of designed G-FIR bandstop digital filter with group delay in passband at 12 obtained by MOCSA .....	79
Fig. 4.32 Magnitude response, impulse response, the passband and stopband errors of designed G-FIR bandstop digital filter with group delay in passband at 12 obtained by NSGA-III .....	80
Fig. 4.33 Convergence curve of designed G-FIR bandstop digital filter with group delay in passband at 12 obtained by MOCSA .....	80
Fig. 4.34 Magnitude response, impulse response, the passband and stopband errors of designed G-FIR bandstop digital filter with group delay in passband at 14 obtained by MOCSA .....	82
Fig. 4.35 Magnitude response, impulse response, the passband and stopband errors of designed G-FIR bandstop digital filter with group delay in passband at 14 obtained by NSGA-III .....	83
Fig. 4.36 Convergence curve of designed G-FIR bandstop digital filter with group delay in passband at 14 obtained by MOCSA .....	83
Fig. 5.1 Magnitude, group delay, magnitude errors and group delay errors of designed IIR lowpass digital filter in Example 1 obtained by constrained MOCSA .....	93
Fig. 5.2 Convergence curve of designed IIR lowpass digital filter in Example 1 obtained by constrained MOCSA .....	94
Fig. 5.3 Magnitude, group delay, magnitude errors and group delay errors of designed IIR highpass digital filter in Example 2 obtained by constrained MOCSA .....	97
Fig. 5.4 Convergence curve of designed IIR highpass digital filter in Example 1 obtained by constrained MOCSA .....	97
Fig. 5.5 Magnitude, group delay, magnitude errors and group delay errors of designed IIR bandpass digital filter in Example 3 obtained by constrained MOCSA .....	100
Fig. 5.6 Convergence curve of designed IIR bandpass digital filter in Example 3 obtained by constrained MOCSA .....	100

## LIST OF ABBREVIATIONS/SYMBOLS

FIR	Finite Impulse Response
IIR	Infinite Impulse Response
CSA	Cuckoo Search Algorithm
MOCSA	Multiobjective Cuckoo Search Algorithm
NSGA-III	Non-dominated Sorting Genetic Algorithm III
GA	Genetic Algorithm
DE	Differential Evolution
PSO	Particle Swarm Optimization
LP-FIR	Linear-phase FIR
G-FIR	General FIR

## CHAPTER 1 Introduction to Digital Filters

### 1.1 Introduction

A digital filter is a mathematical system which operates numerical calculation on a discrete-time sampled signal to extract or remove its specific components. A continuous-time analog signal is usually sampled by a certain frequency to be converted into a corresponding set of discrete numerical sequences. These sequences can be operated by filtering processing in a digital filter system to obtain the desired components of a signal.

Compared to analog filters, digital filters contain three representative advantages including:

**Reliability:** The characteristics of digital filters stay stable without disadvantages of aging or tolerance. The coefficients of a designed digital filters can be permanently fixed and used.

**Accuracy:** The word length of filter coefficients can be precisely controlled to assure its accuracy. A longer word length, especially with more decimal parts, leads to higher accuracy. Approximation of ideal sharp cutoff is available if sufficiently long word length is provided.

**Flexibility:** Filtering characteristics are easy to modify by changing the filter coefficients.

With these advantages, digital filters play a very important role in nowadays society. Digital filters are being used in plenty of practical applications, such as communication, electrical systems and astronautic industry, etc.

In view of the finiteness of impulse response, digital filters can be divided into finite impulse response (FIR) digital filters and infinite impulse response (IIR) digital filters. Meanwhile, in view of the filter shape, digital filters mainly include four types called lowpass, highpass, bandpass and bandstop filters.

### 1.2 Analog-to-digital Conversion

For a continuous-time analog signal  $x(t)$ , its sampled signal  $x_s(t)$  with a period of  $T$  seconds can be represented to be a set of numerical impulses that

$$x_s(t) = x(t) \sum_{n=-\infty}^{\infty} \delta(t - nT) = \sum_{n=-\infty}^{\infty} x(nT) \delta(t - nT) \quad (1.1)$$

where  $\delta(t)$  is a unit impulse function that

$$\delta(t) = \begin{cases} 1 & t = 0 \\ 0 & t \neq 0 \end{cases} \quad (1.2)$$

The sampling frequency  $w_s$  is calculated by

$$w_s = \frac{2\pi}{T} \quad (1.3)$$

### 1.2.1 Limitation of Sampling Frequency

An original signal  $x(t)$  can be decomposed into a series of components with different frequencies. Let the highest frequency among those components as  $w_m$ , then the sampling frequency  $w_s$  must follow the below limitation that

$$w_s \geq 2w_m \quad (1.4)$$

### 1.2.2 Normalized Frequency

For the mathematical expression of a digital filter system, the analog frequency  $f$  (in samples/second) is often normalized with respect to the sampling frequency  $f_s$  (in samples/second) such that a normalized digital frequency  $v$  (in radians/sample) can be derived as [1]

$$v = 2f/f_s \quad (1.5)$$

When the previous analog frequency is equal to the sampling frequency that  $f = f_s$ , then we have normalized frequency  $v = 2$  corresponding to  $2\pi$  in radians/sample to represent a cycle of the base band in frequency spectrum.

For convenient visualization due to the periodicity of frequency band with a period of 2 (in normalized frequency), the normalized frequency adopts

$$w = \frac{v}{2}, \quad 0 \leq v \leq 2 \quad (1.6)$$

where the half normalized frequency  $w$  (in half-cycle/sample) is in the range of 0 to 1.

### 1.3 Z-transform to A Digital Filter

A digital filter can be closely expressed by a transfer function in frequency domain for further design, optimization and realization. The transfer function of a digital filter can be calculated by taking the z-transform [1] of its impulse response which is a discrete output signal with an impulse input of magnitude “1” at the beginning input but “0” at all latter inputs to a digital filter.

The impulse response of a digital filter can be expressed as

$$\mathbf{h} = \sum_{n=0}^{\infty} h(nT)\delta(t - nT) \quad (1.7)$$

where  $T$  is the sampling period;  $h(nT)$  represents the  $n$ th sampled discrete impulse response. For simplicity, (1.7) can be simplified as

$$\mathbf{h} = \sum_{n=0}^{\infty} h(n)\delta(t - nT) \quad (1.8)$$

Fig. 1.1 shows the input-filtering-output correspondence of a digital filter for its impulse response.

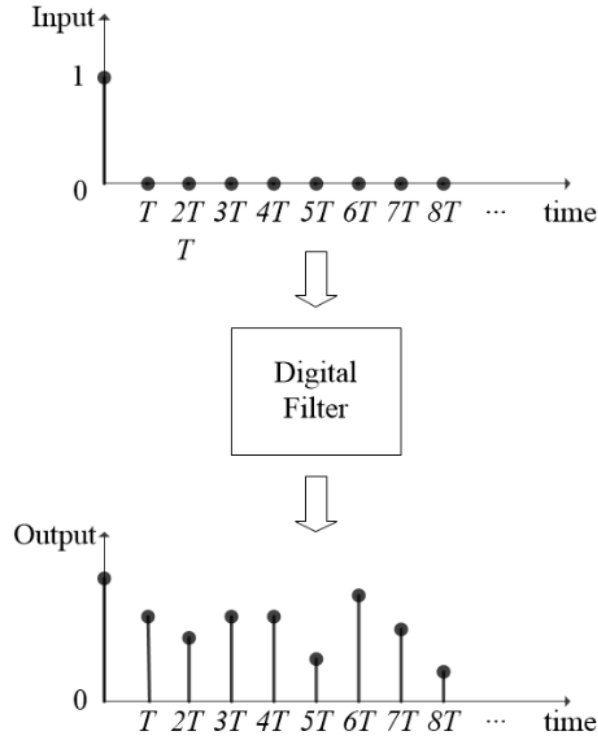


Fig. 1.1 Input-filtering-output correspondence of a digital filter for its impulse response

The z-transform of a digital filter can be expressed as

$$H(w) = \sum_{n=0}^{\infty} h(n)z^{-n} \Big|_{z=e^{jwT}} = \sum_{n=0}^{\infty} h(n)e^{-jnwT} \quad (1.9)$$

Where  $H(w)$  is named as the frequency response of a digital filter.

Normally, the coefficients of the transfer function of a digital filter are real numbers, which result in an even function of frequency for its magnitude response while an odd function for its phase response that [1]

$$|H(-w)| = |H(w)| \quad (1.10)$$

$$\theta(-w) = -\theta(w) \quad (1.11)$$

Hence, a digital filter can be described entirely over the positive half of the baseband  $0 \leq w \leq 1$  (in normalized frequency) rather than the whole baseband  $-1 \leq w \leq 1$ .

## 1.4 Four Main Types of Ideal Filter Shapes [1]

### 1.4.1 Ideal Lowpass Digital Filter

An ideal lowpass digital filter has a magnitude response of one at lower frequencies but that of zero at higher frequencies. The magnitude response of an ideal lowpass digital filter with an ideal cutoff frequency  $w_c$  is defined as

$$|H_{LP}(w)| = \begin{cases} 1 & \text{for } |w| \leq w_c \\ 0 & \text{for } |w| \geq w_c \end{cases} \quad (1.12)$$

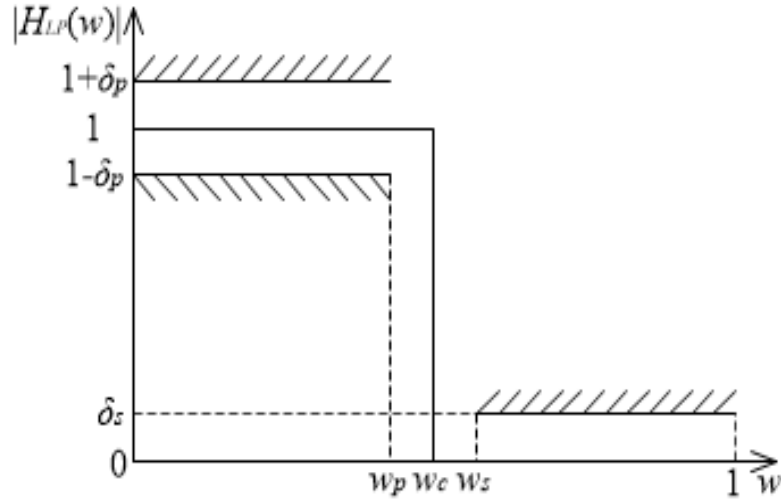


Fig. 1.2 Magnitude response of an ideal lowpass digital filter

The magnitude response of an ideal lowpass digital filter is shown in Fig. 1.2. The magnitude response in passband is limited within the range of  $1 - \delta_p$  to  $1 + \delta_p$  and the magnitude response in stopband is limited within the range of 0 to  $\delta_s$ .  $\delta_p$  represents the acceptable peak error in passband while  $\delta_s$  represents that in stopband. The ideal cutoff frequency shall normally be  $w_c$  but practically the magnitude response can not be strictly sharp at frequency  $w_c$ . Hence, a passband cutoff frequency  $w_p$  and a stopband cutoff frequency  $w_s$  are used to retain a transition band, which formulates a more achievable requirement for approximation.

### 1.4.2 Ideal Highpass Digital Filter

An ideal highpass digital filter has a magnitude response of zero at lower frequencies but that of one at higher frequencies. The magnitude response of an ideal highpass digital filter with an ideal cutoff frequency  $w_c$  is defined as

$$|H_{HP}(w)| = \begin{cases} 0 & \text{for } |w| \leq w_c \\ 1 & \text{for } w_c \leq |w| \leq \pi \end{cases} \quad (1.13)$$

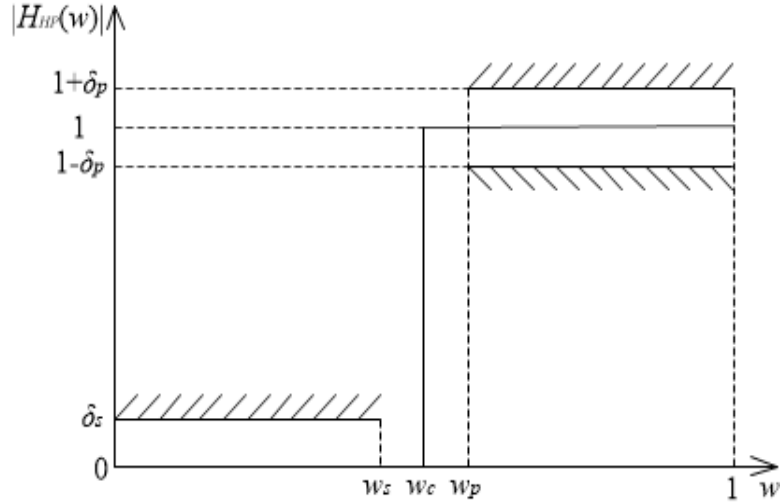


Fig. 1.3 Magnitude response of an ideal highpass digital filter

The magnitude response of an ideal highpass digital filter is shown in Fig. 1.3. The magnitude response in passband is limited within the range of  $1 - \delta_p$  to  $1 + \delta_p$  and the magnitude response in stopband is limited within the range of 0 to  $\delta_s$ .  $\delta_s$  represents the acceptable peak error in stopband while  $\delta_p$  represents that in passband. The ideal cutoff frequency shall normally be  $w_c$  but practically the magnitude response can not be strictly sharp at frequency  $w_c$ . Hence, a stopband cutoff frequency  $w_s$  and a passband cutoff frequency  $w_p$  are used to retain a transition band, which formulates a more achievable requirement for approximation.

### 1.4.3 Ideal Bandpass Digital Filter

An ideal bandpass digital filter has a magnitude response of zero at lower and higher frequencies but that of one at middle frequencies. The magnitude response of an ideal bandpass digital filter with an ideal cutoff frequency  $w_c$  is defined as

$$|H_{BP}(w)| = \begin{cases} 0 & \text{for } |w| \leq w_{c1} \\ 1 & \text{for } w_{c1} \leq |w| \leq w_{c2} \\ 0 & \text{for } w_{c2} \leq |w| \leq \pi \end{cases} \quad (1.14)$$

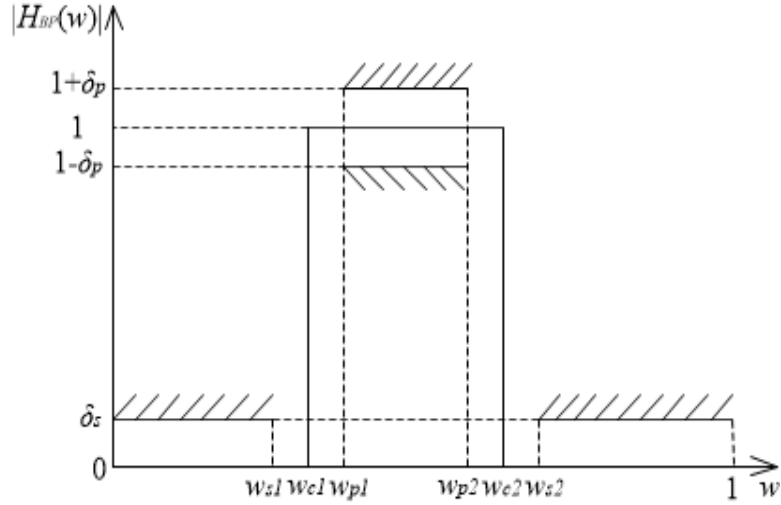


Fig. 1.4 Magnitude response of an ideal bandpass digital filter

The magnitude response of an ideal bandpass digital filter is shown in Fig. 1.4. The magnitude response in passband is limited within the range of  $1 - \delta_p$  to  $1 + \delta_p$  and the magnitude response in stopband is limited within the range of 0 to  $\delta_s$ .  $\delta_s$  represents the acceptable peak error in stopband while  $\delta_p$  represents that in passband. The ideal cutoff frequency shall normally be  $w_{c1}$  and  $w_{c2}$  but practically the magnitude response can not be strictly sharp at both frequencies  $w_{c1}$  and  $w_{c2}$ . Hence, two stopband cutoff frequencies  $w_{s1}$  and  $w_{s2}$  as well as two passband cutoff frequencies  $w_{p1}$  and  $w_{p2}$  are used to retain two transition bands on both sides of passband, which formulates a more achievable requirement for approximation.

#### 1.4.4 Ideal Bandstop Digital Filter

An ideal bandstop digital filter has a magnitude response of one at lower and higher frequencies but that of zero at middle frequencies. The magnitude response of an ideal bandstop digital filter with an ideal cutoff frequency  $w_c$  is defined as

$$|H_{BS}(w)| = \begin{cases} 1 & \text{for } |w| \leq w_{c1} \\ 0 & \text{for } w_{c1} \leq |w| \leq w_{c2} \\ 1 & \text{for } w_{c2} \leq |w| \leq \pi \end{cases} \quad (1.15)$$



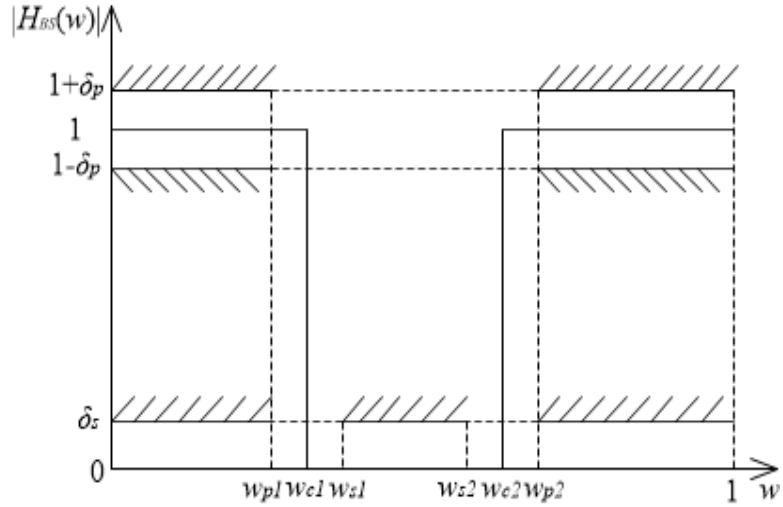


Fig. 1.5 Magnitude response of an ideal bandstop digital filter

The magnitude response of an ideal bandstop digital filter is shown in Fig. 1.5. The magnitude response in passband is limited within the range of  $1 - \delta_p$  to  $1 + \delta_p$  and the magnitude response in stopband is limited within the range of 0 to  $\delta_s$ .  $\delta_p$  represents the acceptable peak error in passband while  $\delta_s$  represents that in stopband. The ideal cutoff frequency shall normally be  $w_{c1}$  and  $w_{c2}$  but practically the magnitude response can not be strictly sharp at both frequencies  $w_{c1}$  and  $w_{c2}$ . Hence, two passband cutoff frequencies  $w_{p1}$  and  $w_{p2}$  as well as two stopband cutoff frequencies  $w_{s1}$  and  $w_{s2}$  are used to retain two transition bands on both sides of stopband, which formulates a more achievable requirement for approximation.

## CHAPTER 2 Introduction to Evolutionary Algorithms

### 2.1 Introduction

In this chapter, a special type of practical problems called optimization problems is discussed. For solving an optimization problem, an effective kind of methods, evolutionary algorithms, is introduced. The basic introduction of evolutionary algorithms includes biological origin, correspondence to computational optimization process and development of some typical evolutionary algorithms. Finally, the basic methodologies of a general evolutionary algorithm are described in detail where Genetic Algorithm (GA) is used as an example for clear illustration.

### 2.2 Optimization Problems

For a computational system, if a specific input is provided, this system would process such input through some computational steps and results in a corresponding output [2]. Sometimes this computational system may be so complicated that it is not easy to describe its computational steps directly. However, once this system is fully configured, it is very simple to obtain the output from a given input. Input, computational steps and output are the three main components of such computational system.

However, some computation systems are mainly forward-going and can not be simply inverted. although it is easy to proceed the input-computation-output process, the reversed operation of finding the input of an obtained output may be very difficult. It may require much more calculations trying to backtrack the original input through a set of reversed computational steps. An optimization problem can be expressed as searching for the potential input which leads to a given output. It aims at identifying a potentially particular solution by a sufficient search in an enormous space of possibilities. Such space of possibilities induces a searching space which contains all possible solutions as well as the optimal one that is being looked for. To find the optimal one in a searching space, exhausting the whole space can be an inevitably successfully method but it is not realistic when the searching space is huge enough.

Hence, some special techniques are required in order to find the optimal solution in a searching space efficiently and accurately. Evolutionary algorithms are currently the most powerful ones in such application.

## 2.3 Evolutionary Algorithms

Evolutionary algorithm is a popular research area in intelligent computing. It derived from biological natural evolution due to the powerful strength that various species overcome natural selection in a fierce competing world for millions of years.

The Darwinian Principles demonstrate the basic process of natural evolution. For a certain species in a living area, a population of individuals are always striving for survival and propagation. The fitness for survival of each individual depends on the combined effect of environmental mildness and its individual abilities of foraging food and protecting itself. That is to say, fitness relates to a possibility of survival and reproduction. An individual with higher fitness is more capable of surviving and have more chance to breed its offspring. As thousands of generations pass, those with higher fitness due to some adaptive characteristics will be predominated and others without such benefits would gradually die out. Then it means evolution on this species happens. Similarly, in a computational optimization problem, a population of possible solutions from the searching space are always being selected depending on their quality on how successful they can solve a problem. A better solution has a higher chance to be kept while a worse one is very possible to be abandoned. The correspondence between a biological evolutionary process and computational optimization process is obvious that an environment corresponds to a problem and each individual in a species population is related to a potential solution. The fitness for a biological individual correlates with the achievement of a solution in an optimization problem. Such correspondence inspired researchers with optimization algorithm based on evolutionary theory.

In the middle of 1960s, Lawrence Jerome Fogel firstly proposed Evolutionary Programming [3] on computer algorithms and established the foundation of the development of further evolutionary algorithms. Afterwards, several advancing evolutionary algorithms based on different mechanisms had been published. A typical one is called Genetic Algorithm (GA) [4], which simulates procedure of inheritance and mutation of genes. There were some prototypes of Genetic Algorithm at that time. Holland summarized all related theories and thus put forward the modern Genetic Algorithm. Besides Genetic Algorithm, other evolutionary algorithms have also gained a lot of achievements. Differential Evolution (DE) [5] and Particle Swarm Optimization (PSO) [6] are the very attractive ones. DE adopted differential operation on the changing of the population while PSO simulates the movement of microscopic particles. Although these algorithms take different theories as simulation models, they share some common points for their methodologies.

## **2.4 Basic Methodologies of An Evolutionary Algorithm**

In this section, basic procedures of a viable evolutionary algorithm are presented. A successful evolutionary algorithm should contain these procedures in adapt to any arbitrary optimization problem. For clear clarification, Genetic Algorithm is taken as an illustration in which each of its steps is illuminated in detail.

### **2.4.1 Configuration of Solutions**

An optimization problem is usually based on a practical application. It often contains abstract concepts or literal descriptions in the original problem context, which requires some suitable operations to transform these information into mathematical expressions so that this problem is capable of being numerical optimized.

First of all, any individual object shall be able to be appropriately converted or mapped into a precise numerical expression corresponding to a specific algorithm, which creates a mapping relation between the original objects and the population of solutions to be optimized [7]. For all types of objects in the context problem, a solution shall contain a number of variables, each of which is prescribed to represent a prescribed type of objects.

Secondly, an efficient optimization should have enough number of competitive solutions to increase the efficiency on searching the optimal one. Those solutions are jointly regarded as a population.

In GA, a solution is called a chromosome and all variables in a solution are named as genes. Rather than the common decimal system, GA adopts binary system to express genes. The number of binary bits for each gene depends on its desired precision. For a given solution, every variable is coded by binary operation and afterward the binary bits of all variables will be configured together as a single-stranded chromosome.

For example, a number “10” in decimal system could be represented as “1010” in binary system. A number with fractional parts can also be binarily coded so long as the numbers of bits for integer part and fractional part has been prescribed respectively in advance. For instance, “14.375” can be represented coded by “1110” for integer part and “011” for fractional part. Then a binary chain “1110011” can be configured to represent the number “14.375” in decimal system, where the former four bits are prescribed for integer part and the rest three bits for fractional part.

If a solution contains two variables “10” and “14.375”, its corresponding chromosome with same precision for each gene can be represented by “10100001110011” where the former seven

bits “1010000” represent “10” with “1010” as integer and “000” as decimal. A detailed representation is shown in Figure 2.1.

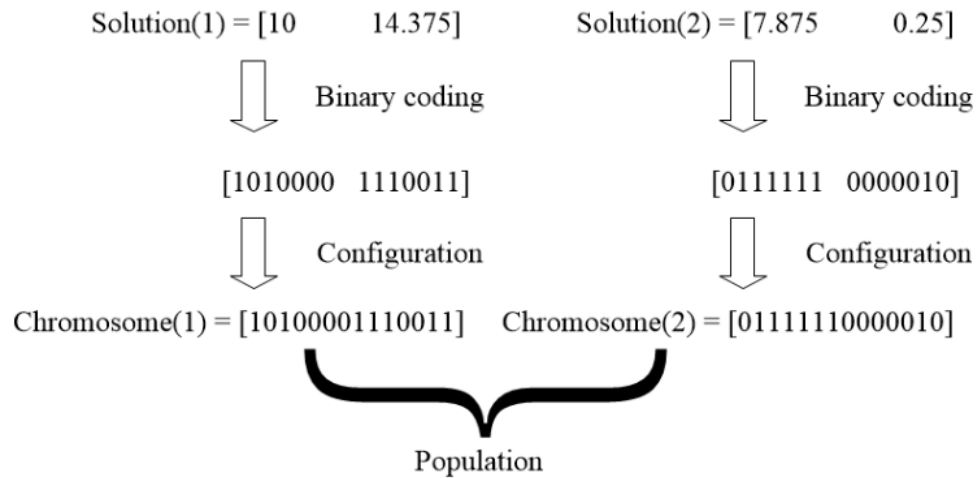


Fig. 2.1 Configuration of a chromosome in GA

#### 2.4.2 Objective Function

An objective function is an indicator which estimates the quality of a solution in an optimization problem. It establishes a target for the whole population to aim at. In other words, all the solutions collectively pursue the objective function and try to satisfy its requirement as possible as they can. Normally, an objective function represents a formulistic measurement by quantizing the levels of quality, which replaces abstract comparison.

In most of the optimization problems, the goal of an optimization procedure is maximizing or minimizing the objective function as much as possible. In a maximization problem, the objective function is always set as fitness function, which aims at searching for the most competitive solution with the largest fitness value. On the other hand, in a minimization problem, the objective function is always set as error function, which tries to find the optimum solution resulting in the least variance from desired quality.

Similarly in GA, an objective function is used to evaluate the qualities of a population of chromosomes. For example, in a minimization problem, a chromosome that leads to a smaller output of the objective function is considered to be better while another chromosome with a larger output is regarded as a worse one.

### 2.4.3 Initialization

It is necessary to provide the first generation of solutions to start a heuristic loop of optimization. Generally, they can be initialized by random values drawn from a random function. However, some special problems might have constraints or principles that help to generate a more applicable set of solutions for initialization at the beginning. This step requires researches to check which initialization method is more suitable.

For initialization of GA, Fig. 2.2 shows how a sample chromosome is initialized by a random function.

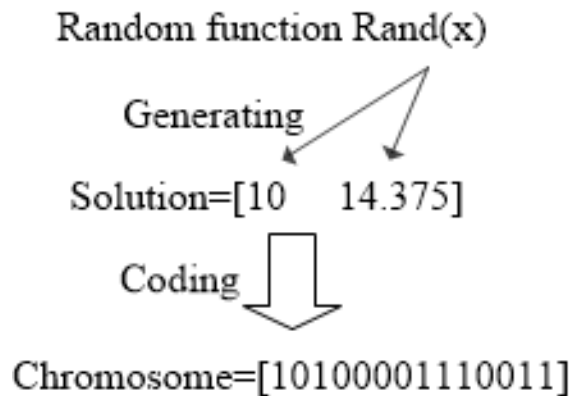


Fig. 2.2 Initialization of a chromosome in GA

### 2.4.4 Elite Selection

Elite Selection is an important process to select elite solutions with better quality as candidates of offspring's parents. A better solution has a larger opportunity to generate its filial solution in order to push quality improvements while a worse one can merely have a rather small possibility to do so [7].

GA introduces a rotatable roulette wheel whose slots are of different sizes based on the proportion of fitness value of every chromosome. Then the cumulative proportional value of each chromosome is calculated according to their indices. Each time when trying to find an elite chromosome, a random number is derived with the range of 0 to 1 representing a random value of proportion. One chromosome with the smallest cumulative proportional value among those larger than the given random number will be pick up as elite. One with a higher fitness value leads to a larger proportion of fitness and a wider range in the cumulative proportional domain. It would have a larger possibility to be selected. It should be noted that each round of elite selection is independent that one chromosome may have more than one time to be selected. A new configured

parent population could have several same chromosomes. This would not cause a problem because subsequent operations are designed to re-diversify the population. Fig 2.3 shows a sample roulette wheel of a population and Fig. 2.4 shows an example of an elite selection.

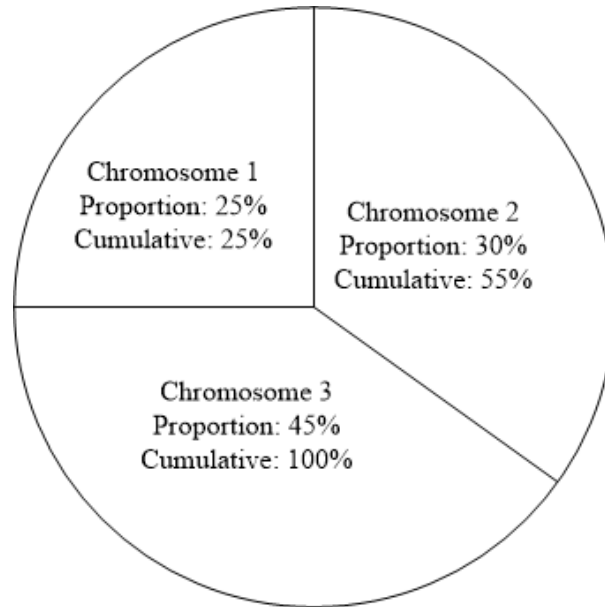


Fig. 2.3 Roulette wheel for a population in GA

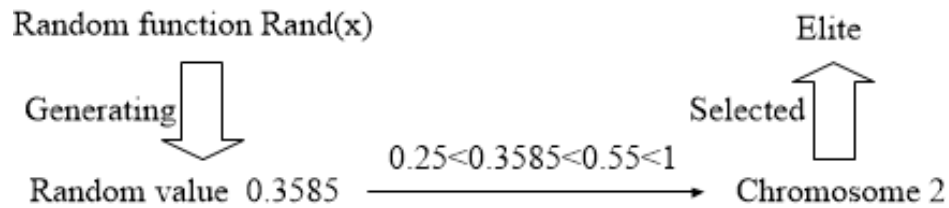


Fig. 2.4 An example of elite selection in GA

## 2.4.5 Variation for New Solutions

To further optimize a population, it is necessary to create new solutions from the existing ones. By taking variation operations on a parent population, new solutions that inherit parts of their parents' characteristics and mutate with some specialities can be generated. In this case, two main steps are required for generating a new population. One represents inheritance of parent solutions while the other represents mutation of new specialities.

### 2.4.5.1 Inheritance

Inheritance of parent solutions is an operation that merge characteristics from two parent solutions into one or two offspring solutions [7]. It decides which two solutions from a population are taken as parents at each time and defines a method to proceed a merging operation. Mostly this

process is based on stochastic probabilities that parent solutions are randomly chosen and the fragments that are being merged on parent solutions are randomly determined. In some algorithms, a parthenogenetic principle is adopted that an offspring only inherits from one parent.

In GA, inheritance of parent solutions is equivalent to crossover on chromosomes. In each time crossover is operated, two random parent chromosomes are fetched and one or two random crossover points is then determined based on some stochastic decisions. A crossover point locates the edge between the reserved parts and merging fragments on a parent chromosome. Afterward, the two fetched parent chromosomes switch their merging fragments to each other and reserve the rest parts. By mean of this, two new offspring chromosomes are generated with characteristics of both of their parents. These operations will cycle until all the parent chromosomes have gone through crossover where each one can only take crossover for one time. A new offspring population after crossover is then created. Fig. 2.5 shows a simple crossover operation with one crossover point on two sample chromosomes.

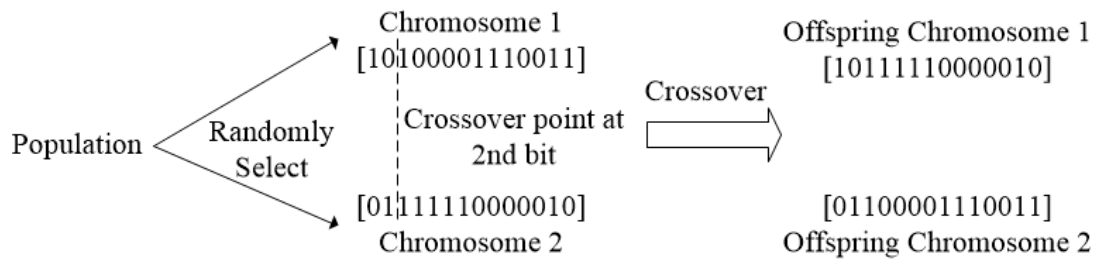


Fig. 2.5 Crossover operation in GA

#### 2.4.5.2 Mutation

Mutation of new specialities applies on a unary solution and produce a mutant offspring with probably slight changes. The mutation operation is always stochastic [7]. The number of mutant points and their locations are both relied on a sequence of independent stochastic decisions. Each location in one solution has an equal probability to mutate, and their decisions are all independent from each other based on their respective deciding variables generated stochastically. The probability of mutation is always small which would merely introduce a little new specialities and reserve most of the characteristics of the original solution. A large probability of mutation might lead to a totally fresh mutant solution with a large number of changes where its original characteristics are swept out.

In GA, each bit of an offspring chromosome after crossover shall go through a mutation-deciding process. A mutant probability is prescribed before mutation-decision. During this process,



each bit is assigned with a random number, called mutation-deciding value, within the range of 0 to 1. These mutation-deciding values are then compared to mutant probability. If the mutation-deciding value of a bit is smaller than mutant probability, this bit will mutate to an opposite binary value such as “0” to “1” or “1” to “0”. Fig. 2.6 shows a simple mutation operation on a sample chromosome.

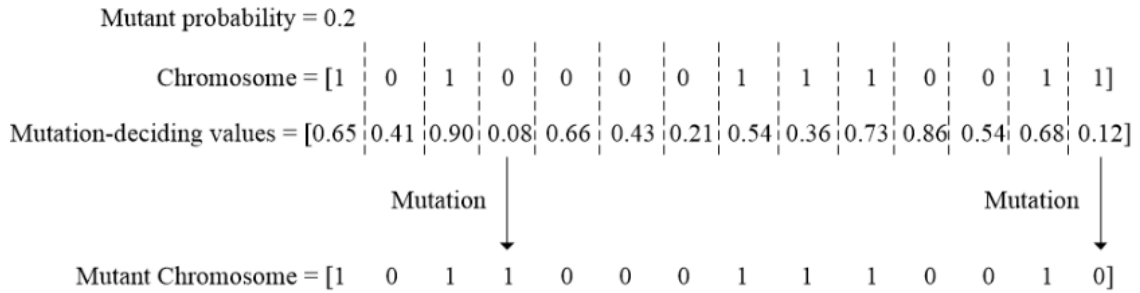


Fig. 2.6 Mutation operation in GA

#### 2.4.6 Survivor Determination

After the offspring solutions are generated, survivor determination which is similar to elite selection will be carried out to determine a population of survivors with the highest quality among a set of candidate solutions. However, survivor determination is rather deterministic that it only concerns about the output of objective function resulting from each candidate solution. In other words, survivor determination is a final evaluation of the output of objective functions related to candidate solutions. Meanwhile, the set of candidate solutions might contain both the original population and its offspring with an objective-based perspective or only reserve the offspring solutions with an age-discriminational view. After survivor determination, the obtained population of survivors will be taken to next generation and a new loop of evolutionary optimization procedure will restart.

GA technically does not have the step of survivor determination. This is not only because the number of offspring chromosomes is exactly the same as that of the original population but also GA employs an age-discriminational view such that only the offspring chromosomes are reserved. During the described steps in sections 2.4.4 and 2.4.5, GA keeps the same population size of original population, selected parent population, offspring population after crossover and offspring population after mutation. In this case, in order to deliver a population with the same population size to the next generation, all the offspring chromosomes will be taken without one missed.

#### **2.4.7 Termination Criterion**

A termination criterion is used to judge whether to stop the optimization procedure in case of endless operations. For a practical optimization problem, a stochastic-based searching evolutionary algorithm can not guarantee to obtain the global optimum. It is possible that an optimization could never reach its goal that the value of objective function never reaches an expected level. This may lead to an endless optimization process where time and resource of calculation are being wasted. In this case, it is necessary to prescribe a termination criterion in advance to prevent possible redundant optimization procedure such as maximum number of iterations or depleted CPU time, variation of the output of objective function within a range of time.

### 3.1 Introduction of CSA

Cuckoo search algorithm (CSA) [8] - [9] is a successful evolutionary optimization method which has been used in a large amount of numerical optimization problems [10]. CSA was first proposed by Xin-She Yang in [8], who described the basic framework and internal approaches of CSA. Afterward, Milan Tuba developed CSA with an a more sophisticated method for searching step [10]. CSA was based on the biological fact that some cuckoo species has a special natural habit of parasitic breeding [10]. For example, the Guira and Ani, will lay their eggs in shared nests, and they may even take others' eggs away so that their own eggs would have more chance to be hatched [11]. CSA was soon implemented on practical engineering problems that its excellent performance on several types of test functions was then presented in [12]. Considering other evolutionary algorithms such as Genetic Algorithm and Particle Swarm Optimization, comparison shows that CSA is superior to these existing algorithms for multimodal objective functions. On one hand, there are fewer parameters to be pre-determined in CSA than in GA and PSO [8]. On the other hand, by implementing a combination of global search and local search, CSA is capable of efficiently traversing the whole searching space and accurately locating the local minima around a local space. Recently, CSA and some other evolutionary algorithms have been successfully applied to the designs of some typical types of FIR digital filters [13] - [15], which has raised people's research interest in this field.

In this chapter, more expansible and updated work on linear phase FIR digital filter design using Cuckoo Search Algorithm is presented. This chapter firstly introduces the detailed description of CSA including algorithm background, methodologies and calculation steps. Then it proposes the configuration process of objective function based on linear-phase type-1 FIR digital filters. Finally, lowpass, highpass, bandpass and bandstop digital filters at different order are taken as design examples and their design results are compared to Park-McClellan Algorithm [16] - [18].

#### 3.1.1 Biological Background of CSA

Cuckoos are some kinds of arboreal birds which have over 100 species. They can be mainly classified into three families such as Cuculidae, Opisthocomidae and Musophagidae. Cuckoos have widely spread around the world from Africa to east Asia. Their main food resource are forest insects but some kinds of molluscs are also accessible [19].

Some cuckoo species are very reproductive due to their special aggressive brooding parasitism. A female cuckoo normally lays around 20 eggs which can be in several different colours and sizes.

Most of the cuckoo don't hatch their own eggs but cheat other host birds for resort [11]. They often target at other host birds, who have just laid eggs. Afterward, cuckoos deposit their own deceitful eggs into the host nest such that the host bird would take their place to hatch the eggs. Moreover, a new born cuckoo chick can be very aggressive to expel the host bird's egg in order to monopolize the host bird's feeding.

### 3.1.2 Biological Rules of CSA for Algorithm Realization

To realize the parasitism behavior of cuckoos into a computer algorithm, the below three rules are regulated as

- (1) Each time a cuckoo only lays one egg, and randomly chooses a foreign nest to deposit;
- (2) High-quality eggs are regarded as best ones and will be inherited to next generations;
- (3) The host nests available is limited, and there is a probability  $p_a \in [0, 1]$  that a cuckoo egg may be discovered by the host bird. In this case, the host bird can either dispose the egg or abandon the nest and build a new nest [19].

### 3.1.3 Levy Flight

For random walking approximation, Levy flights [8] is a very competitive algorithm due to its heavy-tailed probability distribution. Levy flights can be used to generate random numbers with a random direction subjected to a uniform distribution and a step size that is drawn from the Levy distribution [13]. In this case, a symmetric Levy stable distribution is a reliable method to generate step size. By the use of Mantegna algorithm [8], the Levy flight with a parameter  $\beta$  can be calculated by

$$\text{Levy}(\beta) = \frac{u}{|v|^{1/\beta}} \quad (3.1)$$

where  $u$  and  $v$  are drawn from normal distributions [8]. Thus,

$$u = N(0, \sigma_u^2), \quad v = N(0, \sigma_v^2) \quad (3.2)$$

where

$$\sigma_u = \left\{ \frac{\Gamma(1+\beta) \sin(\pi\beta/2)}{\Gamma[(1+\beta)/2] \cdot \beta \cdot 2^{(\beta-1)/2}} \right\}^{1/\beta}, \quad \sigma_v = 1 \quad (3.3)$$

and

$$\Gamma(x) = \int_0^{\infty} e^{-t} t^{x-1} dt \quad (3.4)$$

### 3.1.4 Random Walk

A nest corresponds to an existing solution where several nests provide a number of potential solutions. Each egg in a nest corresponds to a variable in an existing solution while a cuckoo egg corresponds to a new generated value of a specific variable. If a cuckoo egg replaces a host egg, it means a better solution with new updated variables in performance substitutes the old one. Usually, an optimization problem involves a number of variables to be optimized. Thus, Cuckoo search Algorithm has a multiple number of eggs in a nest [13]. A global explorative random walk and local random walk is then applied to simulate the parasitic breeding behavior of cuckoos such that new potentially better solution can be generated and compared. For a  $d$  - dimensional optimization problem, suppose the  $i$ th solution in iteration  $t$  as

$$\mathbf{x}_i(t) = [x_i^1(t) \quad x_i^2(t) \quad \cdots \quad x_i^d(t)]^T \quad (3.5)$$

The global walk for exploring the available searching space can be carried out by using Levy flight described in (3.1) to (3.4) as

$$\mathbf{x}_{i_g}(t) = \mathbf{x}_i(t) + \alpha \times \mathbf{w} \otimes \text{Levy}(\beta) \otimes (\mathbf{x}_i(t) - \mathbf{x}_{best}) \quad (3.6)$$

where  $\alpha$  is a constant scale factor and  $\mathbf{w}$  is a vector comprised of random numbers subjected to the standard normal distribution.  $\text{Levy}(\beta)$  is a vector comprised of a set of numerical values generated by Levy flight. The operator  $\otimes$  means element-wise multiplications.  $\mathbf{x}_{best}$  is the best solution that has ever been obtained from the beginning to current iteration [13].

On the other hand, the local random walk for searching a local minima is generated by

$$\mathbf{x}_{i_l}(t) = \mathbf{x}_i(t) + r \times \mathbf{H}(\epsilon - p_a) \otimes (\mathbf{x}_j(t) - \mathbf{x}_k(t)) \quad (3.7)$$

where  $\mathbf{x}_j(t)$  and  $\mathbf{x}_k(t)$  are two distinct solutions randomly selected from the current population.  $r$  and  $\epsilon$  are random numbers evenly distributed in  $[0, 1]$ .  $\mathbf{H}(\epsilon - p_a)$  is a vector comprised of constant values either at one or zero determined by a Heaviside function that [13]

$$\mathbf{H}(\epsilon - p_a) = \begin{cases} 1 & \epsilon > p_a \\ 0 & \epsilon \leq p_a \end{cases} \quad (3.8)$$

At the end of each iteration, the best solution among  $\mathbf{x}_{i_g}(t)$ ,  $\mathbf{x}_{i_l}(t)$ , and  $\mathbf{x}_i(t)$  is selected as  $\mathbf{x}_i(t + 1)$  for the next iteration.

The pseudocode of CSA is listed in Table 3.1.

Table 3.1 Pseudocode of Cuckoo Search Algorithm

Steps	Description
1	Set $t = 1$ ; Set $\alpha, \beta, p_a$ ; Initialize $\mathbf{x}(1)$ ;
2	Calculate the fitness values of $\mathbf{x}(t)$ ;
3	Generate global walks $\mathbf{x}_g(t)$ and calculate their fitness values;
4	Generate local walks $\mathbf{x}_l(t)$ and calculate their fitness values;
5	Compare $\mathbf{x}_g(t)$ , $\mathbf{x}_l(t)$ , and $\mathbf{x}(t)$ and update $\mathbf{x}(t + 1)$ ;
6	Compare each solution in $\mathbf{x}(t + 1)$ and update $\mathbf{x}_{best}$ ;
7	If convergence criterion is satisfied, optimization procedure is completed; otherwise, return step 2;
8	Output the obtained optimal solution $\mathbf{x}_{best}$ .

### 3.2 Design of Linear-phase Type-1 FIR Digital Filters

An  $N$ th-order linear-phase type-1 FIR (LP-FIR1) filter [1] is an even  $N$  and even symmetrical FIR digital filter consisting of  $(N + 1)$  impulse responses as

$$\mathbf{h} = [h(0), h(1), h(2), \dots, h(n), \dots, h(N - 1), h(N)]^T \quad (3.9)$$

According to its characteristic of even symmetry in impulse responses, it can be found that

$$h(n) = h(N + 1 - n) \text{ for } n = 0, 1, 2, 3, \dots, \left(\frac{N-2}{2}\right) \quad (3.10)$$

The impulse response vector (3.9) can be represented by a distinct coefficient vector  $\mathbf{c}$  which can be expressed as

$$\mathbf{c} = \left[ c_0, c_1, c_2, c_3, \dots, c\left(\frac{N}{2}\right) \right]^T = \left[ h\left(\frac{N}{2}\right), 2h\left(\frac{N}{2} - 1\right), \dots, 2h(2), 2h(1), 2h(0) \right]^T \quad (3.11)$$

The frequency response  $H(w)$  of the LP-FIR1 filter can be expressed as

$$H(w) = e^{-j\left(\frac{N}{2}\right)w} \left\{ h\left(\frac{N}{2} + 1\right) + \sum_{n=0}^{\frac{N-2}{2}} 2h(n) \cos \left[ \left(\frac{N}{2} - n\right) w \right] \right\} = e^{-j\left(\frac{N}{2}\right)w} |H(w)| \quad (3.12)$$

In (3.12), the magnitude response  $|H(w)|$  can be transformed as

$$|H(w)| = \mathbf{c}^T \mathbf{cos}(w) \quad (3.13)$$

$$\mathbf{cos}(w) = \left[ 1 \quad \cos(w) \quad \cos(2w) \quad \cdots \quad \cos\left(\frac{N}{2}w\right) \right]^T \quad (3.14)$$

The design of LP-FIR1 digital filter is to search for an optimal coefficient vector  $\mathbf{c}$  that minimizes the objective function  $e(\mathbf{c})$  in terms of maximum error which is defined as

$$\min_{\mathbf{c}} e(\mathbf{c}) \quad (3.15)$$

where

$$e(\mathbf{c}) = \max_{\text{for } w_i \in \Omega_I} | |H(w_i)| - H_d(w_i) | \quad (3.16)$$

where  $H_d(w_i)$  is the ideal magnitude response of the desired LP-FIR1 digital filter;  $\Omega_I$  is the union of band of interest including both passband and stopband.

For example, for a lowpass digital filter, the objective function  $e(\mathbf{c})$  can be further decomposed into error functions of magnitude in passband and stopband respectively as

$$e(\mathbf{c}) = \max(e_p(\mathbf{c}), e_s(\mathbf{c})) \quad (3.17)$$

When operating on a union set of discrete sampling frequency points,  $w \in \Omega_I = [0, w_p] \cup [w_s, \pi]$ , the two error functions of magnitude response can be approximated by

$$e_p(\mathbf{c}) = \max_{I_{p1} \text{ to } I_{p2}} | |H(\mathbf{c}, w_i)| - H_d(w_i) | \quad (3.18)$$

for  $0 \leq w_i \leq w_p$

$$e_s(\mathbf{c}) = \max_{I_{s1} \text{ to } I_{s2}} | |H(\mathbf{c}, w_i)| - H_d(w_i) | \quad (3.19)$$

for  $w_s \leq w_i \leq \pi$

where  $H_d(w_i) = 1$  in passband and  $H_d(w_i) = 0$  in stopband.

Similarly, the objective function  $e(\mathbf{c})$  of a highpass digital filter can be expressed as

$$e(\mathbf{c}) = \max(e_s(\mathbf{c}), e_p(\mathbf{c})) \quad (3.20)$$

The objective function  $e(\mathbf{c})$  of a bandpass digital filter can be expressed as

$$e(\mathbf{c}) = \max(e_{p1}(\mathbf{c}), e_s(\mathbf{c}), e_{p2}(\mathbf{c})) \quad (3.21)$$

The objective function  $e(\mathbf{c})$  of a bandstop digital filter can be expressed as

$$e(\mathbf{c}) = \max(e_{s1}(\mathbf{c}), e_p(\mathbf{c}), e_{s2}(\mathbf{c})) \quad (3.22)$$

### 3.3 Design Examples and Results

In this section, linear-phase type-1 FIR lowpass, highpass, bandpass and bandstop digital filters of order 24 and 48 are designed. All the filter coefficients are initialized randomly within a specific range of lower bound and upper bound. Design results are compared favourably to Park-McClellan Algorithm.

The linear-phase type-1 FIR lowpass, highpass, bandpass and bandstop digital filter specifications, and CSA parameters are listed in Table 3.2. Lowpass, highpass, bandpass and bandstop normalized cutoff frequencies are specified in Table 3.3. The adopt frequency grids for optimization and for evaluating the peak errors of magnitude are shown in Table 3.4. The design optimization is terminated when the value of the objective function from the best solution stays unchanged during the last 10% continuous iterations. All the optimization designs are carried out using an Intel(R) Core(TM) i7-5500U CPU, 2.40 GHz with 8GB RAM laptop computer.

Table 3.2 Filter specifications and CSA parameters

Symbol	Description	LP		HP		BP		BS	
$c_k^{[U]}$	Upper bound of filter coefficients	0.45		0.675		0.45		1.275	
$c_k^{[L]}$	Lower bound of filter coefficients	-0.95		-0.45		-0.33		-0.185	
$N$	Filter order	24	48	24	48	24	48	24	48
$N_c$	Number of distinct coefficients	13	25	13	25	13	25	13	25
$\tau$	Group delay	12	24	12	24	12	24	12	24
$P_C$	CSA population size	25		25		25		25	
$\beta$	CSA parameter	1.5		1.5		1.5		1.5	
$\alpha$	CSA parameter	0.01		0.01		0.01		0.01	
$p_a$	CSA parameter	0.25		0.25		0.25		0.25	

Table 3.3 LP-FIR1 digital filter cutoff frequencies

	$w_{s1}$	$w_{p1}$	$w_{p2}$	$w_{s2}$



LP	$0.4\pi$	$0.3\pi$	-	-
HP	$0.45\pi$	$0.55\pi$	-	-
BP	$0.25\pi$	$0.35\pi$	$0.6\pi$	$0.7\pi$
BS	$0.4\pi$	$0.3\pi$	$0.65\pi$	$0.55\pi$

Table 3.4 Frequency grids for LP-FIR1 digital filter design

Optimization	$F_o = [0: 0.001: 1]$
Peak magnitude error evaluation	$F_{mag} = [0: 0.001: 1]$

### 3.3.1 Lowpass Digital Filters

#### 3.3.1.1 24th-order Lowpass Digital Filter

The filter coefficients of obtained by CSA are listed in Table 3.5 and design results are listed in Table 3.6. The computational record in terms of CPU seconds and number of iterations for reaching convergence are listed in Table 3.7. Plots of the magnitude response, impulse response, the passband and stopband errors of the designed lowpass digital filters are shown in Fig. 3.1, and its convergence curve is plotted in Fig. 3.2.

Table 3.5 Coefficients of 24th-order LP-FIR1 lowpass digital filter

$h(n)$	Values	$h(n)$	Values
$h(0) = h(24)$	0.015602222754826	$h(7) = h(17)$	-0.040713665580239
$h(1) = h(23)$	-0.019662001462534	$h(8) = h(16)$	-0.071172492458704
$h(2) = h(22)$	-0.026736838577082	$h(9) = h(15)$	-0.016293605259372
$h(3) = h(21)$	-0.014437347989756	$h(10) = h(14)$	0.126601433359116
$h(4) = h(20)$	0.016516376274050	$h(11) = h(13)$	0.282601413553978
$h(5) = h(19)$	0.036242108746287	$h(12)$	0.350222576870181
$h(6) = h(18)$	0.014078010180280		

Table 3.6 Design results of 24th-order LP-FIR1 lowpass digital filter

Algorithm	Peak (Passband)	Peak (Stopband)
CSA	0.044526196060964	0.044690412237109
PM	0.044667506785979	0.044738246884825

Table 3.7 Computational record of 24th-order LP-FIR1 lowpass digital filter

CPU Seconds	Iteration
122.492415	678099

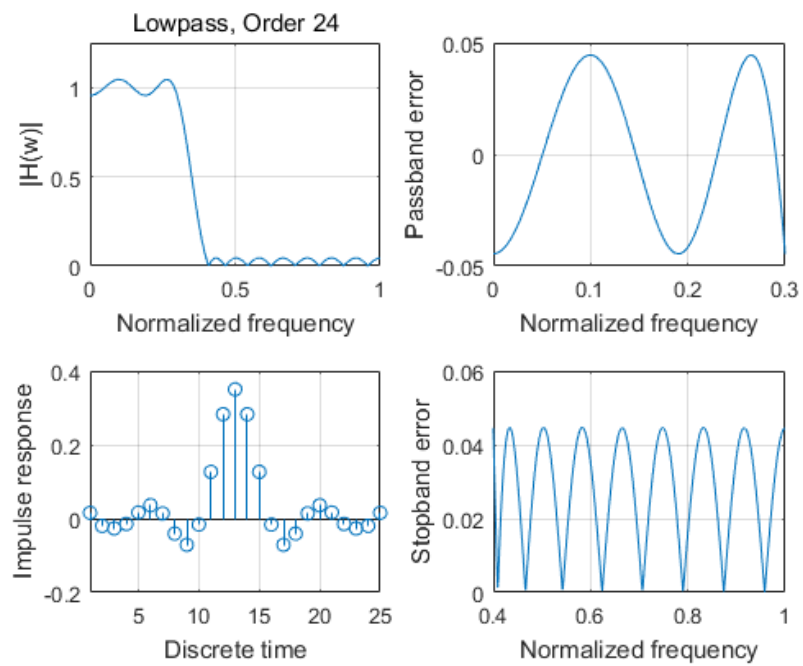


Fig. 3.1 Magnitude response, impulse response, the passband and stopband errors of designed 24th-order LP-FIR1 lowpass digital filter

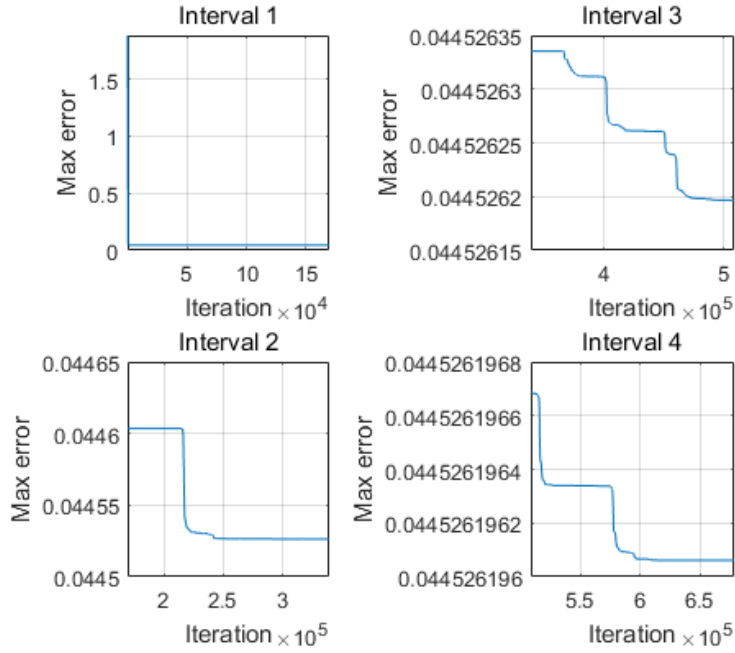


Fig. 3.2 Convergence curve of designed 24th-order LP-FIR1 lowpass digital filter

### 3.3.1.2 48th-order Lowpass Digital Filter

The filter coefficients of obtained by CSA are listed in Table 3.8 and design results are listed in Table 3.9. The computational record in terms of CPU seconds and number of iterations for reaching convergence are listed in Table 3.10. Plots of the magnitude response, impulse response, the passband and stopband errors of the designed lowpass digital filters are shown in Fig. 3.3, and its convergence curves is plotted in Fig. 3.4.

Table 3.8 Coefficients of 48th-order LP-FIR1 lowpass digital filter

$h(n)$	Values	$h(n)$	Values
$h(0) = h(48)$	0.002844114639424	$h(13) = h(35)$	-0.009516655396541
$h(1) = h(47)$	-0.000302320733241	$h(14) = h(34)$	-0.024552215283222
$h(2) = h(46)$	-0.003227868508635	$h(15) = h(33)$	-0.013113103176163
$h(3) = h(45)$	-0.004071333103923	$h(16) = h(32)$	0.019738384929840
$h(4) = h(44)$	-0.000346727330479	$h(17) = h(31)$	0.039589845700028
$h(5) = h(43)$	0.005063411205536	$h(18) = h(30)$	0.014991254801521
$h(6) = h(42)$	0.005609968761438	$h(19) = h(29)$	-0.042230715098655
$h(7) = h(41)$	-0.001359959309635	$h(20) = h(28)$	-0.072755728918604
$h(8) = h(40)$	-0.009413302078598	$h(21) = h(27)$	-0.016373908625510

$h(9) = h(39)$	-0.008230816903790	$h(22) = h(26)$	0.127344674773362
$h(10) = h(38)$	0.004057999776199	$h(23) = h(25)$	0.282872287617703
$h(11) = h(37)$	0.015388182625822	$h(24)$	0.350020414205919
$h(12) = h(36)$	0.010700387342576		

Table 3.9 Design results of 48th-order LP-FIR1 lowpass digital filter

Algorithm	Peak (Passband)	Peak (Stopband)
CSA	0.004605917394988	0.004617517614943
PM	0.004630930079829	0.004620232061237

Table 3.10 Computational record of 48th-order LP-FIR1 lowpass digital filter

CPU Seconds	Iteration
5065.454939	9637933

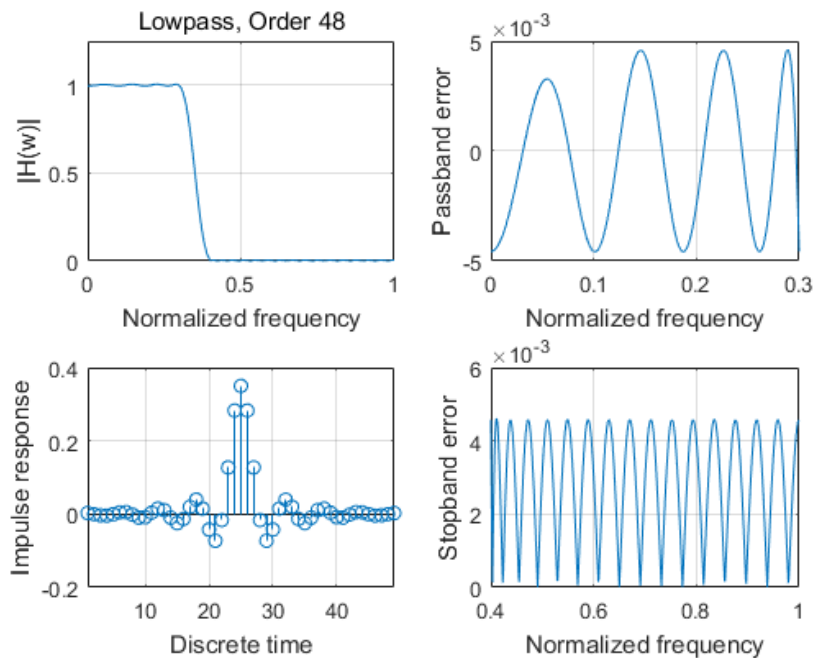


Fig. 3.3 Magnitude response, impulse response, the passband and stopband errors of designed 48th-order LP-FIR1 lowpass digital filter

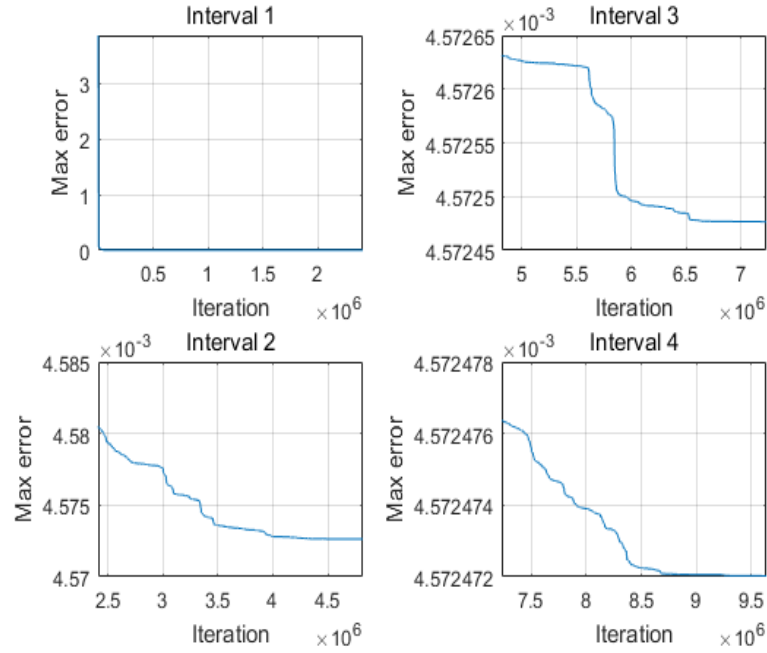


Fig. 3.4 Convergence curve of designed 48th-order LP-FIR1 lowpass digital filter

### 3.3.2 Highpass Digital Filters

#### 3.3.2.1 24th-order Highpass Digital Filter

The filter coefficients of obtained by CSA are listed in Table 3.11 and design results are listed in Table 3.12. The computational record in terms of CPU seconds and number of iterations for reaching convergence are listed in Table 3.13. Plots of the magnitude response, impulse response, the passband and stopband errors of the designed highpass digital filters are shown in Fig. 3.5, and its convergence curve is plotted in Fig. 3.6.

Table 3.11 Coefficients of 24th-order LP-FIR1 highpass digital filter

$h(n)$	Values	$h(n)$	Values
$h(0) = h(24)$	0.00000000042704	$h(7) = h(17)$	-0.057605481098976
$h(1) = h(23)$	0.032847061482731	$h(8) = h(16)$	0.00000000082169
$h(2) = h(22)$	0.00000000070915	$h(9) = h(15)$	0.102388522740894
$h(3) = h(21)$	-0.025312253861246	$h(10) = h(14)$	0.00000000082119
$h(4) = h(20)$	0.00000000054528	$h(11) = h(13)$	-0.317056595714510
$h(5) = h(19)$	0.037271286797722	$h(12)$	0.50000000076811
$h(6) = h(18)$	0.00000000051803		

Table 3.12 Design results of 24th-order LP-FIR1 highpass digital filter

Algorithm	Peak (Stopband)	Peak (Passband)
CSA	0.045082367262490	0.045082367061960
PM	0.045265488163783	0.045062116544123

Table 3.13 Computational information of 24th-order LP-FIR1 highpass digital filter

CPU Seconds	Iteration
46.716542	166583

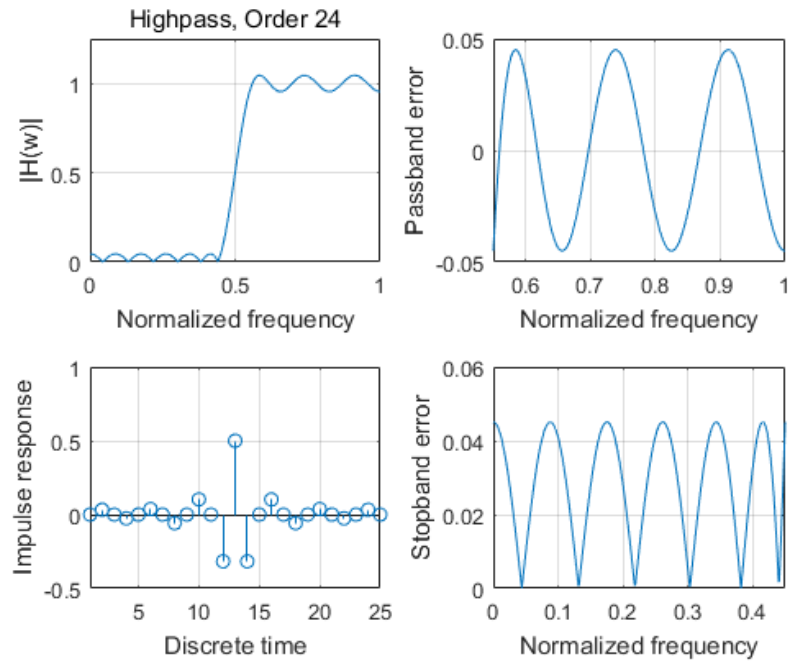


Fig. 3.5 Magnitude response, impulse response, the passband and stopband errors of designed 24th-order LP-FIR1 highpass digital filter

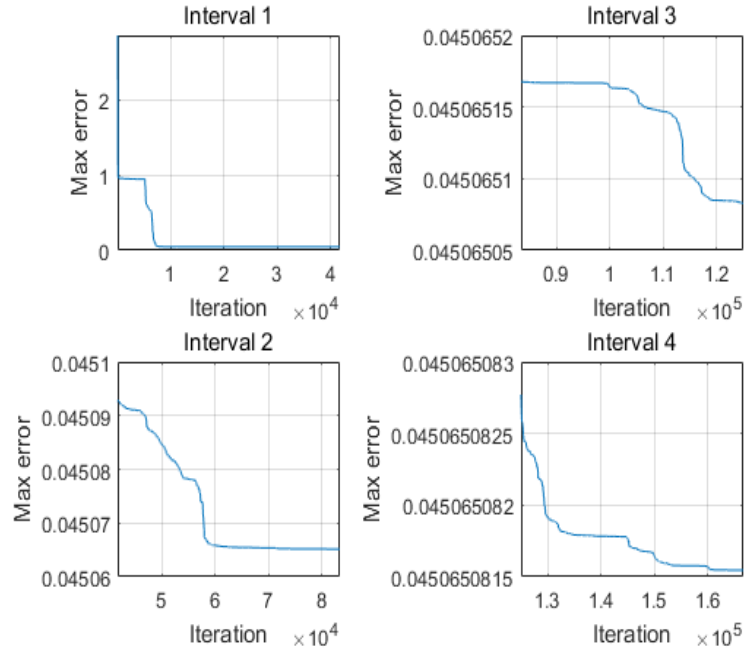


Fig. 3.6 Convergence curve of designed 24th-order LP-FIR1 highpass digital filter

### 3.3.2.2 48th-order Highpass Digital Filter

The filter coefficients of obtained by CSA are listed in Table 3.14 and design results are listed in Table 3.15. The computational record in terms of CPU seconds and number of iterations for reaching convergence are listed in Table 3.16. Plots of the magnitude response, impulse response, the passband and stopband errors of the designed highpass digital filters are shown in Fig. 3.7, and its convergence curve is plotted in Fig. 3.8.

Table 3.14 Coefficients of 48th-order LP-FIR1 highpass digital filter

$h(n)$	Values	$h(n)$	Values
$h(0) = h(48)$	0.000000000274744	$h(13) = h(35)$	0.020943715816087
$h(1) = h(47)$	0.004097749652286	$h(14) = h(34)$	-0.000000000014083
$h(2) = h(46)$	0.000000000378644	$h(15) = h(33)$	-0.028567287969460
$h(3) = h(45)$	-0.003950222433274	$h(16) = h(32)$	0.000000000212389
$h(4) = h(44)$	0.000000000181198	$h(17) = h(31)$	0.040014057993254
$h(5) = h(43)$	0.005811843735690	$h(18) = h(30)$	0.000000000157791
$h(6) = h(42)$	-0.000000000166138	$h(19) = h(29)$	-0.059670733860250
$h(7) = h(41)$	-0.008232450009601	$h(20) = h(28)$	0.000000000045528
$h(8) = h(40)$	-0.000000000233253	$h(21) = h(27)$	0.103671515990105

$h(9) = h(39)$	0.011371368281609	$h(22) = h(26)$	-0.000000000333849
$h(10) = h(38)$	-0.000000000256773	$h(23) = h(25)$	-0.317492688648257
$h(11) = h(37)$	-0.015473106864559	$h(24)$	0.499999999619962
$h(12) = h(36)$	-0.000000000081171		

Table 3.15 Design results of 48th-order LP-FIR1 highpass digital filter

Algorithm	Peak (Stopband)	Peak (Passband)
CSA	0.005058774840816	0.005058774817072
PM	0.005073979553563	0.005073979553563

Table 3.16 Computational information of 48th-order LP-FIR1 highpass digital filter

CPU Seconds	Iteration
13757	30000000

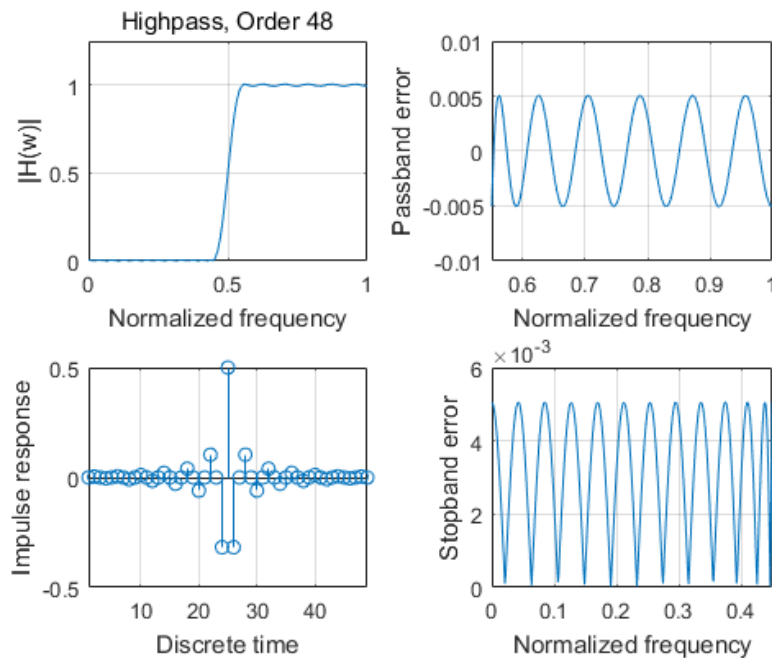


Fig. 3.7 Magnitude response, impulse response, the passband and stopband errors of designed 48th-order LP-FIR1 highpass digital filter



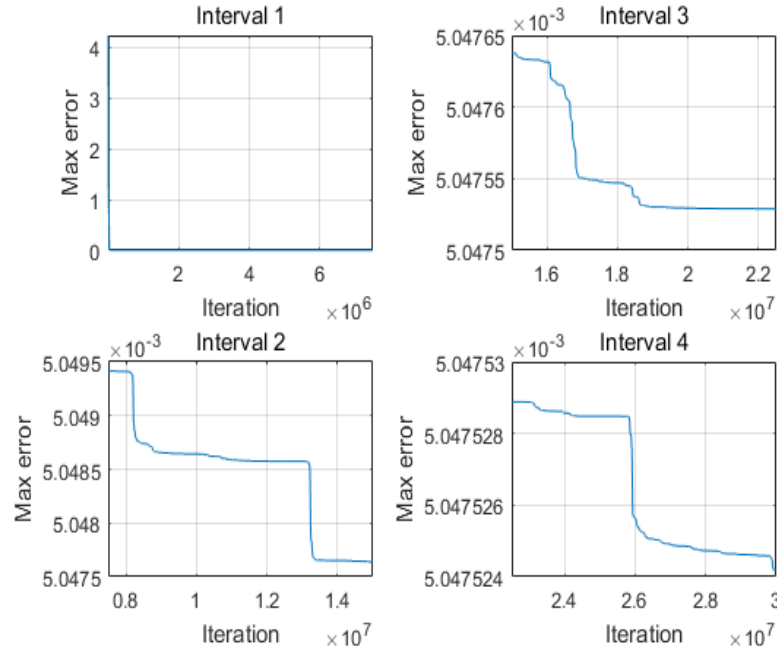


Fig. 3.8 Convergence curve of designed 48th-order LP-FIR1 highpass digital filter

### 3.3.3 Bandpass Digital Filters

#### 3.3.3.1 24th-order Bandpass Digital Filter

The filter coefficients of obtained by CSA are listed in Table 3.17 and design results are listed in Table 3.18. The computational record in terms of CPU seconds and number of iterations for reaching convergence are listed in Table 3.19. Plots of the magnitude response, impulse response, the passband and stopband errors of the designed bandpass digital filters are shown in Fig. 3.9, and its convergence curve is plotted in Fig. 3.10.

Table 3.17 Coefficients of 24th-order LP-FIR1 bandpass digital filter

$h(n)$	Values	$h(n)$	Values
$h(0) = h(24)$	0.005873070364878	$h(7) = h(17)$	0.015522073715187
$h(1) = h(23)$	-0.003134642021242	$h(8) = h(16)$	0.114031977173706
$h(2) = h(22)$	0.023197161313002	$h(9) = h(15)$	-0.047450432177461
$h(3) = h(21)$	-0.043449803354569	$h(10) = h(14)$	-0.275836858534444
$h(4) = h(20)$	-0.053830578635584	$h(11) = h(13)$	0.025635431280225
$h(5) = h(19)$	0.023085898119753	$h(12)$	0.350012567395827
$h(6) = h(18)$	0.011558944930731		

Table 3.18 Design results of 24th-order LP-FIR1 bandpass digital filter

Algorithm	Peak (Stopband1)	Peak (Passband)	Peak (Stopband2)
CSA	0.059582949496635	0.059582949496635	0.059582949496635
PM	0.059543404896685	0.059740130212373	0.059753172716330

Table 3.19 Computational record of 24th-order LP-FIR1 bandpass digital filter

CPU Seconds	Iteration
36.923787	103270

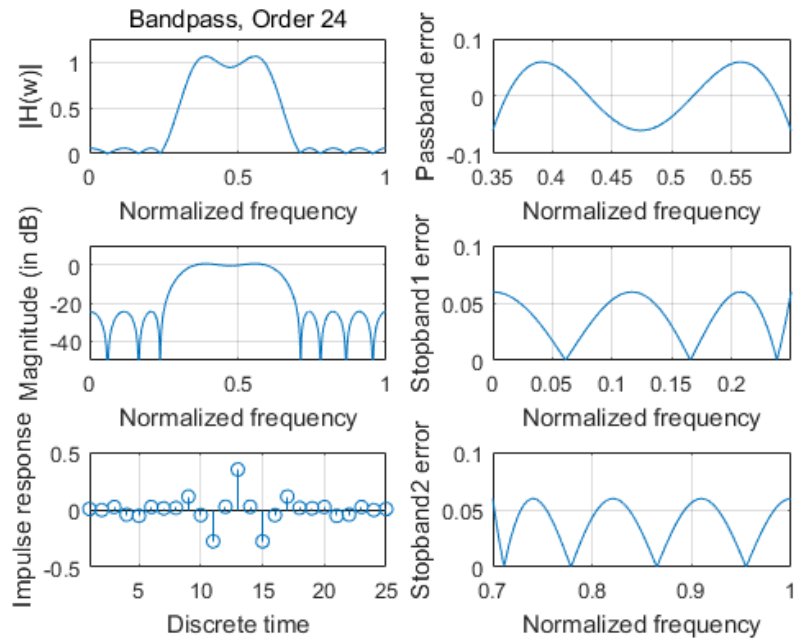


Fig. 3.9 Magnitude response, impulse response, the passband and stopband errors of designed 24th-order LP-FIR1 bandpass digital filter

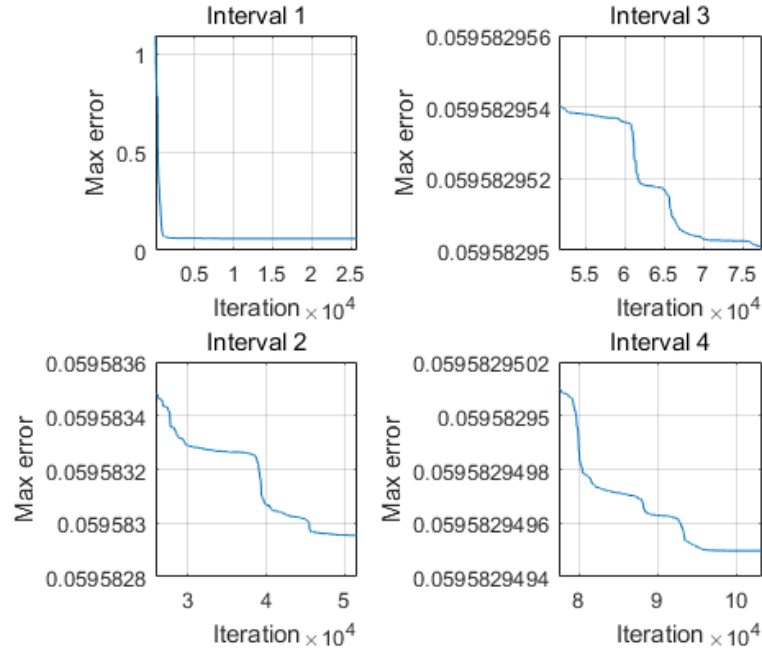


Fig. 3.10 Convergence curve of designed 24th-order LP-FIR1 bandpass digital filter

### 3.3.3.2 48th-order Bandpass Digital Filter

The filter coefficients of obtained by CSA are listed in Table 3.20 and design results are listed in Table 3.21. The computational record in terms of CPU seconds and number of iterations for reaching convergence are listed in Table 3.22. Plots of the magnitude response, impulse response, the passband and stopband errors of the designed bandpass digital filters are shown in Fig. 3.11, and its convergence curve is plotted in Fig. 3.12.

Table 3.20 Coefficients of 48th-order LP-FIR1 bandpass digital filter

$h(n)$	Values	$h(n)$	Values
$h(0) = h(48)$	-0.000338755405739	$h(13) = h(35)$	0.007146131165616
$h(1) = h(47)$	-0.001394990601093	$h(14) = h(34)$	0.023893413054746
$h(2) = h(46)$	-0.000223744629716	$h(15) = h(33)$	-0.035692925449260
$h(3) = h(45)$	-0.007159205454750	$h(16) = h(32)$	-0.051306155900774
$h(4) = h(44)$	0.000126376524088	$h(17) = h(31)$	0.027129935902712
$h(5) = h(43)$	0.009423794361884	$h(18) = h(30)$	0.013623715630051
$h(6) = h(42)$	0.000942183133334	$h(19) = h(29)$	0.017359164043243
$h(7) = h(41)$	0.000997036008702	$h(20) = h(28)$	0.117064836295993
$h(8) = h(40)$	0.003276936087726	$h(21) = h(27)$	-0.048295198569917
$h(9) = h(39)$	-0.018635547345007	$h(22) = h(26)$	-0.277215413086399

$h(10) = h(38)$	-0.011474111235669	$h(23) = h(25)$	0.026104018784016
$h(11) = h(37)$	0.019676219379267	$h(24)$	0.350279305243349
$h(12) = h(36)$	0.006491066057793		

Table 3.21 Design results of 48th-order LP-FIR1 bandpass digital filter

Algorithm	Peak (Stopband1)	Peak (Passband)	Peak (Stopband2)
CSA	0.006683137272674	0.006683137272728	0.006683137272208
PM	0.006700546942702	0.006700259956930	0.006699594292273

Table 3.22 Computational record of 48th-order LP-FIR1 bandpass digital filter

CPU Seconds	Iteration
7598.309211	13742183

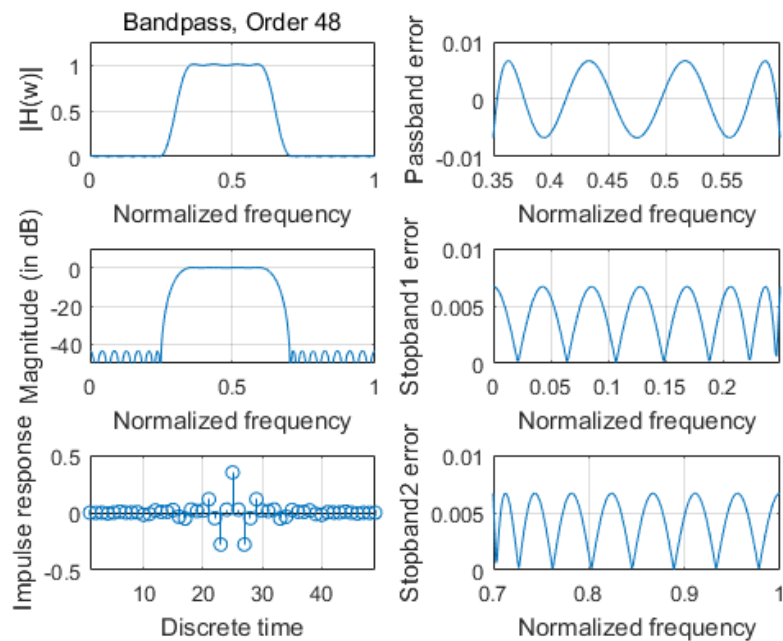


Fig. 3.11 Magnitude response, impulse response, the passband and stopband errors of designed 48th-order LP-FIR1 bandpass digital filter

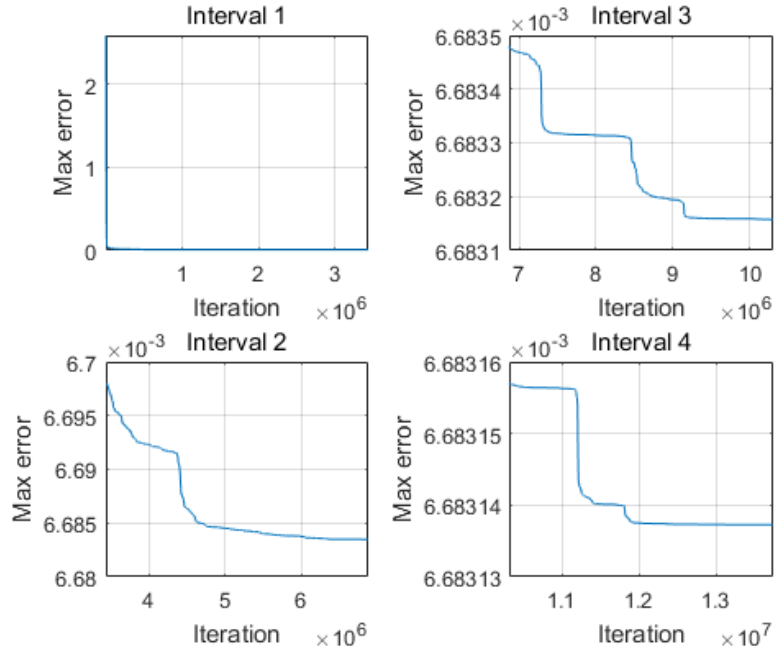


Fig. 3.12 Convergence curve of designed 48th-order LP-FIR1 bandpass digital filter

### 3.3.4 Bandstop Digital Filters

#### 3.3.4.1 24th-order Bandstop Digital Filter

The filter coefficients of obtained by CSA are listed in Table 3.23 and design results are listed in Table 3.24. The computational record in terms of CPU seconds and number of iterations for reaching convergence are listed in Table 3.25. Plots of the magnitude response, impulse response, the passband and stopband errors of the designed bandstop digital filters are shown in Fig. 3.13, and its convergence curve is plotted in Fig. 3.14.

Table 3.23 Coefficients of 24th-order LP-FIR1 bandstop digital filter

$h(n)$	Values	$h(n)$	Values
$h(0) = h(24)$	0.016290826914678	$h(7) = h(17)$	-0.041240368449089
$h(1) = h(23)$	-0.033316831641946	$h(8) = h(16)$	-0.145571615427783
$h(2) = h(22)$	-0.023409617184792	$h(9) = h(15)$	0.044425868837146
$h(3) = h(21)$	0.007020847526987	$h(10) = h(14)$	0.223958170306042
$h(4) = h(20)$	-0.003286142155914	$h(11) = h(13)$	-0.019156949837817
$h(5) = h(19)$	0.015749009775587	$h(12)$	0.744118856875453
$h(6) = h(18)$	0.059959014164242		

Table 3.24 Design results of 24th-order LP-FIR1 bandstop digital filter

Algorithm	Peak (Passband1)	Peak (Stopband)	Peak (Passband2)
CSA	0.053091981387982	0.053045049123189	0.053108368921888
PM	0.053134613120994	0.053022952607939	0.053208962863983

Table 3.25 Computational record of 24th-order LP-FIR1 bandstop digital filter

CPU Seconds	Iteration
19.038659	81936

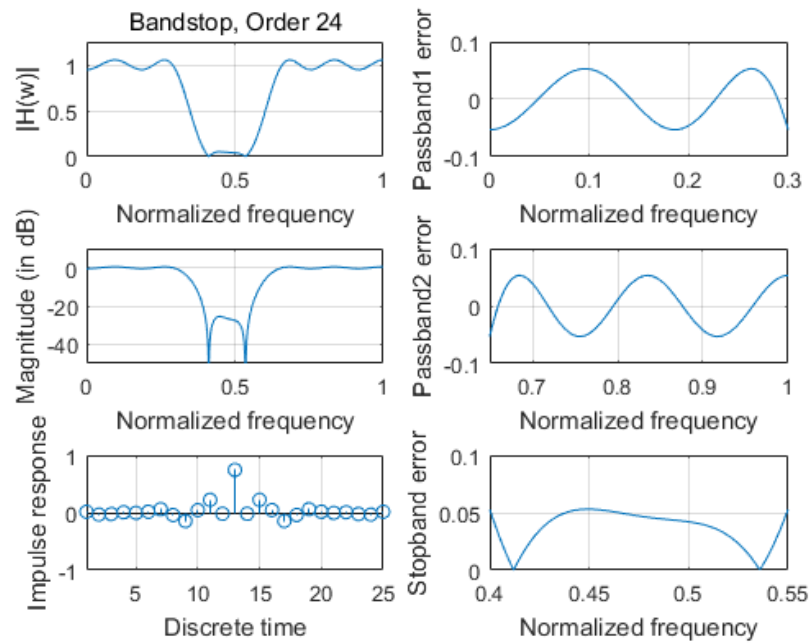


Fig. 3.13 Magnitude response, impulse response, the passband and stopband errors of designed 24th-order LP-FIR1 bandstop digital filter

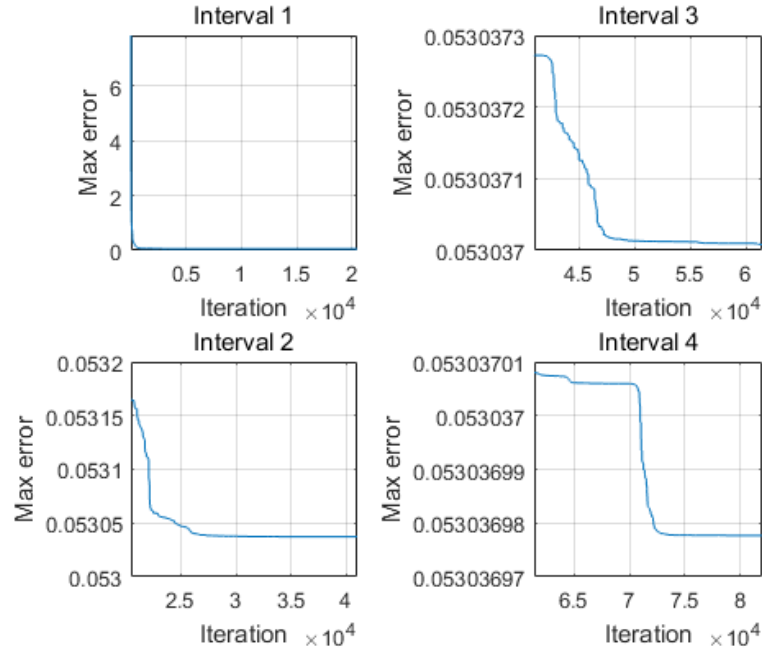


Fig. 3.14 Convergence curve of designed 24th-order LP-FIR1 bandstop digital filter

### 3.3.4.2 48th-order Bandstop Digital Filter

The filter coefficients of obtained by CSA are listed in Table 3.26 and design results are listed in Table 3.27. The computational record in terms of CPU seconds and number of iterations for reaching convergence are listed in Table 3.28. Plots of the magnitude response, impulse response, the passband and stopband errors of the designed bandstop digital filters are shown in Fig. 3.15, and its convergence curve is plotted in Figs. 3.16.

Table 3.26 Coefficients of 48th-order LP-FIR1 bandstop digital filter

$h(n)$	Values	$h(n)$	Values
$h(0) = h(48)$	0.003908043927805	$h(13) = h(35)$	0.009868794246921
$h(1) = h(47)$	-0.001718752622614	$h(14) = h(34)$	-0.023669026618227
$h(2) = h(46)$	-0.005084946782733	$h(15) = h(33)$	-0.040010888786738
$h(3) = h(45)$	-0.000274613515775	$h(16) = h(32)$	0.039306415789148
$h(4) = h(44)$	-0.000069566013098	$h(17) = h(31)$	0.063635673883198
$h(5) = h(43)$	-0.000610392551288	$h(18) = h(30)$	-0.031177716768294
$h(6) = h(42)$	0.009387956456829	$h(19) = h(29)$	-0.043293064617811
$h(7) = h(41)$	0.003609177075744	$h(20) = h(28)$	0.000375177899855
$h(8) = h(40)$	-0.018809927272693	$h(21) = h(27)$	-0.076051548276449

$h(9) = h(39)$	-0.008489112279614	$h(22) = h(26)$	0.034500875604178
$h(10) = h(38)$	0.017470998789566	$h(23) = h(25)$	0.584390536388135
$h(11) = h(37)$	0.006788182462449	$h(24)$	-0.049676563579217
$h(12) = h(36)$	-0.000945273437220		

Table 3.27 Design results of 48th-order LP-FIR1 bandstop digital filter

Algorithm	Peak (Passband1)	Peak (Stopband)	Peak (Passband2)
CSA	0.005042621679150	0.005029606571997	0.005057575531740
PM	0.005861705990205	0.005874023389562	0.005866614940886

Table 3.28 Computational record of 48th-order LP-FIR1 bandstop digital filter

CPU Seconds	Iteration
5438.547879	13083193

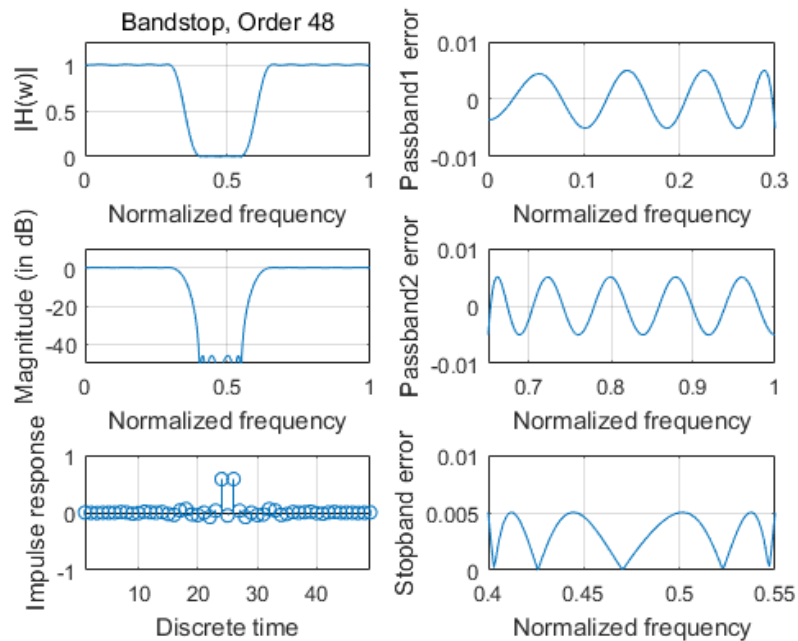


Fig. 3.15 Magnitude response, impulse response, the passband and stopband errors of designed 48th-order LP-FIR1 bandstop digital filter



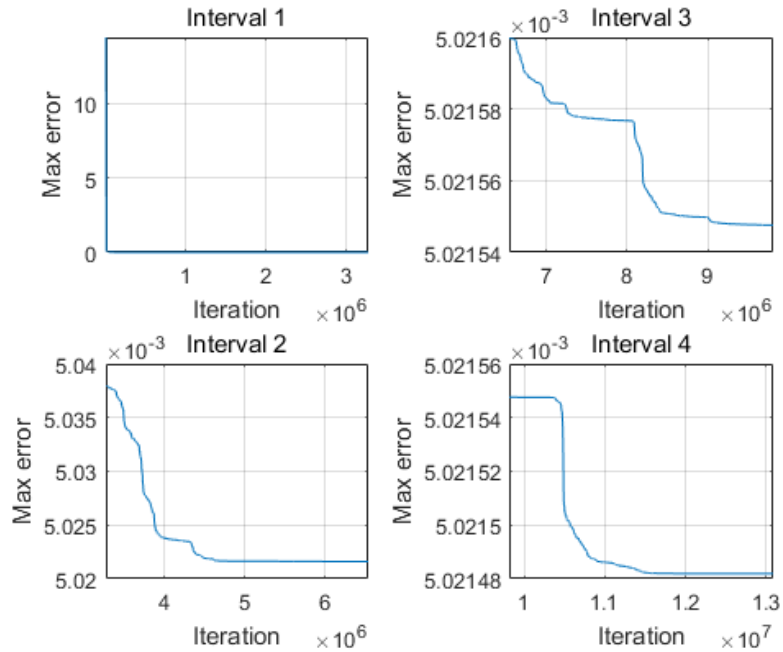


Fig. 3.16 Convergence curve of designed 48th-order LP-FIR1 bandstop digital filter

### 3.4 Conclusion

This chapter has presented the design of linear-phase type-1 FIR digital filters using Cuckoo Search Algorithm. 24th and 48th-order lowpass, highpass, bandpass and bandstop digital filters are chosen for the design and their results are obtained. The results have shown that the peak errors obtained by CSA are mostly smaller than those obtained by the Parks-McClellan algorithm. This denotes the effectiveness of CSA and its better performance on the optimal design than those of Parks-McClellan algorithm.

It should be noted that CSA is a meta-heuristic algorithm which requires a sufficient number of iterations and therefore it takes relatively more optimization time than that of Parks-McClellan algorithm.

In summary, CSA is capable of reaching the global optimum for it utilizes Levy flight with wide-range step length as a special strategy for the global walk. Meanwhile, the local walk is able to improve the existing solutions. In the future, more work can focus on the improvement of CSA, such as other suitable methods for the global walk or an efficient way for the parameter decision.

## CHAPTER 4 General FIR Digital Filter Design Using Multiobjective Cuckoo Search Algorithm

### 4.1 Introduction

In the real life, many practical problems are consisted of various interactive but conflicting objectives to be satisfied simultaneously. These objectives may be contradictory to each other such that an improvement on an objective could lead to serious depravation of some others. It means it is impossible to find a solution that satisfies all the objectives to their respective optimum levels at the same time. A possible solution for this situation is compromising the objectives and trying to optimize them simultaneously until they reach equilibration. A multiobjective optimization problem is defined as searching for an optimal solution within a certain of range to optimize multiple objectives at a balanced optimum level as optimal equilibration.

A number of multiobjective optimization algorithms have been proposed so far. Most of them share a common method, Pareto Front, to determine the potential optimal solution. The Pareto Front, named after a famous mathematician Vilfredo Pareto (1848-1923), is used to find those solutions that can not improve an objective without degrading any one of the others. Then the optimal solution shall be pick up from the Pareto Front. A typical multiobjective optimization algorithm using the Pareto Front is Non-dominated Sorting Genetic Algorithm (NSGA-III) [20]. NSGA-III is able to achieve a minimum point in a swift way and obtain a set of solutions with well-convergence and well-diversity over enough number of iterations. However, the Pareto Front may contain more than one candidate solution and require more standards to finalize the most feasible one. This requires more preparing work including further model-formulation, formula-derivation or objective-based equilibrating methods.

In this chapter, an improvement on CSA in adapt to multiobjective optimization problems is presented as multiobjective Cuckoo Search Algorithm (MOCSA) [21]. MOCSA incorporates a technique of Euclidean distance instead of Pareto Front to realize the objective-based optimal equilibration and determine the optimal solution by simple comparison. MOCSA and NSGA-III are applied on the design of general FIR lowpass, highpass, bandpass and bandstop digital filters at order 24 with different group delay values in passband. Their design results are compared with each other to demonstrate the effectiveness of MOCSA.

### 4.2 Multiobjective Cuckoo Search Algorithm

Multiobjective Cuckoo Search Algorithm follows the steps of the original CSA described in section 3.1 from (3.1) to (3.8). For a minimization problem with  $M$  ( $M \geq 2$ ) objective functions

$f_m(\mathbf{x})$  ( $m = 1, 2, \dots, M$ ) and  $I$  competing solutions, an Euclidean space  $\mathcal{S}^M$  can be formulated that each dimension corresponds to a respective objective function. An Euclidean spatial point with respect to a solution  $\mathbf{x}$  can then be represented by [21]

$$\mathbf{f}(\mathbf{x}) = (f_1(\mathbf{x}), f_2(\mathbf{x}), \dots, f_M(\mathbf{x})) \quad (4.1)$$

The current ideal spatial point  $\mathbf{z}(t)$  obtained at the current iteration  $t$  can be represented by

$$\mathbf{z}(t) = (z_1^{\min}(t), z_2^{\min}(t), \dots, z_M^{\min}(t)) \quad (4.2)$$

where

$$z_m^{\min}(t) = \min \left\{ \min_{i=1 \text{ to } I} f_m(\mathbf{x}_i(t)), z_m^{\min}(t-1) \right\} \quad (4.3)$$

for  $m = 1$  to  $M$

which represents the minimum value of  $f_m(\mathbf{x})$  that has ever reached during the iterative procedure so far. For initialization, all the elements in  $\mathbf{z}(0)$  should be positively infinite such that the current ideal spatial point at the first iteration  $\mathbf{z}(1)$  could be consistently updated.

The Euclidean distance between an Euclidean spatial point  $\mathbf{f}(\mathbf{x})$  in the Euclidean Space  $\mathcal{S}^M$  defined in (4.1) and the current ideal spatial point  $\mathbf{z}(t)$  at the current iteration  $t$  is calculated by

$$d(\mathbf{x}, \mathbf{z}(t)) = \sqrt{\sum_{m=1}^M [f_m(\mathbf{x}) - z_m(t)]^2} \quad (4.4)$$

The usage of Euclidean distance is for comparing the qualities of the candidate solutions. A solution with a smaller Euclidean distance implies its corresponding Euclidean spatial point is closer to the current ideal spatial point in the Euclidean space. It means this solution is more qualified to realize the ideal optimization goal. Concerning the  $i$ th population member  $\mathbf{x}_i(t)$  for  $i = 1, 2, \dots, I$ , the one with the smallest Euclidean distance among the global walk solution  $\mathbf{x}_{i_g}(t)$ , the local walk solution  $\mathbf{x}_{i_l}(t)$  and the existing solution  $\mathbf{x}_i(t)$  is selected as the solution  $\mathbf{x}_i(t+1)$  for the next iteration [21].

The best solution  $\mathbf{x}_{best}$  for the next iteration is updated by that with the smallest Euclidean distance among the new updated population such that the most qualified solution is currently restored.

### 4.3 Design of General FIR Digital Filters

An  $N$ th-order general FIR (G-FIR) digital filter consists of  $(N + 1)$  impulse responses [21]. This series of values can be expressed as a distinct coefficient vector  $\mathbf{c}$  as

$$\mathbf{c} = [c_0, c_1, c_2, c_3, \dots, c_N]^T = [h(0), h(1), h(2), h(3), \dots, h(N)]^T \quad (4.5)$$

The frequency response  $H(w)$  of a general FIR digital filter can be represented by

$$H(w) = \sum_{n=0}^N c_n z^{-n} \Big|_{z=e^{jwT}} = |H(w)|e^{j\theta(w)} \quad (4.6)$$

The group delay of a general FIR digital filter can be expressed as

$$\tau(w) = -\frac{\partial\theta(w)}{\partial wT} \quad (4.7)$$

The objective function for the maximum magnitude error  $e_{mag}(\mathbf{c})$  is defined by

$$e_{mag}(\mathbf{c}) = \max_{\mathbf{c}} | |H(\mathbf{c}, w_i)| - H_d(w_i) | \quad (4.8)$$

for  $\forall w_i \in \Omega_I$

where  $H_d(w_i) = 1$  in passband(s) and  $H_d(w_i) = 0$  in stopband(s); and  $\Omega_I$  denotes union of frequency bands of interest including both passband and stopband.

Similarly, the objective function for the peak group delay error in passband  $e_{gd}(\mathbf{c})$  can be defined by

$$e_{gd}(\mathbf{c}) = \max_{\mathbf{c}} |\tau(\mathbf{c}, w_i) - \tau_d| \quad (4.9)$$

for  $w_{p1} \leq w_i \leq w_{p2}$

where  $\tau_d$  is the ideal value of group delay in passband.

The optimization problem for designing FIR lowpass, highpass, bandpass and bandstop digital filters is searching for an optimal coefficient vector  $\mathbf{c}$  that minimizes the objective functions  $e_{mag}(\mathbf{c})$  and  $e_{gd}(\mathbf{c})$  simultaneously.

### 4.4 Design Examples and Results

In this section, general FIR lowpass, highpass, bandpass and bandstop digital filters of order 24 with group delay values of 10, 12 and 14 in passband are designed. In each example, MOCSA is applied to simultaneously minimize the objective functions  $e_{mag}(\mathbf{c})$  and  $e_{gd}(\mathbf{c})$  as given in (4.8) and (4.9) that

$$f_1(\mathbf{x}) = e_{mag}(\mathbf{c}) \quad (4.10)$$

$$f_2(\mathbf{x}) = e_{gd}(\mathbf{c}) \quad (4.11)$$

All the filter coefficients are initialized randomly. NSGA-III is also considered as a compared method for the above design. Design results obtained by MOCSA are compared favourably to those obtained by NSGA-III.

The parameters of MOCSA and NSGA-III are listed in Table 4.1. Lowpass, highpass, bandpass and bandstop cutoff frequencies are specified in Table 4.2. The adopt frequency grids for optimization and for evaluating the peak errors of magnitude as well as group delay in passband are shown in Table 4.3. The optimization procedure is terminated when the Euclidean distance from the best solution stays unchanged during the last 10% continuous iterations. An Intel(R) Core(TM) i7-5500U CPU, 2.40 GHz with 8GB RAM laptop computer is used to carry out all the optimization designs.

Table 4.1 Parameters of MOCSA and NSGA-III

Symbol	Description	LP	HP	BP	BS
$P_C$	MOCSA population size	25	25	25	25
$\beta$	MOCSA parameter	1.5	1.5	1.5	1.5
$\alpha$	MOCSA parameter	0.01	0.01	0.01	0.01
$p_a$	MOCSA parameter	0.25	0.25	0.25	0.25
$P_N$	NSGA-III population size	25	25	25	25

Table 4.2 G-FIR digital filter cutoff frequencies

	$w_{s1}$	$w_{p1}$	$w_{p2}$	$w_{s2}$
LP	$0.4\pi$	$0.3\pi$	-	-
HP	$0.45\pi$	$0.55\pi$	-	-
BP	$0.25\pi$	$0.35\pi$	$0.6\pi$	$0.7\pi$
BS	$0.4\pi$	$0.3\pi$	$0.65\pi$	$0.55\pi$

Table 4.3 Frequency grids for G-FIR digital filter design

Optimization	$F_o = [0:0.005:1]$
Peak error evaluation	$F_{mag} = [0:0.001:1]$

#### 4.4.1 24th-order Lowpass Digital Filters

##### 4.4.1.1 Lowpass Digital Filter with Group Delay in Passband at 10

The filter coefficients of obtained by MOCSA and NSGA-III are listed in Table 4.4. Design results with respect to magnitude error are listed in Table 4.5 while those with respect to group delay error are listed in Table 4.6. The computational record in terms of CPU seconds and number of iterations for reaching convergence are listed in Table 4.7. Plots of the magnitude response, impulse response, the passband and stopband errors of the designed lowpass digital filter are shown in Fig. 4.1 for MOCSA and Fig. 4.2 for NSGA-III, and the convergence curve of MOCSA is plotted in Fig. 4.3.

Table 4.4 Coefficients of lowpass digital filter with group delay in passband at 10

$h(n)$	MOCSA	NSGA-III
$h(0)$	-0.041198269383307	-0.034890224248738
$h(1)$	-0.011702538139839	-0.014555370991983
$h(2)$	0.020598977457927	0.018330739577806
$h(3)$	0.034541783816633	0.044266200345298
$h(4)$	0.016182632487573	0.016978063996938
$h(5)$	-0.043550613642583	-0.048414388981186
$h(6)$	-0.069194930881171	-0.058180800700933
$h(7)$	-0.013300686397420	-0.023432311806267
$h(8)$	0.120037270622586	0.132565266758704
$h(9)$	0.288262477333900	0.286066899227323
$h(10)$	0.348928018203073	0.347702950604088
$h(11)$	0.280853766720371	0.283737138270304
$h(12)$	0.126197531559139	0.133705706158827
$h(13)$	-0.011966727742320	-0.020992582525051
$h(14)$	-0.075204626283456	-0.067198567108741
$h(15)$	-0.039903258233887	-0.034915860013511
$h(16)$	0.016977945620325	0.012773558474705
$h(17)$	0.033753225785978	0.037815659968352
$h(18)$	0.020114139904307	0.021641529999907
$h(19)$	-0.017070876511376	-0.014942398864603
$h(20)$	-0.025634981014295	-0.023675360674065
$h(21)$	-0.018153349567344	-0.016218102844109
$h(22)$	0.010905964021526	0.003984628680988

$h(23)$	-0.003066466549981	0.006427772194404
$h(24)$	0.000168886777214	-0.004177967194567

Table 4.5 Magnitude error of lowpass digital filter with group delay in passband at 10

Algorithm	Peak (Passband)	Peak (Stopband)
MOCSA	0.052596836181376	0.052670823229299
NSGA-III	0.053154096504146	0.053414337614708

Table 4.6 Group delay error of lowpass digital filter with group delay in passband at 10

Algorithm	Peak (Passband)
MOCSA	0.000545615619879
NSGA-III	0.008370524552788

Table 4.7 Computational record of lowpass digital filter with group delay in passband at 10

Algorithm	CPU Seconds	Iteration
MOCSA	8561.143758	12106139
NSGA-III	248.323372	5863

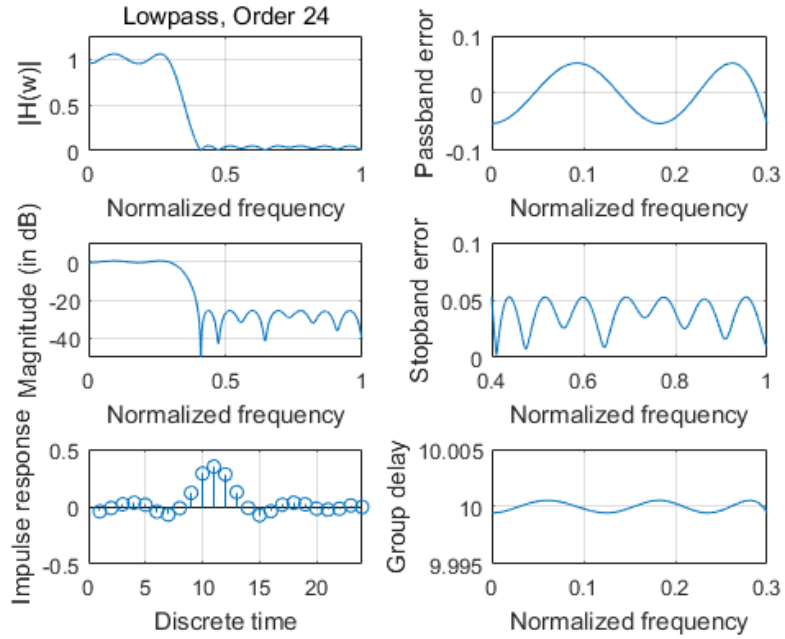


Fig. 4.1 Magnitude response, impulse response, the passband and stopband errors of designed G-FIR lowpass digital filter with group delay in passband at 10 obtained by MOCSA

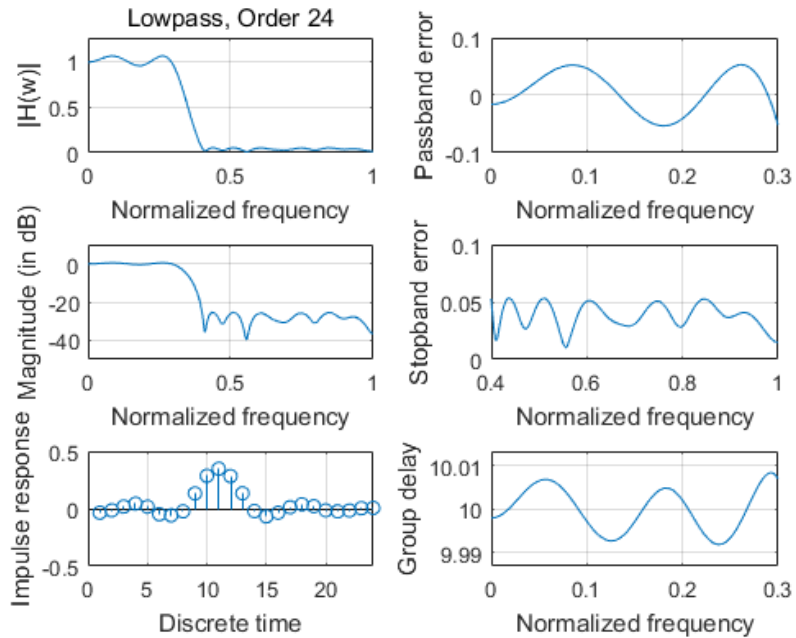


Fig. 4.2 Magnitude response, impulse response, the passband and stopband errors of designed G-FIR lowpass digital filter with group delay in passband at 10 obtained by NSGA-III



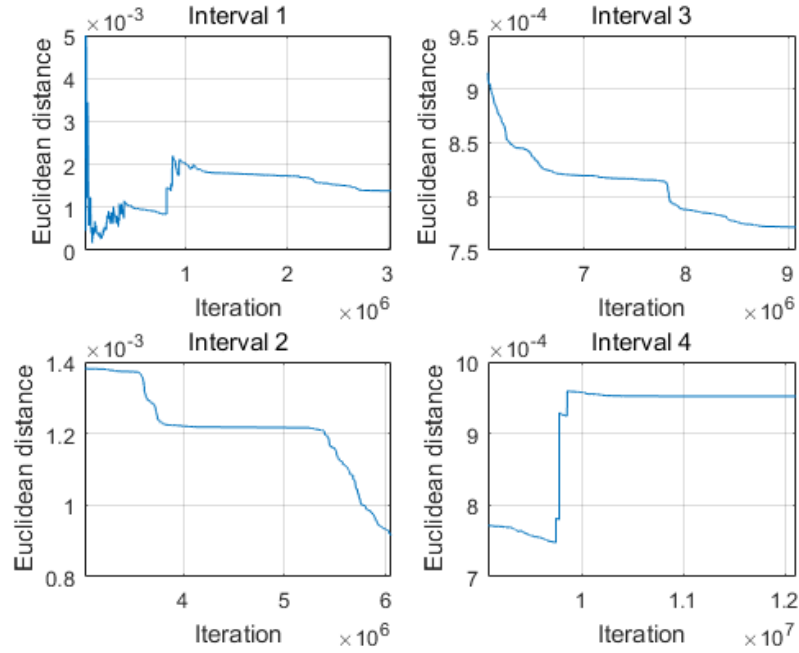


Fig. 4.3 Convergence curve of designed G-FIR lowpass digital filter with group delay in passband at 10 obtained by MOCSA

#### 4.4.1.2 Lowpass Digital Filter with Group Delay in Passband at 12

The filter coefficients of obtained by MOCSA and NSGA-III are listed in Table 4.8. Design results with respect to magnitude error are listed in Table 4.9 while those with respect to group delay error are listed in Table 4.10. The computational record in terms of CPU seconds and number of iterations for reaching convergence are listed in Table 4.11. Plots of the magnitude response, impulse response, the passband and stopband errors of the designed lowpass digital filter are shown in Fig. 4.4 for MOCSA and Fig. 4.5 for NSGA-III, and the convergence curve of MOCSA is plotted in Fig. 4.6.

Table 4.8 Coefficients of lowpass digital filter with group delay in passband at 12

$h(n)$	MOCSA	NSGA-III
$h(0)$	0.013535165952382	0.015505495827124
$h(1)$	-0.016393810496359	-0.018708779428162
$h(2)$	-0.030600620180798	-0.026725383036830
$h(3)$	-0.010080503280016	-0.010466747085602
$h(4)$	0.015273870704195	0.017121203568736
$h(5)$	0.034053420015863	0.035075752003777

$h(6)$	0.017893649453700	0.018960551230898
$h(7)$	-0.041290669072793	-0.043499467328951
$h(8)$	-0.074089875446003	-0.069180971593755
$h(9)$	-0.013065728020069	-0.016850527607509
$h(10)$	0.125652556846760	0.128062517942709
$h(11)$	0.281790231556929	0.279319177054130
$h(12)$	0.351816277073321	0.351731994357483
$h(13)$	0.281709948162901	0.283410310455638
$h(14)$	0.127388588638785	0.124616050521326
$h(15)$	-0.017728601698537	-0.014630030387373
$h(16)$	-0.070011125795146	-0.072107675093053
$h(17)$	-0.038552600082401	-0.038793951006955
$h(18)$	0.009627522065944	0.012343899315996
$h(19)$	0.037673771975495	0.039934633364232
$h(20)$	0.022419255078578	0.018971387845592
$h(21)$	-0.022551958720532	-0.016085139750509
$h(22)$	-0.021413682706359	-0.025128771298926
$h(23)$	-0.019957064352162	-0.016212423788601
$h(24)$	0.014141129928525	0.013733538043933

Table 4.9 Magnitude error of lowpass digital filter with group delay in passband at 12

Algorithm	Peak (Passband)	Peak (Stopband)
MOCSA	0.046065198313971	0.046185882274220
NSGA-III	0.046507218020522	0.046464779221026

Table 4.10 Group delay error of lowpass digital filter with group delay in passband at 12

Algorithm	Peak (Passband)
MOCSA	0.000020504668173
NSGA-III	0.003718899801981

Table 4.11 Computational record of lowpass digital filter with group delay in passband at 12

Algorithm	CPU Seconds	Iteration
MOCSA	1347.678670	1901502
NSGA-III	468.539187	9834

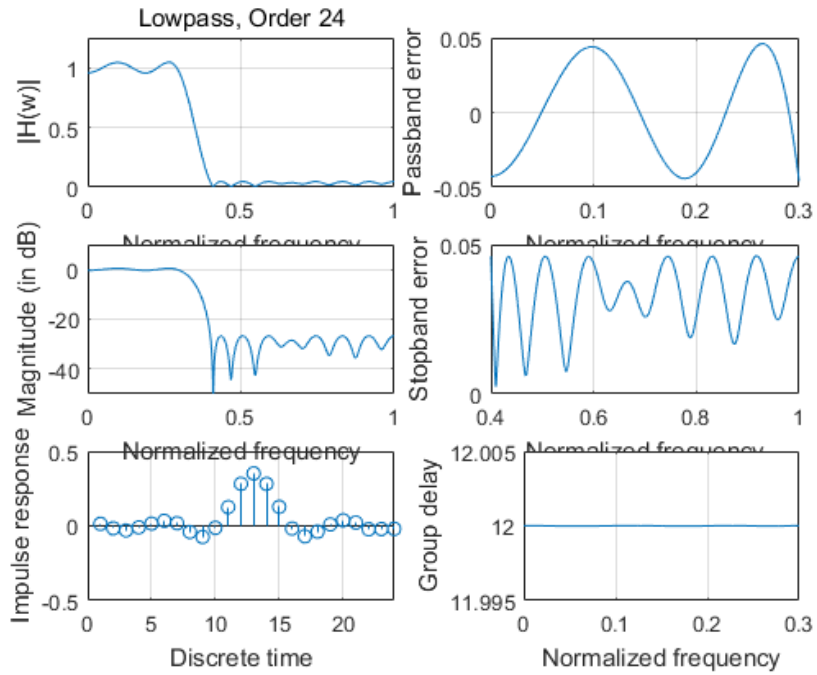


Fig. 4.4 Magnitude response, impulse response, the passband and stopband errors of designed G-FIR lowpass digital filter with group delay in passband at 12 obtained by MOCSA

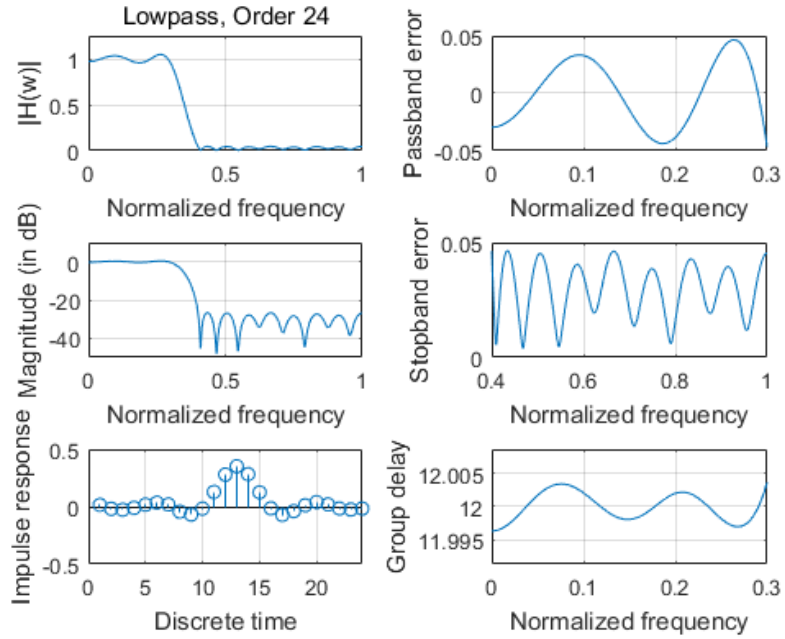


Fig. 4.5 Magnitude response, impulse response, the passband and stopband errors of designed G-FIR lowpass digital filter with group delay in passband at 12 obtained by NSGA-III

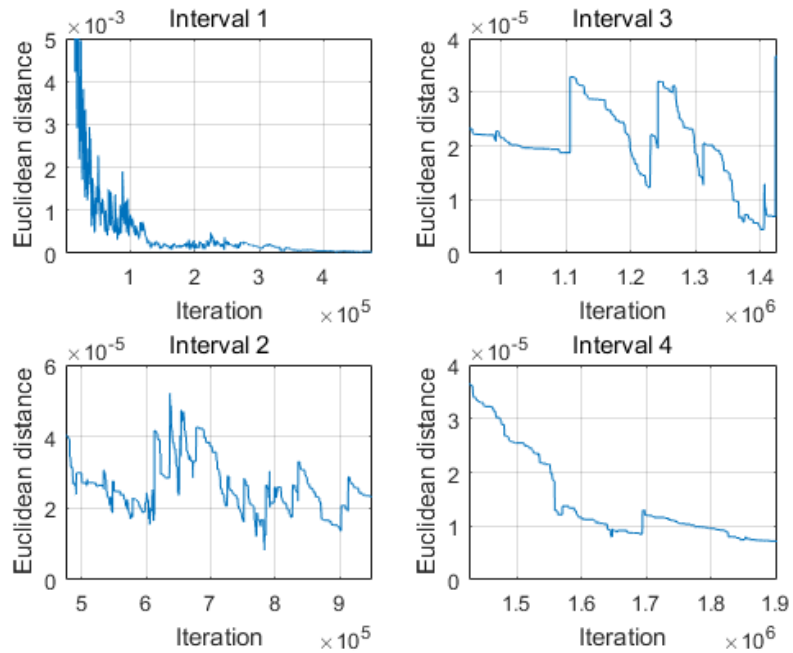


Fig. 4.6 Convergence curve of designed G-FIR lowpass digital filter with group delay in passband at 12 obtained by MOCSA

#### 4.4.1.3 Lowpass Digital Filter with Group Delay in Passband at 14

The filter coefficients of obtained by MOCSA and NSGA-III are listed in Table 4.12. Design results with respect to magnitude error are listed in Table 4.13 while those with respect to group delay error are listed in Table 4.14. The computational record in terms of CPU seconds and number of iterations for reaching convergence are listed in Table 4.15. Plots of the magnitude response, impulse response, the passband and stopband errors of the designed lowpass digital filter are shown in Fig. 4.7 for MOCSA and Fig. 4.8 for NSGA-III, and the convergence curve of MOCSA is plotted in Fig. 4.9.

Table 4.12 Coefficients of lowpass digital filter with group delay in passband at 14

$h(n)$	MOCSA	NSGA-III
$h(0)$	-0.000060451201129	-0.003025624423626
$h(1)$	-0.001607336153554	0.005645000130130
$h(2)$	0.007488600330746	0.002380969367836
$h(3)$	-0.014122534022961	-0.014142558566336
$h(4)$	-0.028639071784242	-0.024911757609482
$h(5)$	-0.014522743300258	-0.016779783444136
$h(6)$	0.016116840110976	0.022691547240656
$h(7)$	0.038581283547434	0.034813373044536
$h(8)$	0.014585982991793	0.013215234212493
$h(9)$	-0.042420817770733	-0.038454021890381
$h(10)$	-0.068139325001451	-0.068178187471455
$h(11)$	-0.021122134913990	-0.019179511118329
$h(12)$	0.134859079352017	0.125566433726659
$h(13)$	0.273000936725557	0.286473248286585
$h(14)$	0.357857722046911	0.346254685530325
$h(15)$	0.277879269113579	0.282411082629091
$h(16)$	0.128717635127549	0.123678623886700
$h(17)$	-0.016514209256488	-0.005742433662816
$h(18)$	-0.072021382900915	-0.083655608750170
$h(19)$	-0.038289810145093	-0.034035049171870
$h(20)$	0.013633870300424	0.013556515691406
$h(21)$	0.032650460614725	0.036622107552164
$h(22)$	0.023883758338048	0.023542666428628
$h(23)$	-0.013329393383173	-0.016704975539084
$h(24)$	-0.041043639974816	-0.036362824312344

Table 4.13 Magnitude error of lowpass digital filter with group delay in passband at 14

Algorithm	Peak (Passband)	Peak (Stopband)
MOCSA	0.052752044407466	0.052789311791234
NSGA-III	0.053034864506350	0.053047188042726

Table 4.14 Group delay error of lowpass digital filter with group delay in passband at 14

Algorithm	Peak (Passband)
MOCSA	0.000398649157843
NSGA-III	0.004335033277854

Table 4.15 Computational record of lowpass digital filter with group delay in passband at 14

Algorithm	CPU Seconds	Iteration
MOCSA	5944.458695	7288980
NSGA-III	227.461914	5058

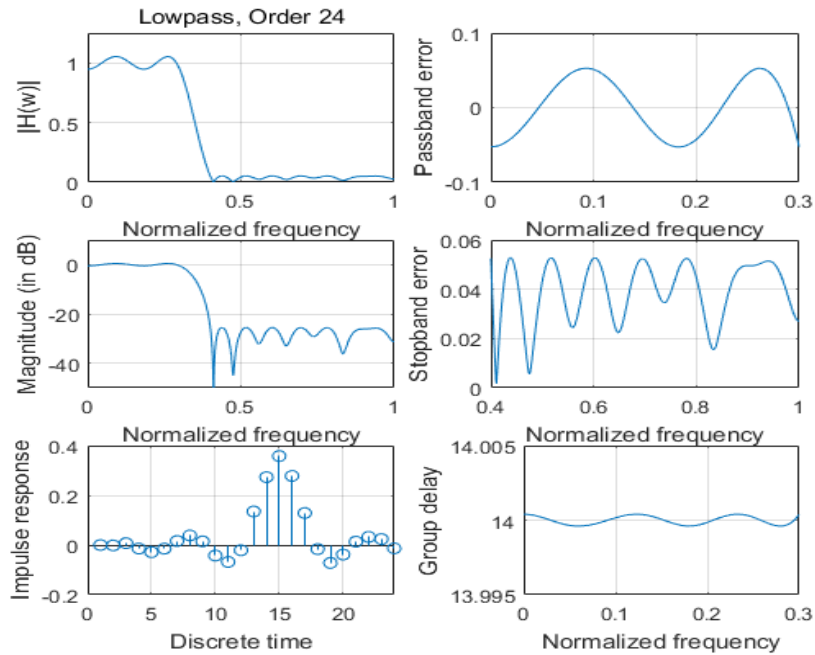


Fig. 4.7 Magnitude response, impulse response, the passband and stopband errors of designed G-FIR lowpass digital filter with group delay in passband at 14 obtained by MOCSA

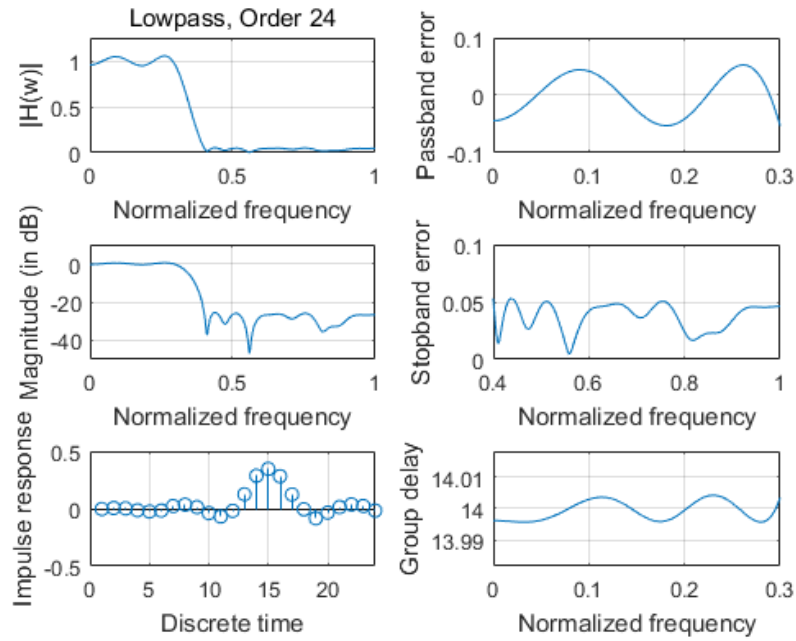


Fig. 4.8 Magnitude response, impulse response, the passband and stopband errors of designed G-FIR lowpass digital filter with group delay in passband at 14 obtained by NSGA-III

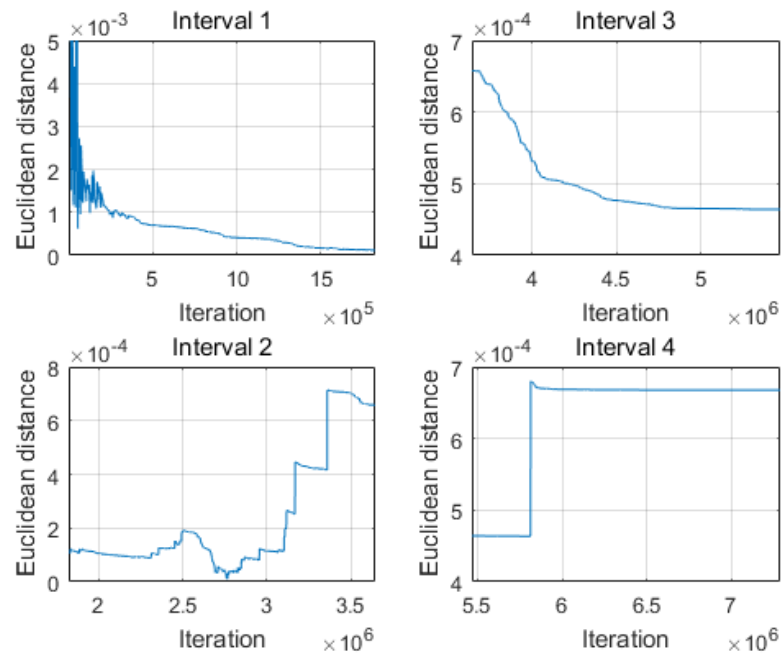


Fig. 4.9 Convergence curve of designed G-FIR lowpass digital filter with group delay in passband at 14 obtained by MOCSA

## 4.4.2 24th-order Highpass Digital Filters

### 4.4.2.1 Highpass Digital Filter with Group Delay in Passband at 10

The filter coefficients of obtained by MOCSA and NSGA-III are listed in Table 4.16. Design results with respect to magnitude error are listed in Table 4.17 while those with respect to group delay error are listed in Table 4.18. The computational record in terms of CPU seconds and number of iterations for reaching convergence are listed in Table 4.19. Plots of the magnitude response, impulse response, the passband and stopband errors of the designed highpass digital filter are shown in Fig. 4.10 for MOCSA and Fig. 4.11 for NSGA-III, and the convergence curve of MOCSA is plotted in Fig. 4.12.

Table 4.16 Coefficients of highpass digital filter with group delay in passband at 10

$h(n)$	MOCSA	NSGA-III
$h(0)$	-0.005494700764422	-0.006988009235285
$h(1)$	-0.054332513603260	-0.039778146318213
$h(2)$	-0.005560223944632	-0.003287272768635
$h(3)$	0.033499245202198	0.047706603197889
$h(4)$	-0.000215376569352	-0.003366750570935
$h(5)$	-0.056124606136280	-0.061645381128061
$h(6)$	0.001525094419797	-0.001327633243464
$h(7)$	0.103960575926926	0.089985698572622
$h(8)$	0.002019908039721	0.000467679828484
$h(9)$	-0.314916980968963	-0.327400248723325
$h(10)$	0.501201679807967	0.509936462868409
$h(11)$	-0.316754812109805	-0.322219947461521
$h(12)$	-0.000022654995965	0.008373126212587
$h(13)$	0.103055817100247	0.091339766599350
$h(14)$	0.001487667379092	-0.004314375769320
$h(15)$	-0.055996001554253	-0.064313717722716
$h(16)$	0.001195236546215	-0.007438567515165
$h(17)$	0.039181000699405	0.042965024408293
$h(18)$	0.006235548389254	-0.002784913861289
$h(19)$	-0.038455083041937	-0.027229372842021
$h(20)$	0.009521174004298	0.012455796552993
$h(21)$	0.010112991551557	0.016649123551283
$h(22)$	0.004653338557117	0.006754628323922



$h(23)$	0.001275386196600	-0.000160751804552
$h(24)$	0.000111716443124	-0.001327002654798

Table 4.17 Magnitude error of highpass digital filter with group delay in passband at 10

Algorithm	Peak (Stopband)	Peak (Passband)
MOCSA	0.062931212642737	0.062762203035294
NSGA-III	0.065651068620897	0.065672129767996

Table 4.18 Group delay error of highpass digital filter with group delay in passband at 10

Algorithm	Peak (Passband)
MOCSA	0.000403657095495
NSGA-III	0.015430694353999

Table 4.19 Computational record of highpass digital filter with group delay in passband at 10

Algorithm	CPU Seconds	Iteration
MOCSA	12423.586642	14966500
NSGA-III	272.569767	5447

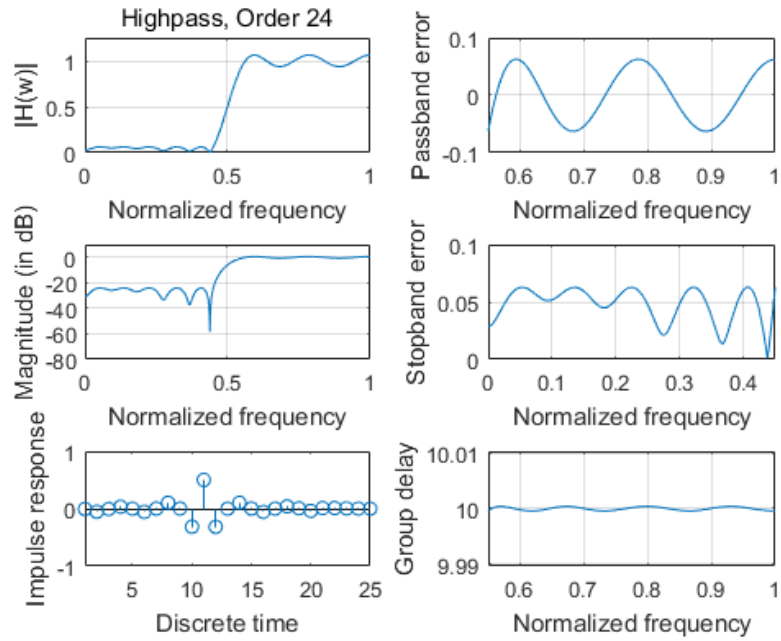


Fig. 4.10 Magnitude response, impulse response, the passband and stopband errors of designed G-FIR highpass digital filter with group delay in passband at 10 obtained by MOCSA

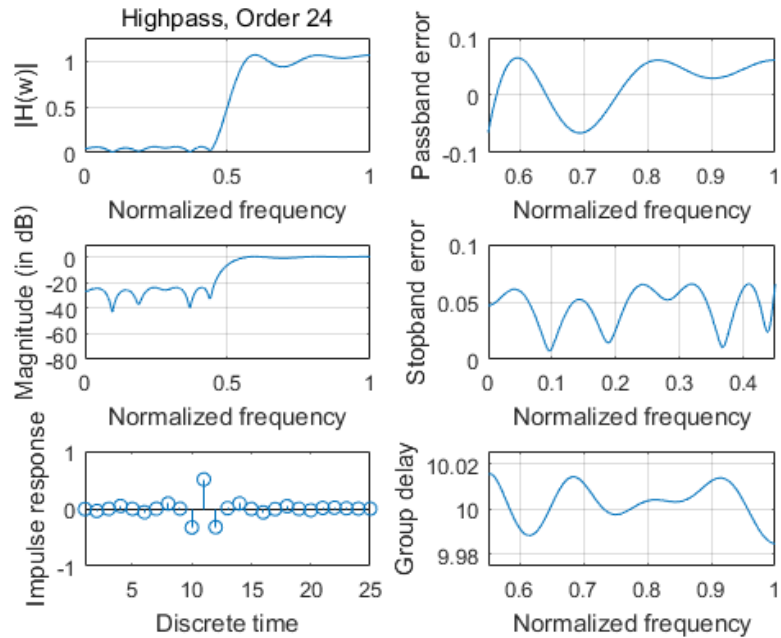


Fig. 4.11 Magnitude response, impulse response, the passband and stopband errors of designed G-FIR highpass digital filter with group delay in passband at 10 obtained by NSGA-III

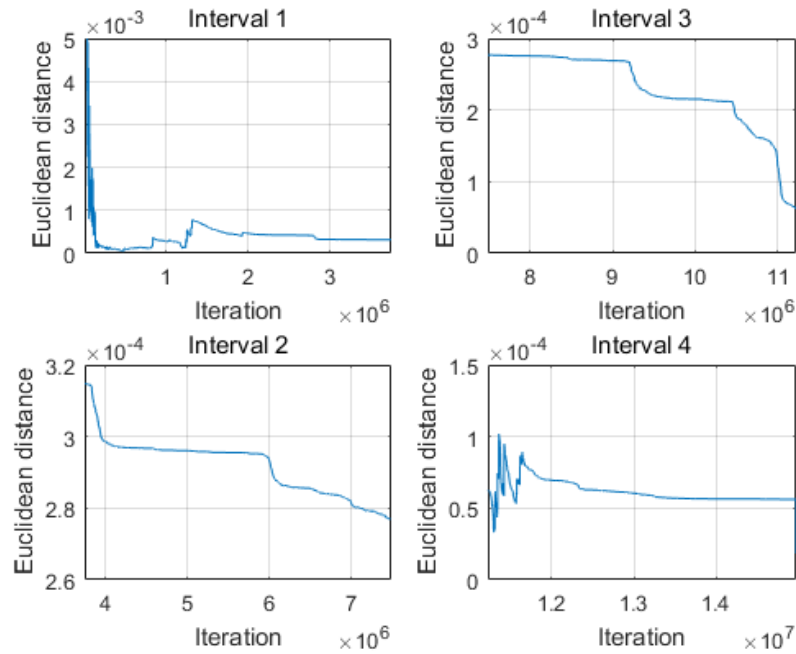


Fig. 4.12 Convergence curve of designed G-FIR highpass digital filter with group delay in passband at 10 obtained by MOCSA

#### 4.4.2.2 Highpass Digital Filter with Group Delay in Passband at 12

The filter coefficients of obtained by MOCSA and NSGA-III are listed in Table 4.20. Design results with respect to magnitude error are listed in Table 4.21 while those with respect to group delay error are listed in Table 4.22. The computational record in terms of CPU seconds and number of iterations for reaching convergence are listed in Table 4.23. Plots of the magnitude response, impulse response, the passband and stopband errors of the designed highpass digital filter are shown in Fig. 4.13 for MOCSA and Fig. 4.14 for NSGA-III, and the convergence curve of MOCSA is plotted in Fig. 4.15.

Table 4.20 Coefficients of highpass digital filter with group delay in passband at 12

$h(n)$	MOCSA	NSGA-III
$h(0)$	-0.001675215493034	-0.001640423119196
$h(1)$	0.030567589936448	0.028789441239145
$h(2)$	-0.003153981941076	-0.000789734235811
$h(3)$	-0.030162804995681	-0.027624301522506

$h(4)$	-0.006257470530900	0.002006791503828
$h(5)$	0.030944299596606	0.036128094215588
$h(6)$	-0.004151306791061	0.000560872431347
$h(7)$	-0.057759642352401	-0.061827799261375
$h(8)$	0.002617052520662	0.001339285695101
$h(9)$	0.105260561729361	0.105424661593389
$h(10)$	0.001196132567202	0.009174624916789
$h(11)$	-0.317380601702831	-0.313761957206108
$h(12)$	0.500190225288344	0.499678839468190
$h(13)$	-0.315927004908013	-0.325910631942135
$h(14)$	0.001091904753222	-0.006185448907321
$h(15)$	0.102234681463712	0.097639432621958
$h(16)$	-0.000078420494503	0.002660561652607
$h(17)$	-0.055080731938677	-0.056658642671228
$h(18)$	0.005484037504044	0.004156502808630
$h(19)$	0.044078607965804	0.037875179446759
$h(20)$	0.005210137139053	0.004286336782926
$h(21)$	-0.023189195584276	-0.023592011437525
$h(22)$	-0.000230886009131	0.003496488274169
$h(23)$	0.031338307159961	0.031595554412682
$h(24)$	-0.001580482608669	-0.000695121954894

Table 4.21 Magnitude error of highpass digital filter with group delay in passband at 12

Algorithm	Peak (Stopband)	Peak (Passband)
MOCSA	0.046374812745406	0.046440998607253
NSGA-III	0.048021545201132	0.047833401391220

Table 4.22 Group delay error of highpass digital filter with group delay in passband at 12

Algorithm	Peak (Passband)
MOCSA	0.000027846540165
NSGA-III	0.001940760275788

Table 4.23 Computational record of highpass digital filter with group delay in passband at 12

Algorithm	CPU Seconds	Iteration
MOCSA	2079.008120	2618404
NSGA-III	586.736733	13099

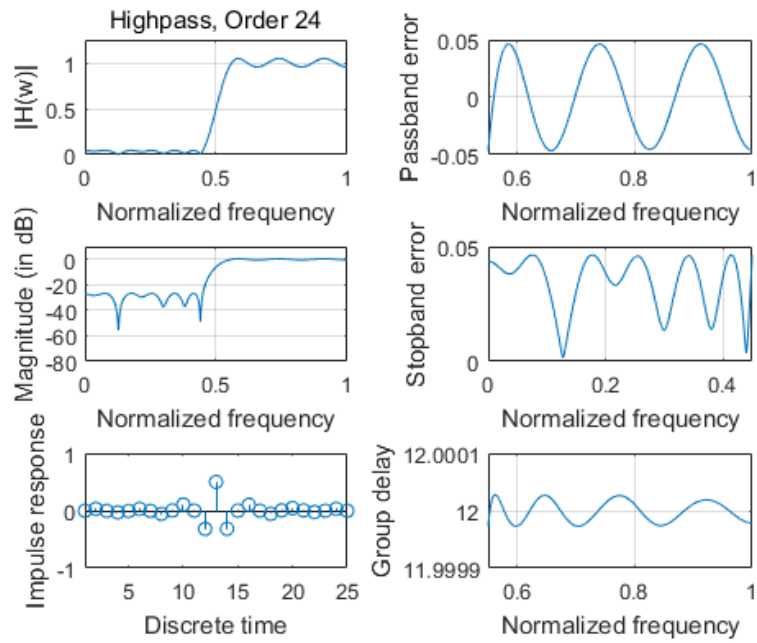


Fig. 4.13 Magnitude response, impulse response, the passband and stopband errors of designed G-FIR highpass digital filter with group delay in passband at 12 obtained by MOCSA

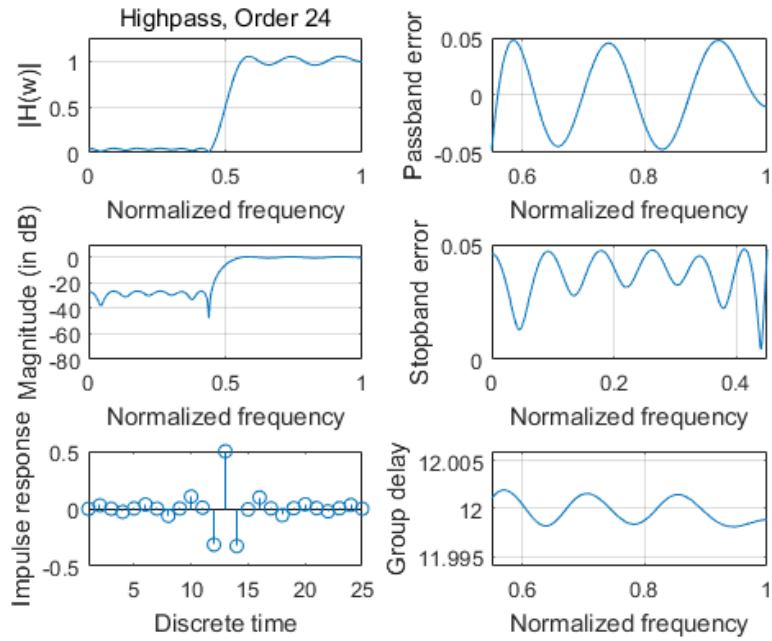


Fig. 4.14 Magnitude response, impulse response, the passband and stopband errors of designed G-FIR highpass digital filter with group delay in passband at 12 obtained by NSGA-III

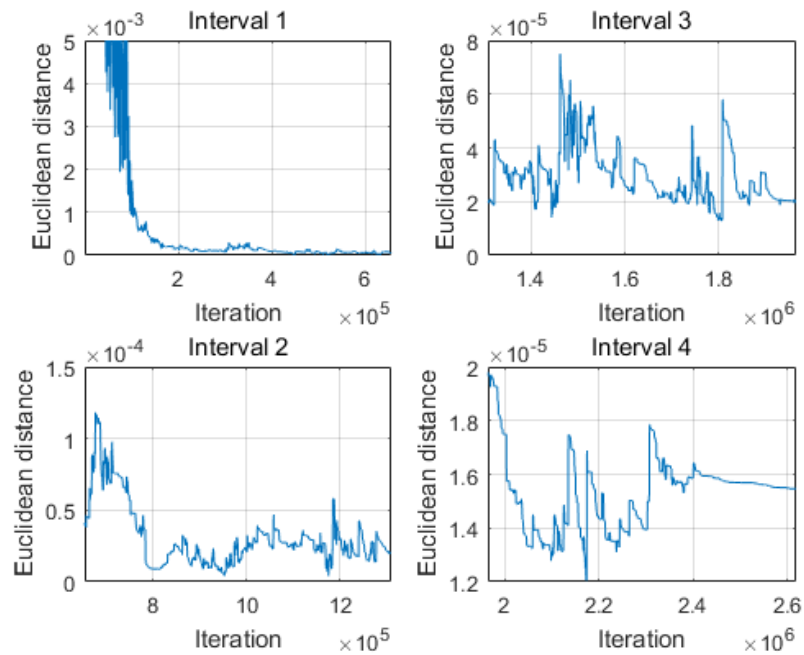


Fig. 4.15 Convergence curve of designed G-FIR highpass digital filter with group delay in passband at 12 obtained by MOCSA

#### 4.4.2.3 Highpass Digital Filter with Group Delay in Passband at 14

The filter coefficients of obtained by MOCSA and NSGA-III are listed in Table 4.24. Design results with respect to magnitude error are listed in Table 4.25 while those with respect to group delay error are listed in Table 4.26. The computational record in terms of CPU seconds and number of iterations for reaching convergence are listed in Table 4.27. Plots of the magnitude response, impulse response, the passband and stopband errors of the designed highpass digital filter are shown in Fig. 4.16 for MOCSA and Fig. 4.17 for NSGA-III, and the convergence curve of MOCSA is plotted in Fig. 4.18.

Table 4.24 Coefficients of highpass digital filter with group delay in passband at 14

$h(n)$	MOCSA	NSGA-III
$h(0)$	0.000189715927521	-0.002811997041032
$h(1)$	0.001669207038640	-0.004663812978790
$h(2)$	0.005499364469888	-0.000038354330207
$h(3)$	0.010958592132011	0.012616891481055
$h(4)$	0.009600026546689	0.012815602164086
$h(5)$	-0.039965497845766	-0.028304050506209
$h(6)$	0.003180190777767	0.004108440286823
$h(7)$	0.035566875442294	0.038789665212909
$h(8)$	-0.001668832776520	-0.002405158505638
$h(9)$	-0.057556120598075	-0.057228569669737
$h(10)$	0.001033324063391	0.000144987203125
$h(11)$	0.102871631399112	0.101201928025161
$h(12)$	-0.000334915169884	0.006524071206849
$h(13)$	-0.317446706150182	-0.319246223329057
$h(14)$	0.500180309880159	0.510111625886739
$h(15)$	-0.316539768231298	-0.318657631144643
$h(16)$	-0.000302558623053	0.005331318109345
$h(17)$	0.100837486759302	0.100990323208555
$h(18)$	-0.001821545517062	-0.000643377400120
$h(19)$	-0.058883535274388	-0.057776779959080
$h(20)$	-0.001423861277780	0.002538538339181
$h(21)$	0.033847584725322	0.045254533956708
$h(22)$	-0.004419496563109	0.000289917257516
$h(23)$	-0.053378064545261	-0.046716715795231
$h(24)$	-0.005100997621485	-0.009417005404971

Table 4.25 Magnitude error of highpass digital filter with group delay in passband at 14

Algorithm	Peak (Stopband)	Peak (Passband)
MOCSA	0.062898584873995	0.062725252692288
NSGA-III	0.063431327828246	0.063420253190410

Table 4.26 Group delay error of highpass digital filter with group delay in passband at 14

Algorithm	Peak (Passband)
MOCSA	0.000458487903323
NSGA-III	0.012003326436762

Table 4.27 Computational record of highpass digital filter with group delay in passband at 14

Algorithm	CPU Seconds	Iteration
MOCSA	2808.501259	3511290
NSGA-III	297.833476	7220

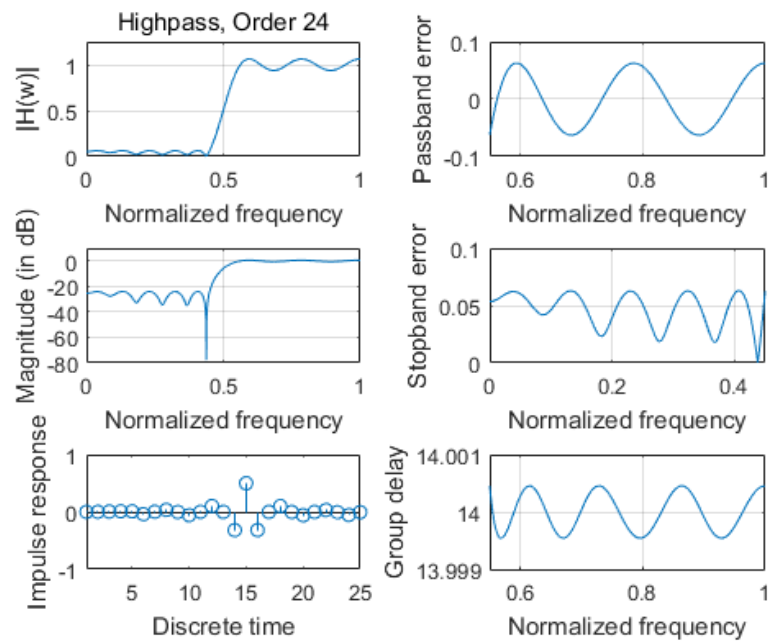


Fig. 4.16 Magnitude response, impulse response, the passband and stopband errors of designed G-FIR highpass digital filter with group delay in passband at 14 obtained by MOCSA



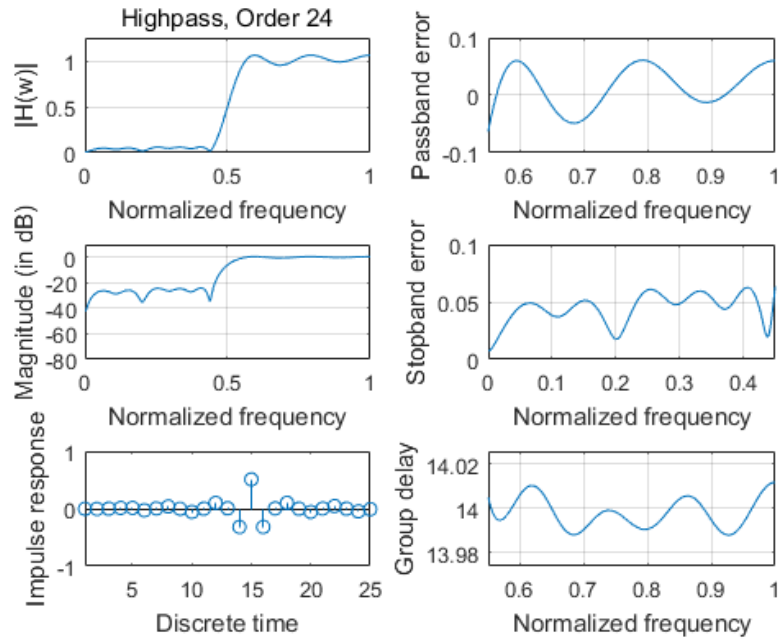


Fig. 4.17 Magnitude response, impulse response, the passband and stopband errors of designed G-FIR highpass digital filter with group delay in passband at 14 obtained by NSGA-III

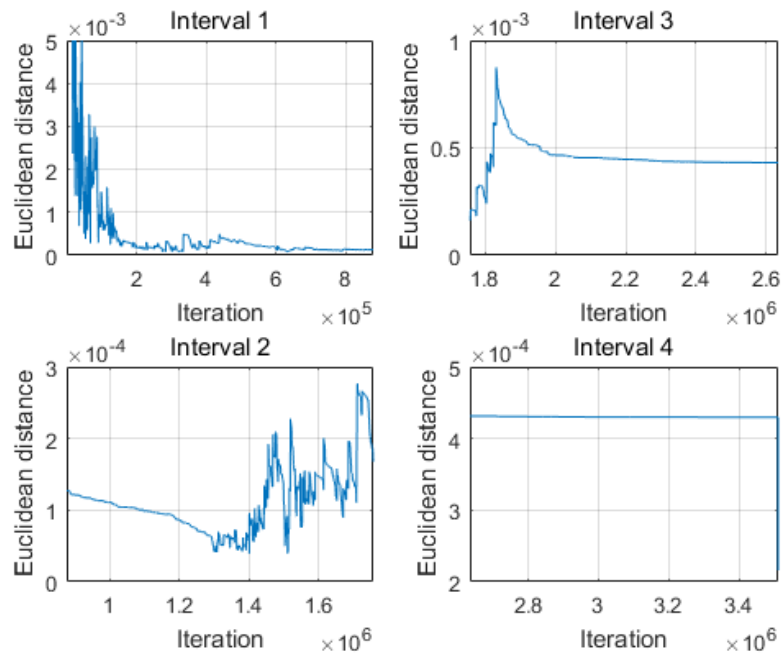


Fig. 4.18 Convergence curve of designed G-FIR highpass digital filter with group delay in passband at 14 obtained by MOCSA

### 4.4.3 24th-order Bandpass Digital Filters

#### 4.4.3.1 Bandpass Digital Filter with Group Delay in Passband at 10

The filter coefficients of obtained by MOCSA and NSGA-III are listed in Table 4.28. Design results with respect to magnitude error are listed in Table 4.29 while those with respect to group delay error are listed in Table 4.30. The computational record in terms of CPU seconds and number of iterations for reaching convergence are listed in Table 4.31. Plots of the magnitude response, impulse response, the passband and stopband errors of the designed bandpass digital filter are shown in Fig. 4.19 for MOCSA and Fig. 4.20 for NSGA-III, and the convergence curve of MOCSA is plotted in Fig. 4.21.

Table 4.28 Coefficients of bandpass digital filter with group delay in passband at 10

$h(n)$	MOCSA	NSGA-III
$h(0)$	0.005430986389361	0.015428932388912
$h(1)$	0.054952478108575	-0.022935152226301
$h(2)$	-0.012815431447323	-0.076844139219472
$h(3)$	-0.055880960011280	0.009335195995019
$h(4)$	0.002491525400599	0.009031209138254
$h(5)$	-0.045430651560580	-0.001725745749316
$h(6)$	-0.014728098727676	0.122564103296319
$h(7)$	0.204568644576432	0.014373971552246
$h(8)$	0.083307096089843	-0.275101194699403
$h(9)$	-0.301674005429034	-0.082325312334294
$h(10)$	-0.153914293976109	0.331929826006284
$h(11)$	0.286589801506166	0.127808117363482
$h(12)$	0.164946213405713	-0.241727746408794
$h(13)$	-0.157127644492924	-0.109674944472053
$h(14)$	-0.078772547017400	0.100205788917136
$h(15)$	0.029456683176514	0.030459383566442
$h(16)$	-0.012720664525222	0.010306905206861
$h(17)$	0.028131361844731	0.040924800018907
$h(18)$	0.046276693673373	-0.038103742320182
$h(19)$	-0.021498029938007	-0.042876879513592
$h(20)$	-0.044795836031356	0.009320452748809
$h(21)$	0.002156244151515	0.013939794691290
$h(22)$	-0.016235989790960	-0.004300401378061

$h(23)$	0.001012831000462	0.006997421717237
$h(24)$	-0.003592261197915	-0.002295269823873

Table 4.29 Magnitude error of bandpass digital filter with group delay in passband at 10

Algorithm	Peak (Stopband1)	Peak (Passband)	Peak (Stopband2)
MOCSA	0.061347203633322	0.061600394139233	0.061511150886210
NSGA-III	0.062560023935884	0.062691098289941	0.061420797889531

Table 4.30 Group delay error of bandpass digital filter with group Delay in passband at 10

Algorithm	Peak (Passband)
MOCSA	0.000697242747409
NSGA-III	0.014194201457874

Table 4.31 Computational record of bandpass digital filter with group delay in passband at 10

Algorithm	CPU Seconds	Iteration
MOCSA	6769.103006	9559146
NSGA-III	278.407725	6964

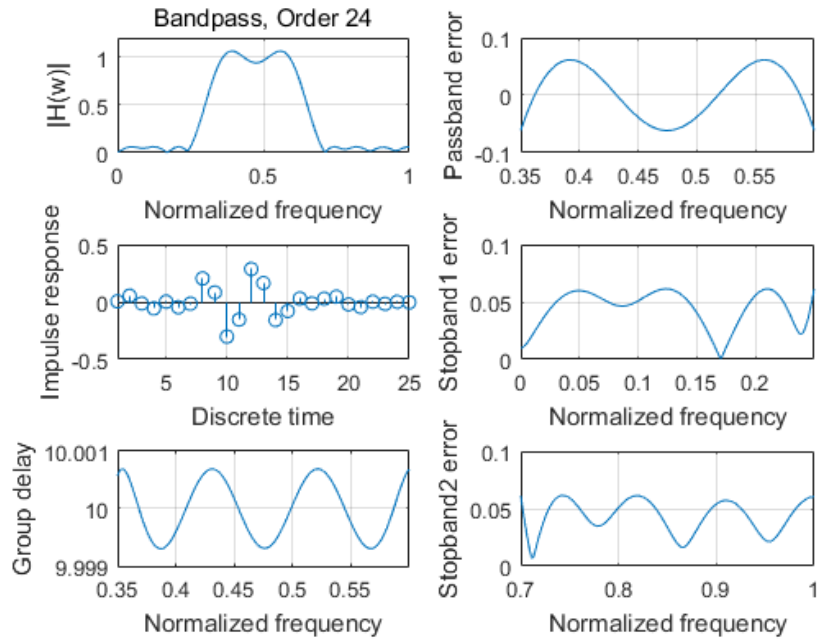


Fig. 4.19 Magnitude response, impulse response, the passband and stopband errors of designed G-FIR bandpass digital filter with group delay in passband at 10 obtained by MOCSA

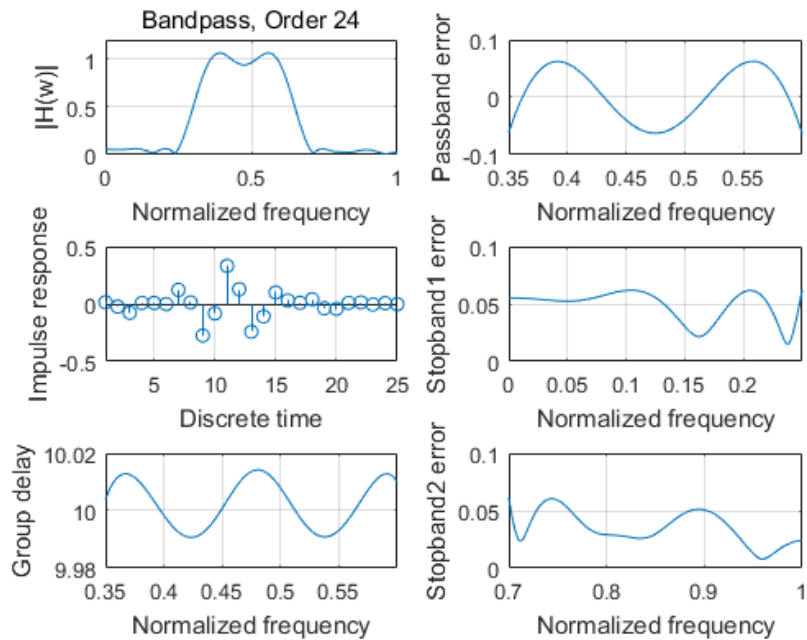


Fig. 4.20 Magnitude response, impulse response, the passband and stopband errors of designed G-FIR bandpass digital filter with group delay in passband at 10 obtained by NSGA-III

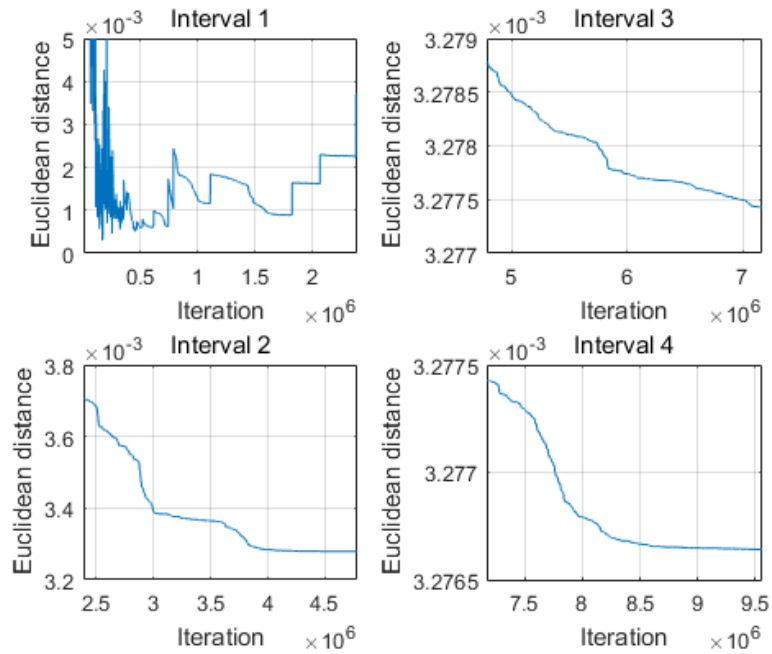


Fig. 4.21 Convergence curve of designed G-FIR bandpass digital filter with group delay in passband at 10 obtained by MOCSA

#### 4.4.3.2 Bandpass Digital Filter with Group Delay in Passband at 12

The filter coefficients of obtained by MOCSA and NSGA-III are listed in Table 4.32. Design results with respect to magnitude error are listed in Table 4.33 while those with respect to group delay error are listed in Table 4.34. The computational record in terms of CPU seconds and number of iterations for reaching convergence are listed in Table 4.35. Plots of the magnitude response, impulse response, the passband and stopband errors of the designed bandpass digital filter are shown in Fig. 4.22 for MOCSA and Fig. 4.23 for NSGA-III, and the convergence curve of MOCSA is plotted in Fig. 4.24.

Table 4.32 Coefficients of bandpass digital filter with group delay in passband at 12

$h(n)$	MOCSA	NSGA-III
$h(0)$	-0.001191522217179	0.003048141506459
$h(1)$	0.004598371465084	0.003694727434776
$h(2)$	-0.005612567970243	0.009670519843770
$h(3)$	0.069080104983046	-0.055520215034369

$h(4)$	0.016192108603444	-0.010231842605478
$h(5)$	-0.037135281545443	0.046954401964552
$h(6)$	-0.003816079934281	0.012168872290850
$h(7)$	-0.033196033228897	0.033902953514733
$h(8)$	-0.062685498028068	0.066565263552653
$h(9)$	0.163396445194271	-0.165885511551674
$h(10)$	0.189157311598212	-0.199642483641960
$h(11)$	-0.227927076818774	0.222525305976030
$h(12)$	-0.271305744214396	0.264638528317406
$h(13)$	0.185688544724823	-0.183874279706602
$h(14)$	0.240091198786329	-0.244940680353214
$h(15)$	-0.090133388592772	0.083354677069625
$h(16)$	-0.116037767378840	0.113111448250574
$h(17)$	0.011057754035267	-0.012799653148681
$h(18)$	-0.015159262222159	0.009370466456723
$h(19)$	0.005666796885008	-0.003239653434532
$h(20)$	0.069134692488655	-0.068845592912893
$h(21)$	0.001053440013482	0.000879273693527
$h(22)$	-0.026020649635451	0.029457978491176
$h(23)$	-0.000142875101177	0.002338417884990
$h(24)$	-0.003927234508290	0.003186750469736

Table 4.33 Magnitude error of bandpass digital filter with group delay in passband at 12

Algorithm	Peak (Stopband1)	Peak (Passband)	Peak (Stopband2)
MOCSA	0.061075373029417	0.061092632312159	0.060882060538963
NSGA-III	0.064950122680827	0.065009803502285	0.064084142414154

Table 4.34 Group delay error of bandpass digital filter with group delay in passband at 12

Algorithm	Peak (Passband)
MOCSA	0.000078604003798
NSGA-III	0.003807656883316

Table 4.35 Computational record of bandpass digital filter with group delay in passband at 12

Algorithm	CPU Seconds	Iteration
MOCSA	6082.247889	7424803
NSGA-III	219.122628	4970

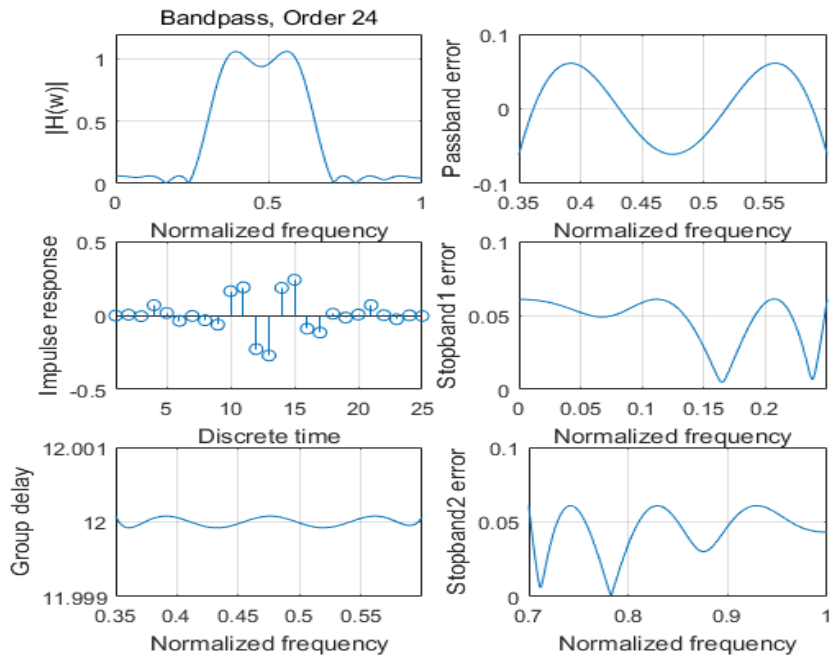


Fig. 4.22 Magnitude response, impulse response, the passband and stopband errors of designed G-FIR bandpass digital filter with group delay in passband at 12 obtained by MOCSA

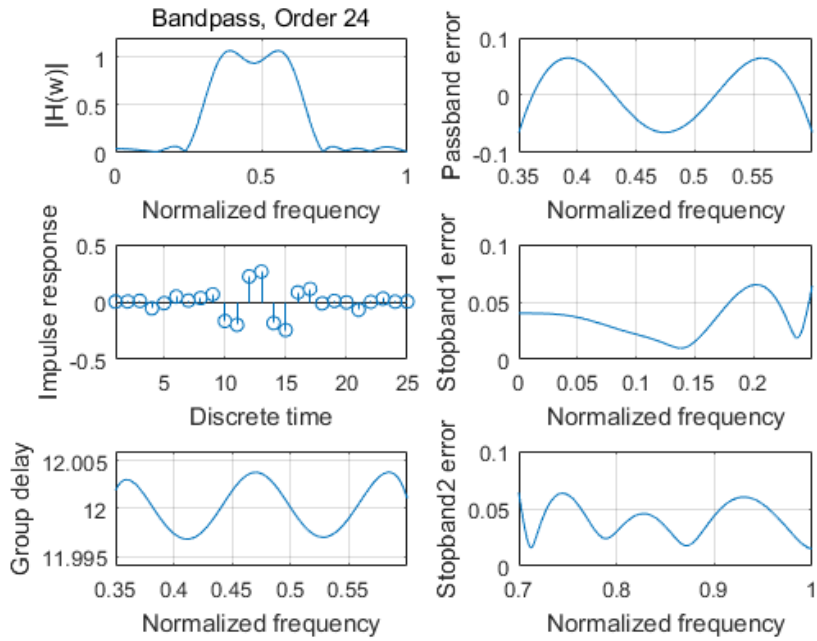


Fig. 4.23 Magnitude response, impulse response, the passband and stopband errors of designed G-FIR bandpass digital filter with group delay in passband at 12 obtained by NSGA-III

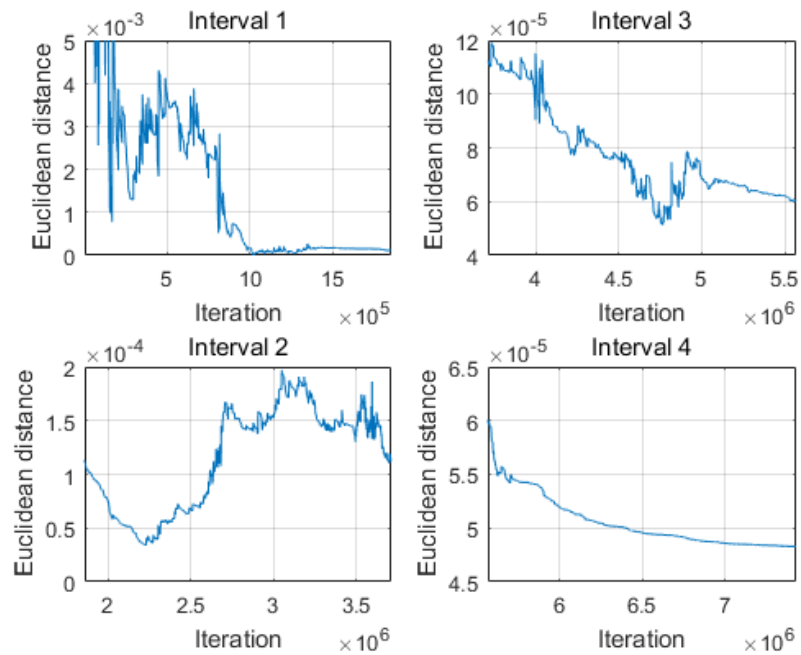


Fig. 4.24 Convergence curve of designed G-FIR bandpass digital filter with group delay in passband at 12 obtained by MOCSA



#### 4.4.3.3 Bandpass Digital Filter with Group Delay in Passband at 14

The filter coefficients of obtained by MOCSA and NSGA-III are listed in Table 4.36. Design results with respect to magnitude error are listed in Table 4.37 while those with respect to group delay error are listed in Table 4.38. The computational record in terms of CPU seconds and number of iterations for reaching convergence are listed in Table 4.39. Plots of the magnitude response, impulse response, the passband and stopband errors of the designed bandpass digital filter are shown in Fig. 4.25 for MOCSA and Fig. 4.26 for NSGA-III, and the convergence curve of MOCSA is plotted in Fig. 4.27.

Table 4.36 Coefficients of bandpass digital filter with group delay in passband at 14

$h(n)$	MOCSA	NSGA-III
$h(0)$	-0.000158409309125	0.002517525690715
$h(1)$	0.000348117438532	0.007987779790538
$h(2)$	-0.000836370771046	0.006655256063427
$h(3)$	0.005662886311499	0.018583905705376
$h(4)$	-0.004189957226333	0.021570973713986
$h(5)$	-0.051407704112385	-0.046034241741658
$h(6)$	-0.002596945210150	-0.016116544127225
$h(7)$	0.058556983789684	0.040725089610432
$h(8)$	0.005938654661087	0.014685464534256
$h(9)$	0.047413121603937	0.033672573884315
$h(10)$	0.050233590169293	0.083943066459743
$h(11)$	-0.188390876086424	-0.131224468729075
$h(12)$	-0.124655209211334	-0.231631888604084
$h(13)$	0.271593472762251	0.176368041149871
$h(14)$	0.219322429154485	0.296888158356687
$h(15)$	-0.243751088508750	-0.125734103869017
$h(16)$	-0.206256973414474	-0.269423074812500
$h(17)$	0.132109787351743	0.053049463881267
$h(18)$	0.093014847013442	0.127020337777304
$h(19)$	-0.016577613863987	-0.000757823734205
$h(20)$	0.002836959499248	0.016622075437980
$h(21)$	-0.014361352264973	0.006523497156257
$h(22)$	-0.073272594365190	-0.074275961850852
$h(23)$	0.012789535852436	-0.011836120482140
$h(24)$	0.022027223026918	0.020102965944567

Table 4.37 Magnitude error of bandpass digital filter with group delay in passband at 14

Algorithm	Peak (Stopband1)	Peak (Passband)	Peak (Stopband2)
MOCSA	0.064549827064764	0.064826771139864	0.064679591909741
NSGA-III	0.064395322900485	0.065337185408170	0.061381925336354

Table 4.38 Group delay error of bandpass digital filter with group delay in passband at 14

Algorithm	Peak (Passband)
MOCSA	0.000008217647183
NSGA-III	0.010551507581969

Table 4.39 Computational record of bandpass digital filter with group delay in passband at 14

Algorithm	CPU Seconds	Iteration
MOCSA	4407.647963	6403848
NSGA-III	191.905443	4491

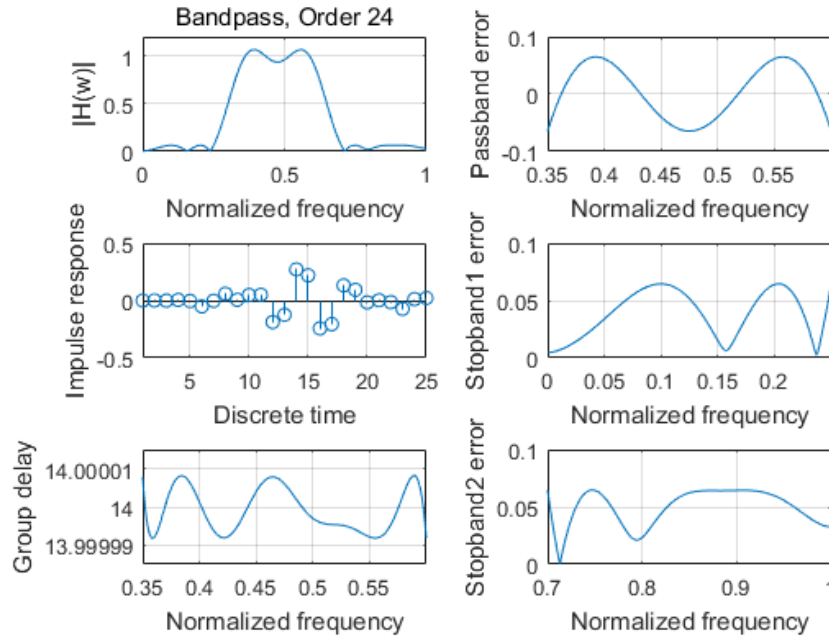


Fig. 4.25 Magnitude response, impulse response, the passband and stopband errors of designed G-FIR bandpass digital filter with group delay in passband at 14 obtained by MOCSA

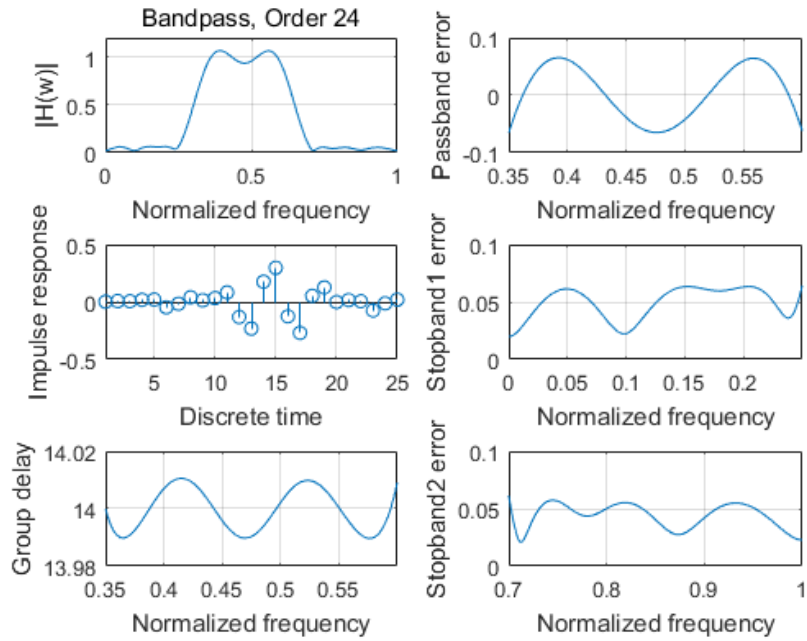


Fig. 4.26 Magnitude response, impulse response, the passband and stopband errors of designed G-FIR bandpass digital filter with group delay in passband at 14 obtained by NSGA-III

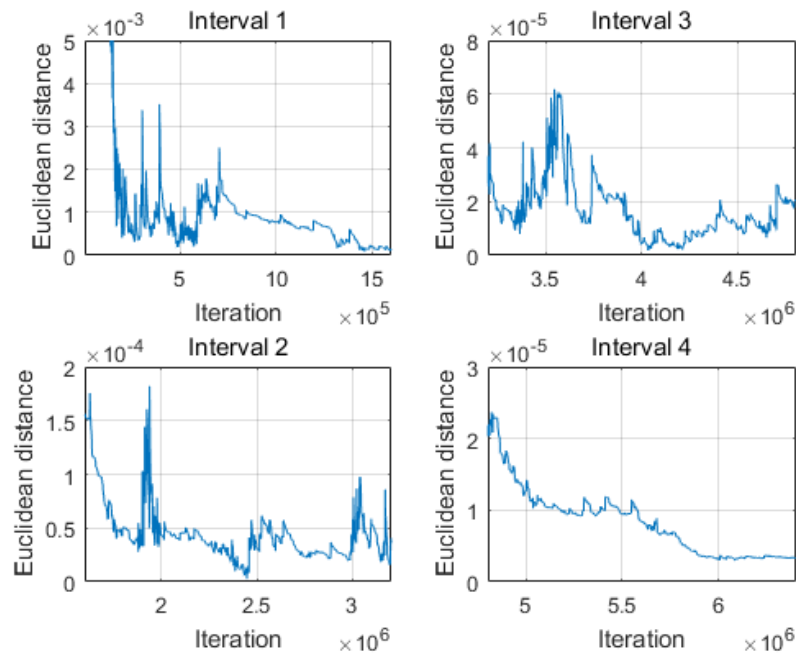


Fig. 4.27 Convergence curve of designed G-FIR bandpass digital filter with group delay in passband at 14 obtained by MOCSA

#### 4.4.4 24th-order Bandstop Digital Filters

##### 4.4.4.1 Bandstop Digital Filter with Group Delay in Passband at 10

The filter coefficients of obtained by MOCSA and NSGA-III are listed in Table 4.40. Design results with respect to magnitude error are listed in Table 4.41 while those with respect to group delay error are listed in Table 4.42. The computational record in terms of CPU seconds and number of iterations for reaching convergence are listed in Table 4.43. Plots of the magnitude response, impulse response, the passband and stopband errors of the designed bandstop digital filter are shown in Fig. 4.28 for MOCSA and Fig. 4.29 for NSGA-III, and the convergence curve of MOCSA is plotted in Fig. 4.30.

Table 4.40 Coefficients of bandstop digital filter with group delay in passband at 10

$h(n)$	MOCSA	NSGA-III
$h(0)$	-0.016271549385357	-0.020891759134752
$h(1)$	-0.044191846217016	-0.035477613233186
$h(2)$	0.043218082019522	0.045409950961097
$h(3)$	0.061899409244757	0.066796459254471
$h(4)$	-0.024809584991104	-0.023197149486721
$h(5)$	-0.034223584964684	-0.040516019189074
$h(6)$	0.003295954738433	0.010395978539926
$h(7)$	-0.072788997928132	-0.076438073724879
$h(8)$	0.035313957311492	0.041839816494008
$h(9)$	0.588573037871458	0.587726752478754
$h(10)$	-0.051247116947269	-0.050086769179649
$h(11)$	0.588185886275092	0.588043756995448
$h(12)$	0.035247287699029	0.042181129053808
$h(13)$	-0.072453372314697	-0.076627542969019
$h(14)$	0.003408699160539	0.009278532554795
$h(15)$	-0.034470988920656	-0.040492736552718
$h(16)$	-0.024931937181908	-0.022148847857980
$h(17)$	0.062052484982118	0.066934431047521
$h(18)$	0.043319253345135	0.044392858866968
$h(19)$	-0.044268952822797	-0.035619743430210
$h(20)$	-0.016337443405922	-0.020256613294678
$h(21)$	0.000029042311447	0.000143832099586
$h(22)$	0.000032479284010	-0.000517808880829

$h(23)$	-0.000007654920649	-0.000105274721732
$h(24)$	-0.000010182566013	0.000220176680256

Table 4.41 Magnitude error of bandstop digital filter with group delay in passband at 10

Algorithm	Peak (Passband1)	Peak (Stopband)	Peak (Passband2)
MOCSA	0.060515728320733	0.060603023881225	0.060604469246464
NSGA-III	0.066005001688474	0.066097315040413	0.065230709820054

Table 4.42 Group delay error of bandstop digital filter with group delay in passband at 10

Algorithm	Peak (Passband)
MOCSA	0.000041857649093
NSGA-III	0.003003702849117

Table 4.43 Computational record of bandstop digital filter with group delay in passband at 10

Algorithm	CPU Seconds	Iteration
MOCSA	433.108879	501553
NSGA-III	463.870783	500001

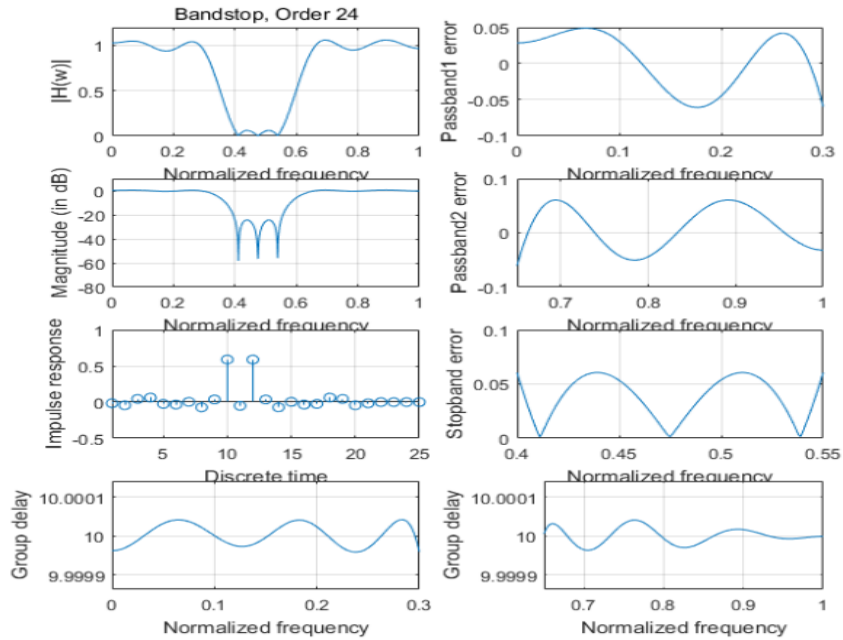


Fig. 4.28 Magnitude response, impulse response, the passband and stopband errors of designed G-FIR bandstop digital filter with group delay in passband at 10 obtained by MOCSA

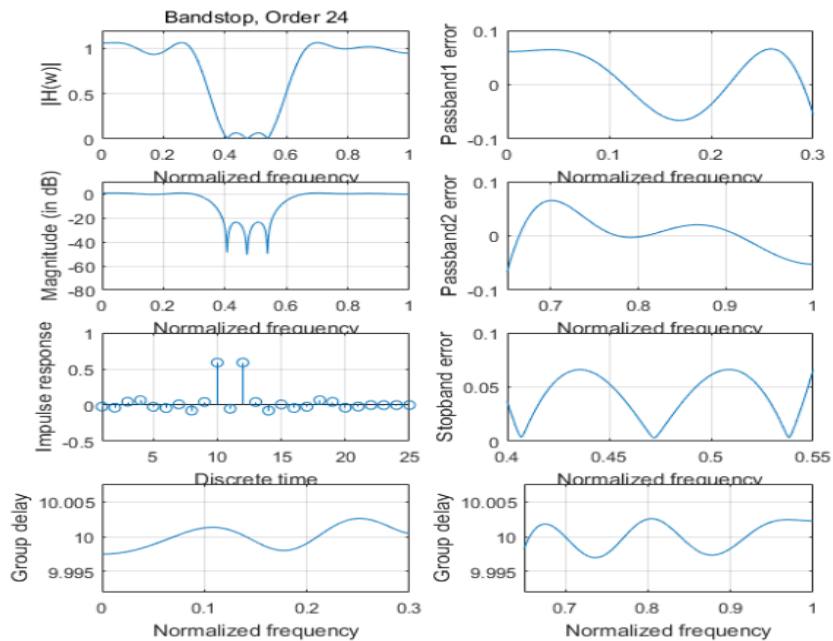


Fig. 4.29 Magnitude response, impulse response, the passband and stopband errors of designed G-FIR bandstop digital filter with group delay in passband at 10 obtained by NSGA-III

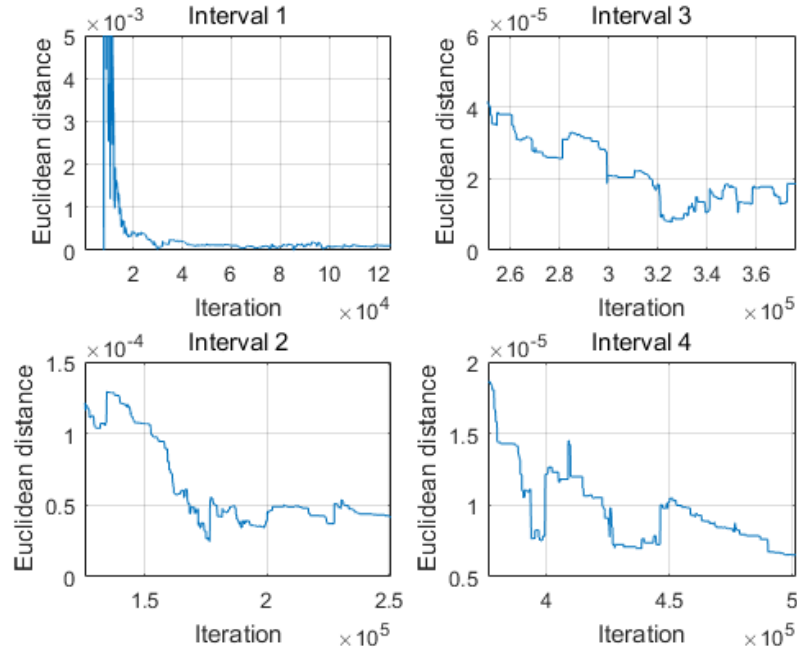


Fig. 4.30 Convergence curve of designed G-FIR bandstop digital filter with group delay in passband at 10 obtained by MOCSA

#### 4.4.4.2 Bandstop Digital Filter with Group Delay in Passband at 12

The filter coefficients of obtained by MOCSA and NSGA-III are listed in Table 4.44. Design results with respect to magnitude error are listed in Table 4.45 while those with respect to group delay error are listed in Table 4.46. The computational record in terms of CPU seconds and number of iterations for reaching convergence are listed in Table 4.47. Plots of the magnitude response, impulse response, the passband and stopband errors of the designed bandstop digital filter are shown in Fig. 4.31 for MOCSA and Fig. 4.32 for NSGA-III, and the convergence curve of MOCSA is plotted in Fig. 4.33.

Table 4.44 Coefficients of bandstop digital filter with group delay in passband at 12

$h(n)$	MOCSA	NSGA-III
$h(0)$	0.016265535979122	-0.005812740708079
$h(1)$	-0.033339532643360	-0.001034575982898
$h(2)$	-0.023377857044211	-0.021855928360500
$h(3)$	0.007037713716130	-0.045151246920947
$h(4)$	-0.003257233431879	0.039052489436224
$h(5)$	0.015763472823043	0.059450970786417

$h(6)$	0.059962584288025	-0.030901174110232
$h(7)$	-0.041258776391504	-0.039038627031482
$h(8)$	-0.145589164010783	-0.000663654945662
$h(9)$	0.044434826701989	-0.076975751560382
$h(10)$	0.223947815053710	0.036369369064707
$h(11)$	-0.019135381416771	0.582045773050688
$h(12)$	0.744099736927598	-0.047870956263024
$h(13)$	-0.019130806211451	0.581810839499140
$h(14)$	0.223948460410035	0.036319485836169
$h(15)$	0.044430928129469	-0.076769765268469
$h(16)$	-0.145590386211484	-0.000611270206111
$h(17)$	-0.041255898236592	-0.039209994637426
$h(18)$	0.059963795480992	-0.030935335698599
$h(19)$	0.015761814946817	0.059563171947518
$h(20)$	-0.003258206770185	0.039083016536470
$h(21)$	0.007038533877668	-0.045203122544525
$h(22)$	-0.023377306845091	-0.021873215240356
$h(23)$	-0.033339805662092	-0.001010326558913
$h(24)$	0.016265343795077	-0.005804285217044

Table 4.45 Magnitude error of bandstop digital filter with group delay in passband at 12

Algorithm	Peak (Passband1)	Peak (Stopband)	Peak (Passband2)
MOCSA	0.053306541094266	0.053028576964483	0.053028890630576
NSGA-III	0.057225380695507	0.057280636850760	0.057000256581570

Table 4.46 Group delay error of bandstop digital filter with group delay in passband at 12

Algorithm	Peak (Passband)
MOCSA	0.000001568313788
NSGA-III	0.000200509782880



Table 4.47 Computational record of bandstop digital filter with group delay in passband at 12

Algorithm	CPU Seconds	Iteration
MOCSA	674.145400	797335
NSGA-III	399.544450	1019667

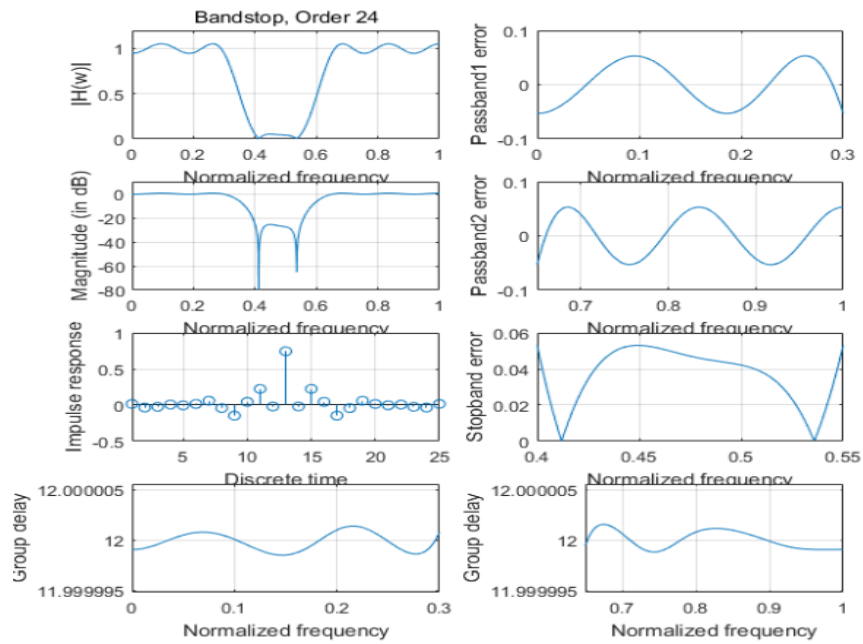


Fig. 4.31 Magnitude response, impulse response, the passband and stopband errors of designed G-FIR bandstop digital filter with group delay in passband at 12 obtained by MOCSA

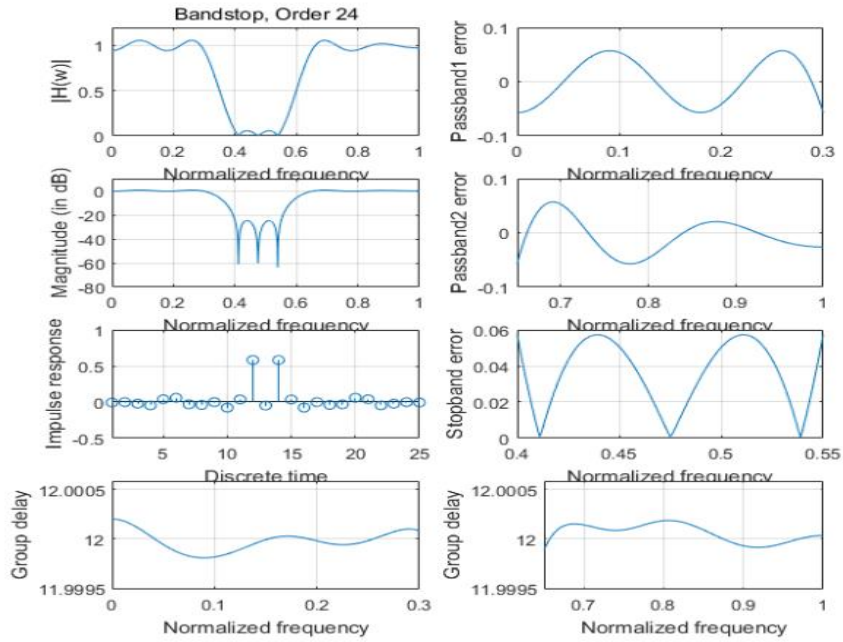


Fig. 4.32 Magnitude response, impulse response, the passband and stopband errors of designed G-FIR bandstop digital filter with group delay in passband at 12 obtained by NSGA-III

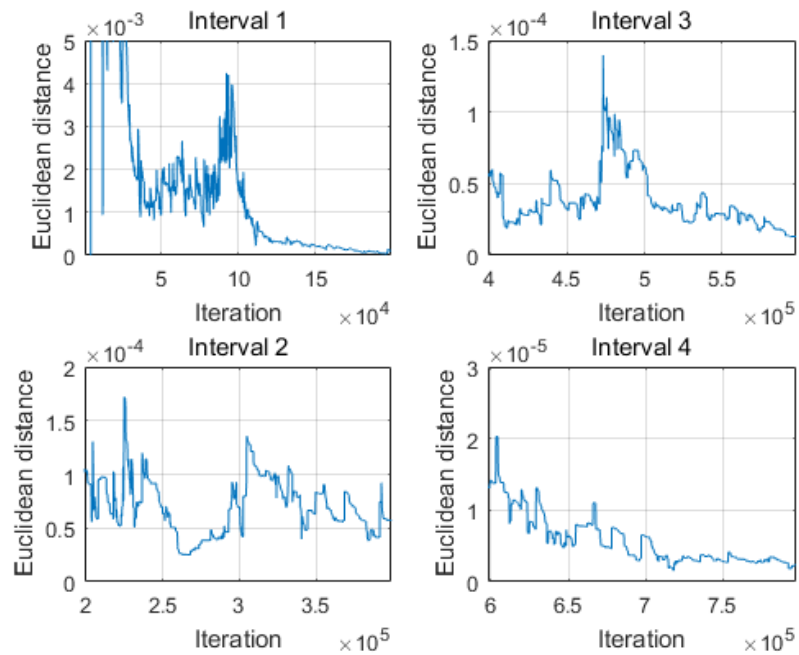


Fig. 4.33 Convergence curve of designed G-FIR bandstop digital filter with group delay in passband at 12 obtained by MOCSA

#### 4.4.4.3 Bandstop Digital Filter with Group Delay in Passband at 14

The filter coefficients of obtained by MOCSA and NSGA-III are listed in Table 4.48. Design results with respect to magnitude error are listed in Table 4.49 while those with respect to group delay error are listed in Table 4.50. The computational record in terms of CPU seconds and number of iterations for reaching convergence are listed in Table 4.51. Plots of the magnitude response, impulse response, the passband and stopband errors of the designed bandstop digital filter are shown in Fig. 4.34 for MOCSA and Fig. 4.35 for NSGA-III, and the convergence curve of MOCSA is plotted in Fig. 4.36.

Table 4.48 Coefficients of bandstop digital filter with group delay in passband at 14

$h(n)$	MOCSA	NSGA-III
$h(0)$	0.000000988620284	-0.000004366673167
$h(1)$	0.000000721967853	-0.000004874317294
$h(2)$	-0.000002984297207	0.000014049071577
$h(3)$	-0.000002693646043	0.000017529101020
$h(4)$	-0.022115813827898	-0.016595845190247
$h(5)$	-0.041499564125230	-0.040567474793168
$h(6)$	0.035345901337625	0.040942683054442
$h(7)$	0.069891482592116	0.060495481052448
$h(8)$	-0.032194074387594	-0.034290101426822
$h(9)$	-0.029748319614457	-0.037528383161795
$h(10)$	-0.005914109023534	-0.002768034113400
$h(11)$	-0.075833408564789	-0.069140345772560
$h(12)$	0.030781729172188	0.036444745407786
$h(13)$	0.587094116939122	0.598006268339232
$h(14)$	-0.050080069900533	-0.047388249848122
$h(15)$	0.587060297909669	0.598206165855378
$h(16)$	0.030775581452847	0.036471816108465
$h(17)$	-0.075803903602138	-0.069310594172484
$h(18)$	-0.005904161097417	-0.002817098154935
$h(19)$	-0.029770301332375	-0.037400583905132
$h(20)$	-0.032204725958382	-0.034236330787208
$h(21)$	0.069905116110613	0.060413985042134
$h(22)$	0.035354927866158	0.040898331330884
$h(23)$	-0.041506551273069	-0.040525140294651
$h(24)$	-0.022121740046043	-0.016566571177104

Table 4.49 Magnitude error of bandstop digital filter with group delay in passband at 14

Algorithm	Peak (Passband1)	Peak (Stopband)	Peak (Passband2)
MOCSA	0.062527047844484	0.062446888080269	0.062298980092027
NSGA-III	0.065215870273564	0.064847515014651	0.064917883976956

Table 4.50 Group delay error of bandstop digital filter with group delay in passband at 14

Algorithm	Peak (Passband)
MOCSA	0.000003997037275
NSGA-III	0.000020395849166

Table 4.51 Computational record of bandstop digital filter with group delay in passband at 14

Algorithm	CPU Seconds	Iteration
MOCSA	3069.845905	2856016
NSGA-III	595.107737	8564

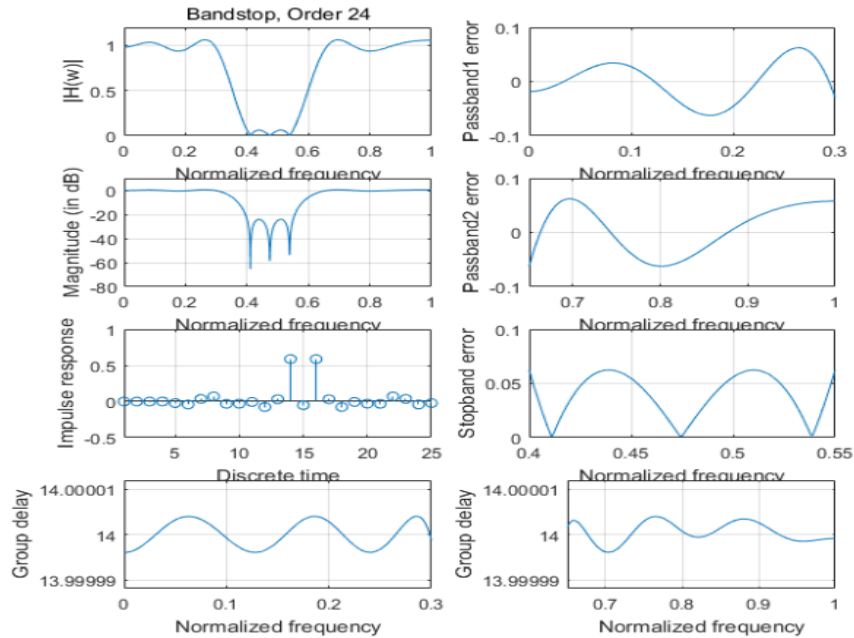


Fig. 4.34 Magnitude response, impulse response, the passband and stopband errors of designed G-FIR bandstop digital filter with group delay in passband at 14 obtained by MOCSA

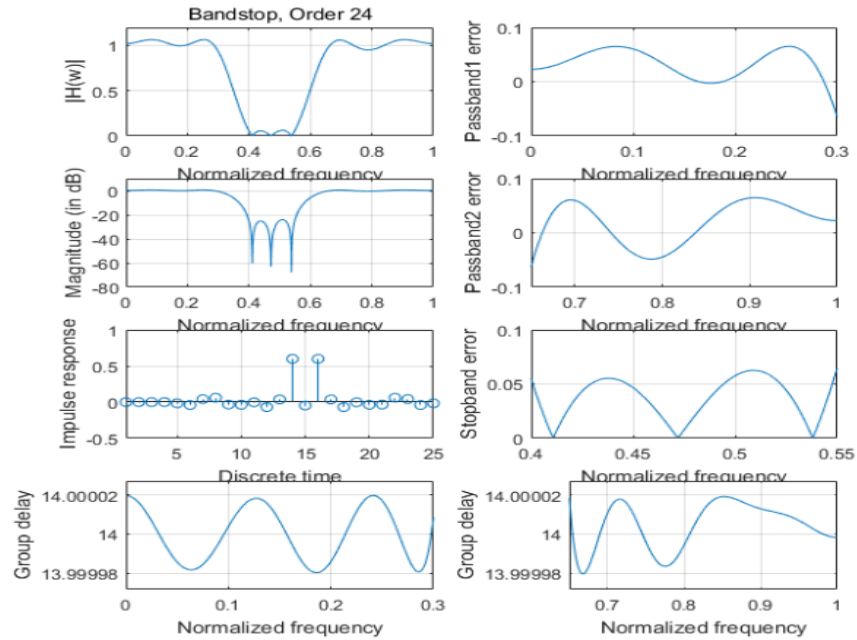


Fig. 4.35 Magnitude response, impulse response, the passband and stopband errors of designed G-FIR bandstop digital filter with group delay in passband at 14 obtained by NSGA-III

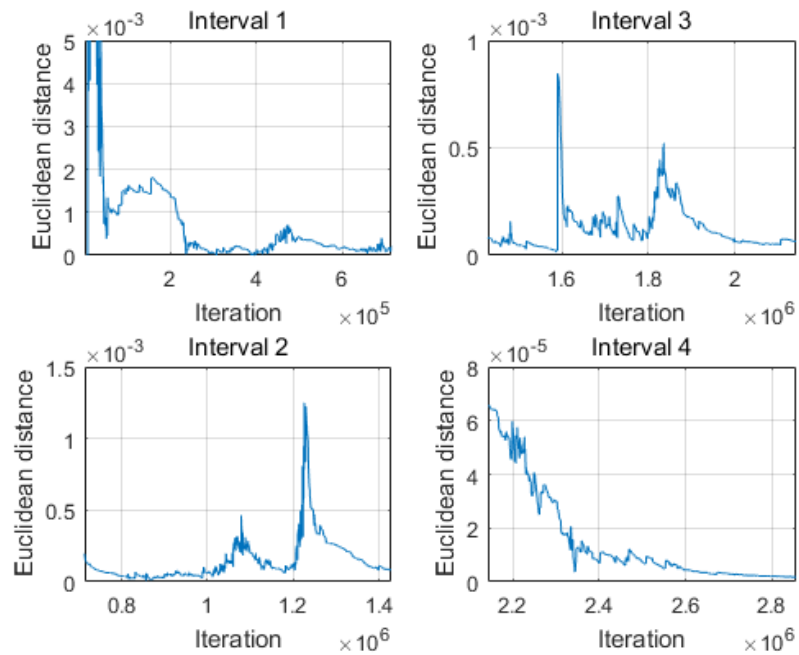


Fig. 4.36 Convergence curve of designed G-FIR bandstop digital filter with group delay in passband at 14 obtained by MOCSA

## 4.5 Conclusion

This chapter has presented the design of general FIR digital filters using multiobjective Cuckoo Search Algorithm. 24th-order lowpass, highpass, bandpass and bandstop digital filters with group delay in passband at 10, 12 or 14 are chosen for the design and their results are obtained. The design results have shown that the peak errors of both magnitude response and group delay in passband obtained by MOCSA are mostly smaller than those obtained by NSGA-III. This denotes that the performance of MOCSA compares favorably with that of NSGA-III certifying the validity and practicability of MOCSA.

MOCSA incorporates a method of Euclidean distance rather than Pareto Front used in NSGA-III. The Pareto Front mainly collects a set of non-dominated solutions but without further objective-based optimal equilibration such that it is difficult to determine which non-dominated solution is the most feasible one that satisfies all the objective functions balancedly at the optimal equilibrating level. It requires more comparing standard or objective-configuration which may increase uncertainty and inaccuracy of subsequent operations.

Nevertheless, the method of Euclidean distance is capable of combining objective-based equilibrating operations and the searching for the optimal solution into one simple step. An Euclidean space is formulated where each objective function represents one of its dimension. It combines separate objective functions into an abstract mathematical spatial model. A changing current ideal spatial point is located according to the best values of all the objective functions that has ever obtained so far, which has become an ideal goal for the optimized population to pursue. A smaller Euclidean distance between the current ideal spatial point and another Euclidean spatial point resulting from a candidate solution implies this solution is more qualified as it obtains a set of objective outputs closer to the ideal ones. During the calculation of Euclidean distance, each objective function has been equilibrated to a coordinative level due to the equal weight for its corresponding dimension. Meanwhile, the best solution can be easily determined after a simple comparison of distinct Euclidean distances. Thus, MOCSA using a method of Euclidean distance shall be a more effective and persuasive technique than NSGA-III using Pareto Front. Design results of general FIR digital filters obtained by MOCSA compare favorably with those of NSGA-III.

## CHAPTER 5 IIR Digital Filter Design Using Constrained Multiobjective Cuckoo Search Algorithm

### 5.1 Introduction

Chapter 4 presents a successful design of general FIR digital filters using multiobjective Cuckoo Search Algorithm. In addition, another possible application for MOCSA may be linear-phase IIR digital filter design. So far several researches on IIR digital filter design using multiobjective algorithms have been proposed. Yu Wang introduced a framework to apply different multiobjective evolutionary algorithms in [21], then an early multiobjective algorithm, NSGA-II, was implemented on a lower-order IIR digital filter design in [22] and the results were persuasive. This arises an interest on whether MOCSA can be applied on the same practical application.

Compared to FIR filter design, IIR filter design requires several limitations to obtain a reasonable result. These limitations include stability constraints and magnitude control and so on. However, the previous MOCSA only concerns about satisfying the given objective functions. If any specific condition is required, MOCSA may not be able to take account of as it is operated without limitations. In such case, it is necessary to derive some suitable improvement for MOCSA in adapt to such multiobjective optimization problems with specific constraints.

In this chapter, an improving version of MOCSA called constrained multiobjective Cuckoo Search Algorithm is presented for IIR digital filter design. This improving approach adopts a constrained Euclidean distance to incorporate other constraints into the evaluation of the quality of a solution. As an illustration, several examples of cascade-form IIR digital filter design are proposed and their results are compared to those of the state-of-the-art design in [23].

### 5.2 Constrained Multiobjective Cuckoo Search Algorithm

Constrained multiobjective Cuckoo Search Algorithm follows the steps of the original MOCSA described in sections 3.1 and 4.2. Suppose an minimization problem is further subjected to  $Q$  inequality constraints, which are expressed in terms of

$$g_q(\mathbf{x}) \leq 0 \quad \text{for } q = 1 \text{ to } Q \quad (5.1)$$

Meanwhile, for any inequality constraint in terms of  $s(\mathbf{x}) \geq 0$ , it can be converted into an expression of  $-s(\mathbf{x}) \leq 0$  such that

$$g(\mathbf{x}) = -s(\mathbf{x}) \leq 0 \quad (5.2)$$

which means any arbitrary inequality constraint can be expressed in terms of (5.1).

To evaluate whether all the inequality constraints are satisfied, a penalty factor  $\eta$  is defined by

$$\eta = \sum_{q=1}^Q \left[ \varphi \left( g_q(\mathbf{x}) \right) \right]^2 \quad (5.3)$$

where  $\varphi(x)$  is a sectional-continuous function defined as

$$\varphi(x) = \begin{cases} 0 & x \leq 0 \\ x & x > 0 \end{cases} \quad (5.4)$$

Then the penalty factor  $\eta$  is merged with the original Euclidean distance and a constrained Euclidean distance is formulated by

$$d_{cons}(\mathbf{z}, \mathbf{x}) = \sqrt{\sum_{m=1}^M [f_m(\mathbf{x}) - z_m^{\min}]^2 + \eta} \quad (5.5)$$

where (5.5) can be expressed more precisely that

$$d_{cons}(\mathbf{z}, \mathbf{x}) = \sqrt{\sum_{m=1}^M [f_m(\mathbf{x}) - z_m^{\min}]^2 + \sum_{q=1}^Q \left[ \varphi \left( g_q(\mathbf{x}) \right) \right]^2} \quad (5.6)$$

If any one or more inequality constraints are not satisfied, the penalty factor  $\eta$  will be a positive value due to a positive quadratic sum, which will enlarge the Euclidean distance. When compared with other potential solutions, one with a larger constrained Euclidean distance will be less capable to be selected. Otherwise, if all the inequality constraints are satisfied, the penalty factor  $\eta$  will become zero such that these satisfied constraints will no longer have an effect on the Euclidean distance.

By the use of penalty factor and constrained Euclidean distance, inequality constraints are now taken into consideration that those solutions which satisfy the constraints would have a higher chance to be chosen.

### 5.3 Design of IIR Digital Filters

For convenience, suppose that both the denominator and the numerator of a transfer function are of the same order. The cascade-form transfer function of an even  $N$ th-order IIR digital filter can be [1].

$$H(z) = b_0 \prod_{n=1}^{N/2} \frac{1 + b_{1n}z^{-1} + b_{2n}z^{-2}}{1 + a_{1n}z^{-1} + a_{2n}z^{-2}} \quad (5.7)$$



where  $b_{1n}$  and  $a_{1n}$  for  $i = 1, 2$  and  $n = 1$  to  $N/2$  are real-valued coefficients, and  $b_0$  is a scaling constant. The corresponding coefficient vector  $\mathbf{c}$  consisting of  $(2N + 1)$  distinct coefficients can be formulated by

$$\mathbf{c} = [b_{11} \quad b_{21} \quad a_{11} \quad a_{21} \quad \cdots \quad a_{1,N/2} \quad a_{2,N/2} \quad b_0]^T \quad (5.8)$$

The stability condition of an IIR digital filter is

$$\begin{cases} -2 < a_{1i} < 2 \\ -1 < a_{2i} < 1 \\ a_{2i} > |a_{1i}| - 1 \end{cases} \quad \text{for } i = 1 \text{ to } N/2 \quad (5.9)$$

The group delay  $\tau(w)$  can be expressed as

$$\tau(w) = -\frac{\partial \theta(w)}{\partial wT} \quad (5.10)$$

The relationship between the maximum passband ripple  $R_p$  (in dB) and its corresponding peak error in passband magnitude response  $\delta_p$  [24] is

$$\delta_p = \mathcal{P}(R_p) = \frac{10^{R_p/20} - 1}{10^{R_p/20} + 1} \quad (5.11)$$

Similarly, the relationship between the minimum stopband attenuation  $A_s$  (in dB) and its corresponding peak error in stopband magnitude response  $\delta_s$  [24] is

$$\delta_s = \mathcal{S}(A_s) = 10^{-A_s/20} \quad (5.12)$$

The max-error function of passband magnitude response  $e_{mag,p}(\mathbf{c})$  can be calculated by

$$e_{mag,p}(\mathbf{c}) = \max_{\mathbf{c}} | |H(\mathbf{c}, w_i)| - 1 | \quad (5.13)$$

for  $i = I_{w_{p1}}$  to  $I_{w_{p2}}$ ;  $w_{p1} \leq w_i \leq w_{p2}$

Then the objective function of passband magnitude response is derived as

$$f_{mag,p}(\mathbf{c}) = \varphi(e_{mag,p}(\mathbf{c}) - \mathcal{P}(R_{p0})) \quad (5.14)$$

where  $R_{p0}$  is the required maximum passband ripple;  $\varphi(x)$  is the same sectional-continuous function defined in (5.4) that

$$\varphi(x) = \begin{cases} 0 & x \leq 0 \\ x & x > 0 \end{cases} \quad (5.15)$$

Similarly, the max-error function of stopband magnitude response  $e_{mag,s}(\mathbf{c})$  can be calculated by

$$e_{mag,s}(\mathbf{c}) = \max_{\mathbf{c}} |H(\mathbf{c}, w_i)| \quad (5.16)$$

for  $i = I_{w_{s1}}$  to  $I_{w_{s2}}$ ;  $w_{s1} \leq w_i \leq w_{s2}$

Then the objective function of stopband magnitude response is derived as

$$f_{mag,s}(\mathbf{c}) = \varphi(e_{mag,s}(\mathbf{c}) - \mathcal{S}(A_{s0})) \quad (5.17)$$

where  $A_{s0}$  is the required minimum stopband attenuation.

The max-error function of the group delay response in passband  $e_{gd}(\mathbf{c})$  can be calculated by

$$e_{gd}(\mathbf{c}) = \max_{\mathbf{c}} |\tau(\mathbf{c}, w_i) - \tau_d| \quad (5.18)$$

for  $i = I_{w_{p1}}$  to  $I_{w_{p2}}$ ;  $w_{p1} \leq w_i \leq w_{p2}$

where  $\tau_d$  is the prescribed group delay in passband.

Then the objective function of passband group delay response is derived as

$$f_{gd}(\mathbf{c}) = \varphi(e_{gd}(\mathbf{c}) - \delta_{gd}) \quad (5.19)$$

where  $\delta_{gd}$  is the required passband group delay error.

From (5.14), (5.17) and (5.19), these three objective functions can be summarized as positive excessive errors beyond error-based requirements with respect to maximum errors of magnitude response in passband and in stopband as well as that of group delay in passband. While any one of the error-based requirements is satisfied, the values of its corresponding objective function would be reduced to zero.

To prevent the magnitude response in the transition band from exceeding its required maximum value, a magnitude limitation for transition band can be applied such that

$$H(\mathbf{c}, w_i) \leq 1 \quad (5.20)$$

for  $i = I_{w_{t1}}$  to  $I_{w_{t2}}$ ;  $w_i \in \mathbf{T}$

where  $\mathbf{T}$  is the transition band;

Afterwards, (5.20) can be converted into an inequality constraint that

$$\begin{aligned} \mathbf{g}(\mathbf{c}) &= \max_{\mathbf{c}}(H(\mathbf{c}, w_i) - 1) \leq 0 \\ &\text{for } i = I_{w_{t1}} \text{ to } I_{w_{t2}}; w_i \in \mathbf{T} \end{aligned} \quad (5.21)$$

The multiobjective optimization problem for the IIR digital filter design is searching for an optimal coefficient vector  $\mathbf{c}$  that minimizes the objective functions  $f_{mag,p}(\mathbf{c})$ ,  $f_{mag,s}(\mathbf{c})$  and  $f_{gd}(\mathbf{c})$ , subjected to  $\mathbf{g}(\mathbf{c}) \leq 0$ , simultaneously.

#### 5.4 Design Examples and Results

In this section, three examples with respect to cascade-form IIR lowpass, highpass and bandpass digital filters are designed. Constrained MOCSA is applied to optimize several randomly initialized coefficient vectors  $\mathbf{c}$  described in (5.8) to reach an optimal solution which minimizes the objective functions  $f_{mag,p}(\mathbf{c})$ ,  $f_{mag,s}(\mathbf{c})$  and  $f_{gd}(\mathbf{c})$  subjected to  $\mathbf{g}(\mathbf{c}) \leq 0$  simultaneously as shown in (5.14), (5.17), (5.19) and (5.21).

In each iteration during the optimization process, all coefficient pairs  $(a_{1,n}, a_{2,n})$  for  $n = 1$  to  $N/2$ , derived from a coefficient vector  $\mathbf{c}$ , is checked by the stability condition as shown in (5.9). If one coefficient exceeds any of its bounds, it will automatically be limited to a value that is a little deviated from that bound within the available range.

Then the cascade-form IIR digital filter design is regarded as a 3-objective and 1-constrained minimization problem. The objective functions and inequality constraint are

$$f_1(\mathbf{c}) = f_{mag,p}(\mathbf{c}) \quad (5.22)$$

$$f_2(\mathbf{c}) = f_{mag,s}(\mathbf{c}) \quad (5.23)$$

$$f_3(\mathbf{c}) = f_{gd}(\mathbf{c}) \quad (5.24)$$

$$\mathbf{g}_1(\mathbf{c}) = \mathbf{g}(\mathbf{c}) \leq 0 \quad (5.25)$$

To evaluate the performance of the obtained results, maximum passband ripple  $R_p$  and minimum stopband attenuation  $A_s$  are used for evaluating the magnitude response. Besides, the maximum group delay deviation  $Q_\tau$  is used for evaluating the obtained group delay in passband [23]. They can be expressed as

$$R_p = \mathcal{P}^{-1}(\delta_p) = 20 \log \frac{1+\delta_p}{1-\delta_p} \quad \text{dB} \quad (5.26)$$

$$A_s = \mathcal{S}^{-1}(\delta_s) = -20 \log \delta_s \quad \text{dB} \quad (5.27)$$

$$Q_\tau = \frac{100(\tau_{max} - \tau_{min})}{2\tau_{ave}} \quad (5.28)$$

$$\tau_{ave} = \frac{\tau_{max} + \tau_{min}}{2} \quad (5.29)$$

$$\tau_{max} = \max_{w_{p1} \leq w_i \leq w_{p2}} \tau(\mathbf{c}, w_i) \quad (5.30)$$

$$\tau_{min} = \min_{w_{p1} \leq w_i \leq w_{p2}} \tau(\mathbf{c}, w_i) \quad (5.31)$$

The parameters of constrained MOCSA are listed in Table 5.1. The adopted frequency grids for optimization and for evaluating the peak errors of magnitude response and group delay are shown in Table 5.2. The optimization procedure is terminated when the value of constrained Euclidean distance from the best solution reaches zero. All the optimization designs are carried out using an Intel(R) Core(TM) i7-5500U CPU, 2.40 GHz with 8GB RAM laptop computer. The design results obtained by constrained MOCSA is compared with the state-of-the-art methods in [23].

Table 5.1 Parameters of constrained MOCSA

Symbol	Description	Example number		
		1	2	3
$c_{bn}^{[U]}$	Upper bound of filter numerator coefficients	10	10	10
$c_{bn}^{[L]}$	Lower bound of filter numerator coefficients	-10	-10	-10
$c_{a_{1n}}^{[U]}$	Upper bound of filter denominator coefficients	2	2	2
$c_{a_{1n}}^{[L]}$	Lower bound of filter denominator coefficients	-2	-2	-2
$c_{a_{2n}}^{[U]}$	Upper bound of filter denominator coefficients	1	1	1
$c_{a_{2n}}^{[L]}$	Lower bound of filter denominator coefficients	-1	-1	-1
$P_C$	Constrained MOCSA population size	25	25	25
$\beta$	Constrained MOCSA parameter	1.5	1.5	1.5
$\alpha$	Constrained MOCSA parameter	0.01	0.01	0.01
$p_a$	Constrained MOCSA parameter	0.25	0.25	0.25
$M$	Number of objective functions	3	3	3
$Q$	Number of inequality constraints	1	1	1

Table 5.2 Frequency grids for IIR digital filter design

Optimization	$F_o = [0: 0.001: 1]$
Peak error evaluation	$F_{mag} = [0: 0.001: 1]$

### 5.4.1 Example 1

A 10th-order IIR lowpass digital filter is taken as Example 1. The filter specification is listed in Table 5.3. Performance requirements of the designed lowpass digital filter is listed in Table 5.4. Design results obtained by constrained MOCSA and the state-of-the-art methods in [23] are listed in Table 5.5. The computational record in terms of CPU seconds and number of iterations for reaching convergence are listed in Table 5.6. The filter coefficients are listed in Table 5.7. Plots of the magnitude response, group delay response in passband of the designed lowpass digital filter is plotted in Fig. 5.1, and its convergence curve is plotted in Fig. 5.2.

Table 5.3 Filter specification of designed IIR lowpass digital filter in Example 1

Parameters	Values
Filter order $N$	10
Prescribed group delay in passband $\tau_d$	9.794
Passband cutoff frequency $w_p$	$0.4\pi$
Stopband cutoff frequency $w_s$	$0.56\pi$

Table 5.4 Performance requirements of designed IIR lowpass filter in Example 1

Parameters	Values
Maximum Passband Ripple $R_p$ (in dB)	0.2062
Minimum Stopband Attenuation $A_s$ (in dB)	50
Maximum Passband Group Delay Error $\delta_{gd}$	0.0156

Table 5.5 Design results of the IIR lowpass digital filter in Example 1

Item	Constrained MOCSA	Design 6A-2 [23]
$\tau_{ave}$	9.794399577864011	9.794423016597630
Peak Error (Passband Magnitude)	0.011868683611219	0.011870695865662
Peak Error (Stopband Magnitude)	0.003161351898799	0.003162390333019
Peak Error (Passband Group Delay)	0.015562525173081	0.015596828111102
Max PB Ripple (in dB)	0.206189834044407	0.206224795410127
Min SB Attenuation (in dB)	50.002543179060879	49.999690524800108
Peak Group Delay Deviation $Q_\tau$	0.158652772086015	0.159006931670001

Table 5.6 Computational record of designed IIR lowpass digital filter in Example 1

CPU Seconds	Iteration
19452.414738	27405467

Table 5.7 Coefficients of designed IIR lowpass digital filter in Example 1

Coefficients	Constrained MOCSA	Design 6A-2 [23]
$b_{11}$	0.771233721582970	-3.12106567253477
$b_{21}$	0.905174158410587	2.68530049526446
$a_{11}$	-1.117788398030811	-0.11179975016549
$a_{21}$	0.319475690574235	0.889727435575185
$b_{12}$	-1.910332982693807	-1.90790617507112
$b_{22}$	2.532382059156775	2.52337146187117
$a_{12}$	-1.017729282085868	-0.274378028479404
$a_{22}$	0.412836443260116	0.501262056741384
$b_{13}$	1.607196259736642	1.5787090685769
$b_{23}$	0.858482285837439	0.826473842394122
$a_{13}$	-0.255912675115420	-0.54060105290066
$a_{23}$	0.504065894027731	0.43671035480304
$b_{14}$	0.413684290551802	0.414726315268322
$b_{24}$	0.986487015072431	0.987612884176495
$a_{14}$	-0.547622269093634	-1.01380963236256
$a_{24}$	0.447122449946612	0.40886408235382
$b_{15}$	-3.124584784917951	0.774046366958724
$b_{25}$	2.691982199025045	0.901783828125454

$a_{15}$	-0.108542060596776	-1.10861455395675
$a_{25}$	0.889736068014168	0.313607374418091
$b_0$	0.007869661374600	0.008027005381132

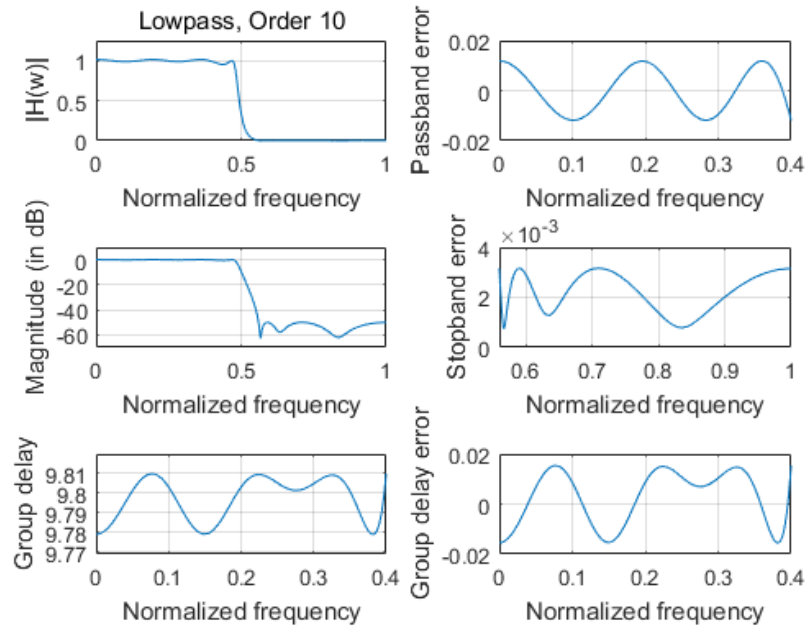


Fig. 5.1 Magnitude, group delay, magnitude errors and group delay errors of designed IIR lowpass digital filter in Example 1 obtained by constrained MOCSA

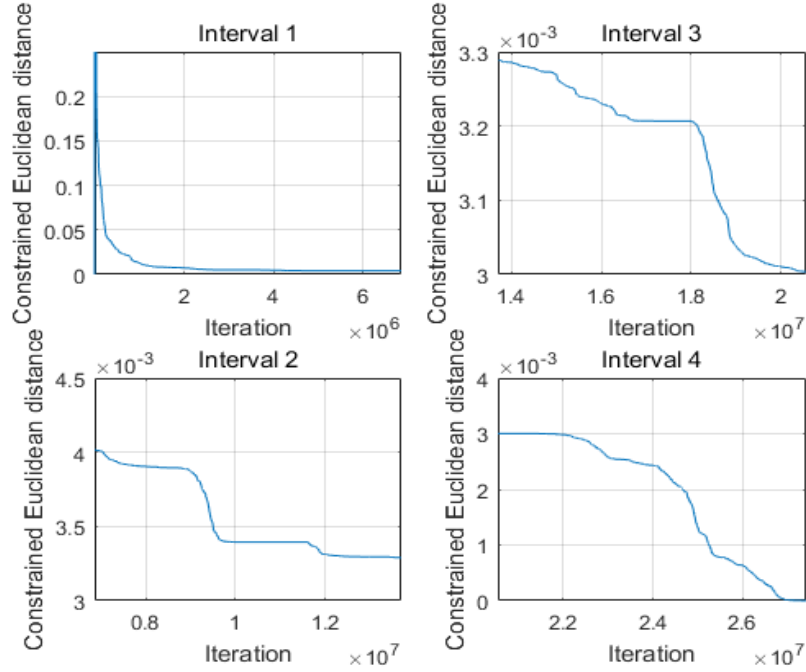


Fig. 5.2 Convergence curve of designed IIR lowpass digital filter in Example 1 obtained by constrained MOCSA

### 5.4.2 Example 2

A 14th-order IIR highpass digital filter is taken as Example 2. The filter specification is listed in Table 5.8. Performance requirements of the designed highpass digital filter is listed in Table 5.9. Design results obtained by constrained MOCSA and the state-of-the-art methods in [23] are listed in Table 5.10. The computational record in terms of CPU seconds and number of iterations for reaching convergence are listed in Table 5.11. The filter coefficients are listed in Table 5.12. Plots of the magnitude response, group delay response in passband of the designed highpass digital filter is plotted in Fig. 5.3, and its convergence curve is plotted in Fig. 5.4.

Table 5.8 Filter specification of designed IIR highpass digital filter in Example 2

Parameters	Values
Filter order $N$	14
Prescribed group delay in passband $\tau_d$	18.026
Passband cutoff frequency $w_p$	$0.4\pi$
Stopband cutoff frequency $w_s$	$0.6\pi$



Table 5.9 Performance requirements of designed IIR highpass filter in Example 2

Parameters	Values
Maximum Passband Ripple $R_p$ (in dB)	0.1
Minimum Stopband Attenuation $A_s$ (in dB)	73.5
Maximum Passband Group Delay Error $\delta_{gd}$	0.0048

Table 5.10 Design results of the IIR highpass digital filter in Example 2

Item	Constrained MOCSA	Design 2A-2 [23]
$\tau_{ave}$	18.024797027462974	18.026183112666885
Peak Error (Passband Magnitude)	0.005755947749258	0.006790271254761
Peak Error (Stopband Magnitude)	0.000205391481994	0.000211274606277
Peak Error (Passband Group Delay)	0.004799635706881	0.004808198009012
Max PB Ripple (in dB)	0.099992158112681	0.117960906457033
Min SB Attenuation (in dB)	73.748351428970849	73.503053979105616
Peak Group Delay Deviation $Q_\tau$	0.026277766619671	0.026673411553407

Table 5.11 Computational record of designed IIR highpass digital filter in Example 2

CPU Seconds	Iteration
38942.358445	50095881

Table 5.12 Coefficients of designed IIR highpass digital filter in Example 2

Coefficients	Constrained MOCSA	Design 2A-2 [23]
$b_{11}$	5.060640991321257	2.21835429452429
$b_{21}$	-5.019206348621768	2.85636737945374
$a_{11}$	1.109283021817947	0.259174061827646
$a_{21}$	0.475407010949268	0.891680083261076
$b_{12}$	1.306267431645476	2.98641105930971
$b_{22}$	1.953911704067707	2.31138312475541
$a_{12}$	0.930969293040202	0.45712541764001
$a_{22}$	0.537619813502240	0.661037748241962
$b_{13}$	-0.670738540599476	2.64495424169767
$b_{23}$	1.015415666665229	2.39779691098628

$a_{13}$	1.280377872186614	0.649627461625722
$a_{23}$	0.486812281485523	0.548167411024861
$b_{14}$	2.263858421551114	1.35635467775126
$b_{24}$	2.158583043342977	2.18981357486249
$a_{14}$	1.376323244637665	0.904591938293396
$a_{24}$	0.481391755065284	0.505675195044766
$b_{15}$	-1.069402626965190	-1.82897334812934
$b_{25}$	0.939896398151080	1.00853880306649
$a_{15}$	0.477038373055354	1.09139256637325
$a_{25}$	0.673183430442082	0.476325040367744
$b_{16}$	0.907329377690136	-0.663358215601436
$b_{26}$	-1.289172501422315	0.998194138629152
$a_{16}$	0.660274773066742	1.27777133174557
$a_{26}$	0.551753628134415	0.475588825228783
$b_{17}$	2.982818383049278	-1.06177430783363
$b_{27}$	2.445302046485580	0.990742722296121
$a_{17}$	0.278163655075763	1.32115805301893
$a_{27}$	0.890352066477236	0.441010398317931
$b_0$	0.000139015122317	0.000425484520156998

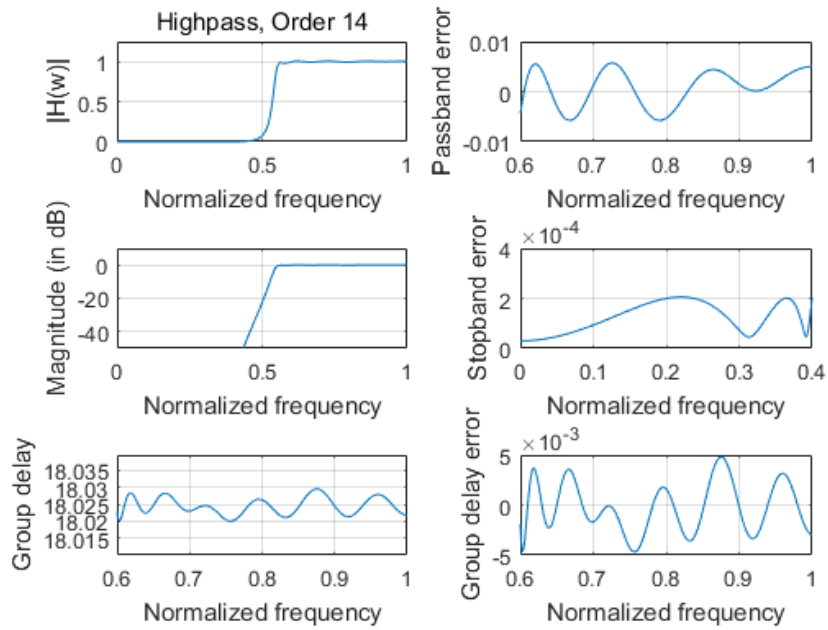


Fig. 5.3 Magnitude, group delay, magnitude errors and group delay errors of designed IIR highpass digital filter in Example 2 obtained by constrained MOCSA

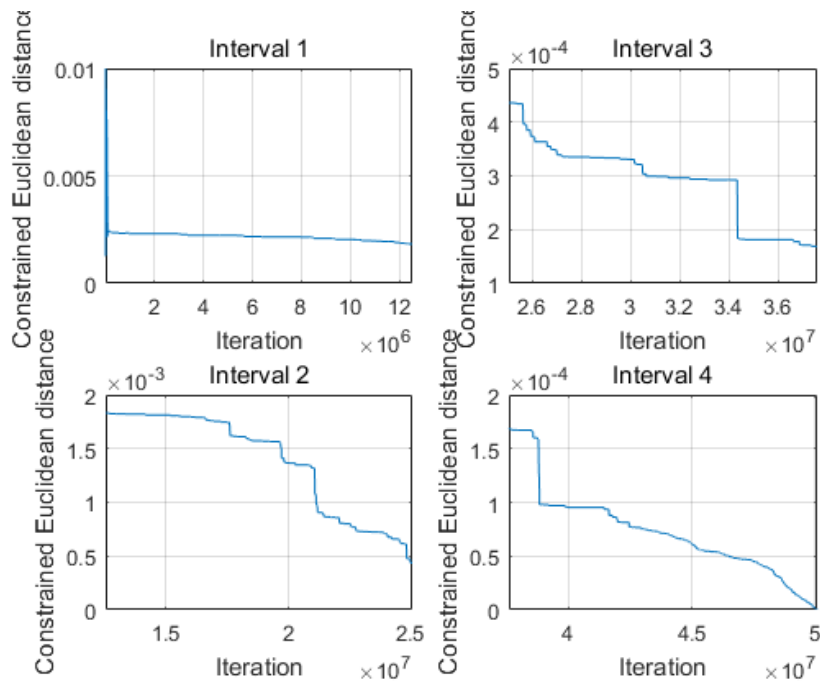


Fig. 5.4 Convergence curve of designed IIR highpass digital filter in Example 2 obtained by constrained MOCSA

### 5.4.3 Example 3

A 14th-order IIR bandpass digital filter is taken as Example 3. The filter specification is listed in Table 5.13. Performance requirements of the designed bandpass digital filter is listed in Table 5.14. Design results obtained by constrained MOCSA and the state-of-the-art methods in [23] are listed in Table 5.15. The computational record in terms of CPU seconds and number of iterations for reaching convergence are listed in Table 5.16. The filter coefficients are listed in Table 5.17. Plots of the magnitude response, group delay response in passband of the designed bandpass digital filter is plotted in Fig. 5.5, and its convergence curve is plotted in Fig. 5.6.

Table 5.13 Filter specification of designed IIR bandpass digital filter in Example 3

Parameters	Values
Filter order $N$	14
Prescribed group delay in passband $\tau_d$	25.542
Stopband1 cutoff frequency $w_{s1}$	$0.2\pi$
Passband lower cutoff frequency $w_{p1}$	$0.3\pi$
Passband higher cutoff frequency $w_{p2}$	$0.5\pi$
Stopband2 cutoff frequency $w_{s2}$	$0.7\pi$

Table 5.14 Performance requirements of designed IIR bandpass filter in Example 3

Parameters	Values
Maximum Passband Ripple $R_p$ (in dB)	1
Minimum Stopband Attenuation $A_s$ (in dB)	41.37
Maximum Passband Group Delay Error $\delta_{gd}$	0.000323

Table 5.15 Design results of the IIR bandpass digital filter in Example 3

Item	Constrained MOCSA	Design 3A-2 [23]
$\tau_{ave}$	25.542422471444112	25.542193451951263
Peak Error (Passband Magnitude)	0.058398293388670	0.059398878295131
Peak Error (Stopband Magnitude)	0.008544695889586	0.008544696148768
Peak Error (Passband Group Delay)	0.000322896688463	0.000322978540844
Max PB Ripple (in dB)	1.015637878550494	1.033080328785178
Min SB Attenuation (in dB)	41.366067788941137	41.366067525475572
Peak Group Delay Deviation $Q_\tau$	0.001264111086021	0.001264490230447

Table 5.16 Computational record of designed IIR bandpass digital filter in Example 3

CPU Seconds	Iteration
40036.549898	50463991

Table 5.17 Coefficients of designed IIR bandpass digital filter in Example 3

Coefficients	Constrained MOCSA	Design 3A-2 [23]
$b_{11}$	-1.189945600692348	-2.59581077068361
$b_{21}$	1.434683922568414	1.6149887104464
$a_{11}$	-0.987788975162247	0.153429290303372
$a_{21}$	0.737464115433211	0.799478405171291
$b_{12}$	1.275283578445253	-1.65640776341346
$b_{22}$	1.519471639766574	0.997535372573892
$a_{12}$	-0.544357075412447	-0.009433276703322
$a_{22}$	0.653531537053280	0.705563625173497
$b_{13}$	-2.596205173320341	-1.19002732412408
$b_{23}$	1.615988246270158	1.43432461034507
$a_{13}$	-0.677654407368676	-1.16782796759126
$a_{23}$	0.667832499113604	0.81379190616821
$b_{14}$	-1.654703801518034	-0.61539101425476
$b_{24}$	0.995533015368855	1.51414977842702
$a_{14}$	-0.248341016919758	-0.988004732500114
$a_{24}$	0.664962202659086	0.737470179439671
$b_{15}$	-0.615218073330092	-0.170279773338488
$b_{25}$	1.514065752725853	1.53212350370819
$a_{15}$	0.153287665810598	-0.248490595991584
$a_{25}$	0.799539136532461	0.665002560048283
$b_{16}$	-0.170550311914843	1.27641783778647
$b_{26}$	1.533172247905208	1.51984836792041
$a_{16}$	-1.167663624736823	-0.677587050173636
$a_{26}$	0.813874476772697	0.668071316673186
$b_{17}$	1.968299743256314	1.96926336909199
$b_{27}$	0.922949856470389	0.923231953452632
$a_{17}$	-0.009812603421707	-0.544100922886046
$a_{27}$	0.705642536197661	0.653350919814536
$b_0$	0.002682393295273	0.002680119463696

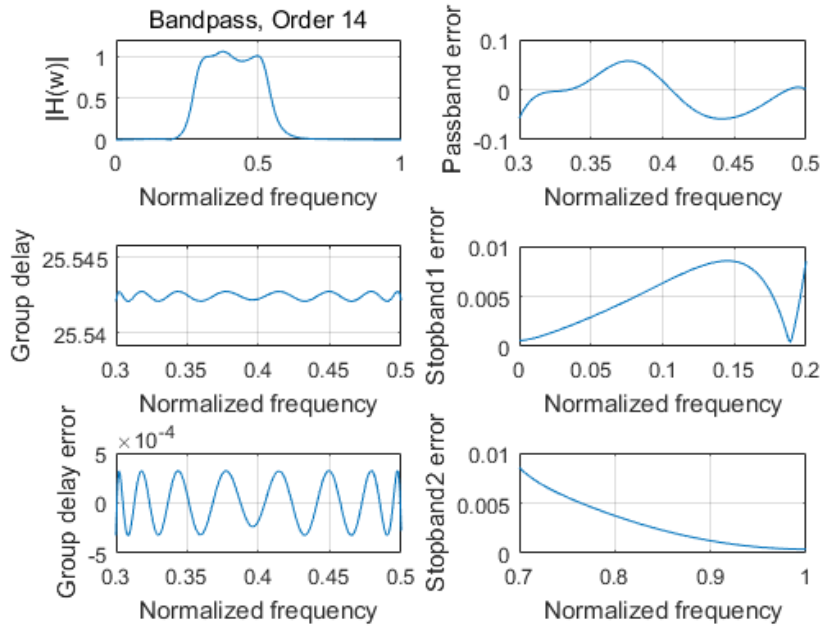


Fig. 5.5 Magnitude, group delay, magnitude errors and group delay errors of designed IIR bandpass digital filter in Example 3 obtained by constrained MOCSA

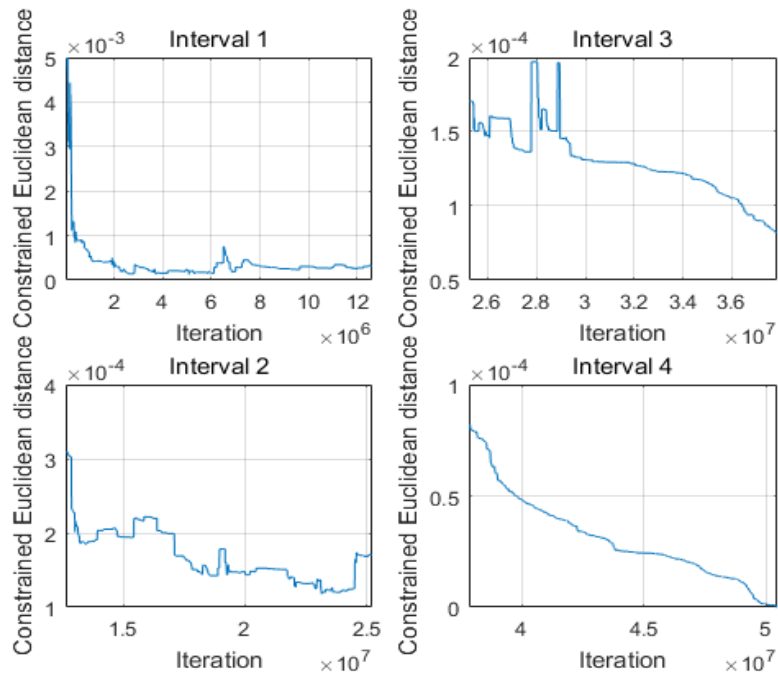


Fig. 5.6 Convergence curve of designed IIR bandpass digital filter in Example 3 obtained by constrained MOCSA

## 5.5 Conclusion

This chapter has presented the design of cascade-form IIR digital filters using constrained multiobjective Cuckoo Search Algorithm. Positive excessive errors beyond error-based requirements with respect to maximum errors of magnitude response in passband and in stopband as well as that of group delay in passband are formulated as three objective functions while a limitation of magnitude response in transition band is formulated as single inequality constraint. Three filter examples including 10th-order lowpass, 14-order highpass and 14h-order bandpass digital filters with prescribed values of group delay in passband are presented. The obtained design results including maximum passband ripple, minimum stopband attenuation and maximum group delay deviation indicates slightly better results can be obtained as compared to the state-of-the-art design results, which has shown the effectiveness of constrained MOCSA.

## CHAPTER 6 Conclusion Remarks

In this thesis, basic background of digital filters and evolutionary algorithms are firstly introduced. Multiple versions of Cuckoo Search Algorithm focusing on single objective, multiobjective and constrained multiobjective optimization problems are presented, respectively. For each version of CSA, comparison on specific digital filter design with other techniques is used to illustrate its effectiveness and applicability.

Chapter 3 has presented the design of linear-phase type-1 FIR digital filters using original Cuckoo Search Algorithm. Design results have shown that the peak errors obtained by CSA are mostly smaller than those obtained by the Parks-McClellan algorithm. Levy flight with wide-range step length is utilized as a special strategy for the global walk to assure reaching the global optimum and the local walk is able to improve an existing solution within a small range to orientate the direction toward the local minima.

Chapter 4 has presented the design of general FIR digital filters using multiobjective Cuckoo Search Algorithm. Design results with respect to smaller peak error of both magnitude response and group delay in passband obtained by MOCSA indicates that MOCSA compares favorably with NSGA-III, which verifies its validity. MOCSA incorporates a method of Euclidean distance combining objective-based equilibrating operations and the searching for the optimal solution into one simple step. During the calculation of Euclidean distance, each objective function has been equilibrated to a coordinative level due to the equal weight for its corresponding dimension. Meanwhile, the best solution can be easily determined after a simple comparison of distinct Euclidean distances.

Chapter 5 has presented the design of cascade-form IIR digital filters using constrained multiobjective Cuckoo Search Algorithm. Slightly smaller peak passband ripple as well as maximum group delay deviation and slightly larger minimum stopband attenuation are obtained by constrained MOCSA as compared to the state-of-the-art methods, which has shown the effectiveness of constrained MOCSA.



## REFERENCES

- [1] H. K. Kwan, Global Optimization Algorithms and Design Applications, Edition 1.2, by Hon Keung Kwan, dfisp.org, March 2018, ISBN13: 9781988307046.
- [2] A. E. Eiben and J. E. Smith, Introduction to Evolutionary Computing, Edition 2, Leiden, Netherlands, 2003, ISBN: 9783662448731
- [3] L. J. Fogel, A. J. Owens and M. J. Walsh, "Artificial intelligence through a simulation of evolution", Biophysices and Cybernetic Systems, pp. 131-156, 1965.
- [4] J. H. Holland, "Genetic algorithms and the optimal allocation of trials", SIAM Journal of Computing, vol. 2, pp. 88-105, 1973.
- [5] R. Stone and K. Price, "Differential evolution – a simple and efficient heuristic for global optimization over continuous spaces", Journal of Global Optimization, vol. 11, pp. 341-359, 1997.
- [6] J. Kennedy and R. Eberhart, "Particle swarm optimization", Proceedings of IEEE International Conference on Neural Networks, vol. IV, pp. 1941-1948, 1995.
- [7] A. E. Eiben and J. E. Smith, Introduction to Evolutionary Computing, Amsterdam, Netherlands, 2003, ISBN: 9783662448731.
- [8] X. S. Yang, Nature-Inspired Metaheuristic Algorithms, Luniver Press, 2nd edition, 2010.
- [9] I. F. Jr., X. S. Yang, D. Fister and I. Fister, "Cuckoo search: A brief literature review," in Cuckoo Search and Firefly Algorithm, Studies in Computational Intelligence, vol. 516, Switzerland: Springer International Publishing, 2014, pp. 49-62.
- [10] M. Tuba, M. Subotic and N. Stanarevic, "Modified cuckoo search algorithm for unconstrained optimization problems", in Proceedings of the European Computing Conference (ECC 2011), Paris, France, 2011, pp. 263-268.
- [11] R. B. Payne, M. D. Sorenson, and K. Klitz, The Cuckoos, Oxford University Press, (2005).
- [12] X. S. Yang and S. Deb, "Engineering optimisation by cuckoo search", Int. J. Mathematical Modelling and Numerical Optimisation, vol.1, no. 4, pp. 330-343, 2010.
- [13] H. K. Kwan and J. Liang, "Minimax design of linear phase FIR filters using cuckoo search algorithm", in Proceedings of 8th International Conference on Wireless Communications and Signal Processing (WCSP 2016), Yangzhou, Jiangsu, China, October 13-15, 2016, pp. 1-4.
- [14] H. K. Kwan and R. Raju, "Minimax design of linear phase FIR differentiators using artificial bee colony algorithm", in Proceedings of 8th International Conference on Wireless

- Communications and Signal Processing (WCSP 2016), Yangzhou, Jiangsu, China, October 13-15, 2016, pp. 1-4.
- [15] H. K. Kwan and M. Zhang, "Minimax design of linear phase FIR Hilbert transformer using teaching-learning-based optimization", in Proceedings of 8th International Conference on Wireless Communications and Signal Processing (WCSP 2016), Yangzhou, Jiangsu, China, October 13-15, 2016, pp. 1-4.
- [16] T. W. Parks and J. H. McClellan, "Chebyshev approximation for non-recursive digital filters with linear phase," IEEE Trans. Circuits Theory, vol. CT-19, pp. 189-194, 1972.
- [17] J. H. McClellan and T. W. Parks, "A unified approach to the design of optimum FIR linear-phase digital filters," IEEE Transactions on Circuit Theory, vol. 20, no. 6, pp. 697-701, 1973.
- [18] L. R. Rabiner, J. H. McClellan, and T. W. Parks. "FIR digital filter design techniques using weighted Chebyshev approximation," Proceedings of the IEEE, vol. 63, number 4, pp. 595-610, 1975.
- [19] I. F. Jr., D. Fister and I. Fister, "A comprehensive review of cuckoo search: variants and hybrids", Int. J. Mathematical Modelling and Numerical Optimisation, vol. 4, no. 4, pp. 387-409, 2013.
- [20] K. Deb and H. Jain, "An evolutionary many-objective optimization algorithm using reference-point-based nondominated sorting approach, Part I: Solving problems with box constraints", IEEE Transactions on Evolutionary Computation, vol. 18, no. 4, pp. 577-601, August, 2014.
- [21] Y. Wang, B. Li and Y. Chen, "Applied soft computing", vol. 11, issue 2, pp. 1851-1857, March, 2011.
- [22] R. C. Sanghvi, H. B. Soni, "Multi-objective IIR filter design using nondominated sorting genetic algorithm-II", Indian Journal of Science and Technology, vol. 9, issue 47, December, 2016.
- [23] R. C. Nongpiur, D. J. Shpak and A. Antoniou, "Improved design method for nearly linear-phase IIR filters using constrained optimization", IEEE Transactions on Signal Processing, vol. 61, issue 4, pp. 895-906, 2012.
- [24] A. Antoniou, Digital Signal Processing, Signals, Systems, and Filters, McGraw-Hill, 2006.

## VITA AUCTORIS

NAME: Jiajun Liang

PLACE OF BIRTH: Guangzhou, China

YEAR OF BIRTH: 1992

EDUCATION: The Affiliated High School of South China Normal University, Guangzhou, China, 2008

South China University of Technology, B.Sc.,  
Guangzhou, China, 2011

University of Windsor, M.A.Sc., Windsor, ON, 2016

PUBLICATION

1. H. K. Kwan and J. Liang, "Minimax design of linear phase FIR filters using cuckoo search algorithm", in Proceedings of 8th International Conference on Wireless Communications and Signal Processing (WCSP 2016), Yangzhou, Jiangsu, China, October 13-15, 2016, pp. 1-4.
2. J. Liang and H. K. Kwan, "FIR filter design using multiobjective cuckoo search algorithm", in Proceedings of 30th IEEE Canadian Conference on Electrical and Computer Engineering (CCECE2017), Windsor, Ontario, Canada, May 1-3, 2017, pp. 1-4.
3. J. Liang and H. K. Kwan, "IIR filter design using constrained multiobjective cuckoo search algorithm", in Proceedings of 31th IEEE Canadian Conference on Electrical and Computer Engineering (CCECE2018), Quebec City, Quebec, Canada, May 13-16, 2018, pp. 1-4.
4. H. K. Kwan, J. Liang and A. Jiang, "Sparse FIR filter design using iterative MOCSA", in Proceedings of 61st IEEE International Midwest Symposium on Circuits and Systems (MWSCAS2018), Windsor, Ontario, Canada, August 5-8, 2018, pp. 1-4. (Submitted)